UNCLASSIFIED

AD NUMBER
ADB805183

LIMITATION CHANGES

TO:
Approved for public release; distribution is unlimited.

FROM:
Distribution authorized to DoD only; Administrative/Operational Use; 1944. Other requests shall be referred to National Aeronautics and Space Administration, Washington, DC. Pre-dates formal DoD distribution statements. Treat as DoD only.

AUTHORITY

NASA TR Server website

THIS PAGE IS UNCLASSIFIED

REPORT No. 803

WIND-TUNNEL INVESTIGATION OF THE EFFECTS OF PROFILE MODIFICATION AND TABS ON THE CHARACTERISTICS OF AILERONS ON A LOW-DRAG AIRFOIL

By ROBERT M. CRANE and RALPH W. HOLTZCLAW

SUMMARY

An investigation has been made to determine the effect of control-surface profile modifications on the aerodynamic characteristics of an NACA low-drag airfoil equipped with a 0.20-chord and a 0.15-chord aileron. Tab characteristics have been obtained for 0.20-aileron chord tabs on two of the 0.20-chord ailerons.

Thickening the aileron profile or thickening and beveling the trailing edge of the aileron was found to reduce the aileron effectiveness, reduce the slope of the wing-section lift curve, and reduce the hinge-moment coefficients. Thinning the profile had the opposite effect. The effects of profile thickness on the aileron characteristics decreased with increasing angle of attack, there being practically no effect at an angle of attack of 12°. For the thickened and beveled trailing edges the effects were maximum for the bevel, the length of which was 20 percent of the aileron chord, and decreased for both increasing and decreasing bevel lengths. Thickening the profile or thickening and beveling the trailing edge caused a slight increase in minimum profile-drag coefficient, but thinning the profile had no effect.

It is demonstrated that deviations of the order of ±0.005-aileron chord from the specified profile on the ailerons of a typical pursuit airplane can cause stick-force variations of ±20 pounds for a large rate of roll at an indicated airspeed of 300 miles per hour. It is also shown that the danger of overbalance at small deflections of closely balanced ailerons can be diminished by thickening of the aileron profile if the internal-balance chord is simultaneously reduced to maintain the same stick force for a large rate of roll.

Thickening and beveling the trailing edge on a typical aileron installation caused a reduction of 50 percent in the control force for a large rate of roll at high speed. When used in conjunction with internal balance, the thickened and beveled profile resulted in a 30-percent reduction in the nose balance required for a given control force at high speed. Under these conditions, the variation of control force with rate of roll was more nearly linear for the aileron of normal profile than for the ailerons with thickened and beveled trailing edges.

Basic data are presented from which the effect of tabs can be calculated for specific cases. The data are sufficient for the solution of problems of fixed tabs with a differential linkage, as well as simple and spring-linked balancing tabs.

INTRODUCTION

With every increase in size and speed of modern high-performance airplanes, the problem of attaining adequate lateral control without excessive control forces becomes less amenable to solution by simple aerodynamic balancing methods. Of the various methods of aerodynamic balance available, one of the most efficient is the sealed internal nose balance. However, sufficient control lightness frequently cannot be satisfactorily attained by the use of an internal nose balance alone. The necessary balance may be so large that the required control-surface deflection cannot be obtained, or structural necessities of the main surfaces may be such that adequate balance cannot be incorporated in the design. Aileron profile offers a convenient means of adjusting the aileron control characteristics. The efficacy of profile variations in modifying aerodynamic characteristics, and the consequent necessity of fabricating to close tolerances, must be appreciated when it is desired to obtain specified aileron characteristics on any one airplane or to maintain a reasonable constancy of characteristics in a number of airplanes of the same design. Previous experiments have indicated that thickening and beveling the control-surface trailing edge is a powerful means of adjusting hinge-moment characteristics. Results of tests reported in references 1, 2, and 3 have shown tabs to be an effective means of adjusting hinge-moment characteristics when used as fixed tabs in conjunction with a differential linkage, or as simple or spring-linked balancing tabs.

The purpose of the tests reported herein was to obtain quantitative data on the effects of aileron profile and trailing-edge modifications and the effects of tabs on the characteristics of ailerons on a low-drag airfoil, and to form a logical basis for the specification of aileron tolerances.

COEFFICIENTS AND CORRECTIONS

The coefficients used in the presentation of results follow:

c_{d_0} airfoil section profile-drag coefficient (d_0/qc)

c_h aileron section hinge-moment coefficient (h/qc_a^2)

c_{h_t} tab section hinge-moment coefficient (h_t/qc_t^2)

c_l airfoil section lift coefficient (l/qc)

c_m airfoil section pitching-moment coefficient (m/qc^2)

c_n airfoil section normal-force coefficient (n/qc)

P/q internal static pressure at aileron nose divided by dynamic pressure

Δc_{d_o} increment of c_{d_o} due to deflecting the aileron from neutral

Δc_h increment of c_h due to deflecting the aileron from neutral

$\Delta c_h'$ c_h of up-aileron minus c_h of down-aileron

Δc_l increment of c_l due to deflecting the aileron from neutral

$\Delta c_l'$ c_l of down-aileron minus c_l of up-aileron

$\Delta P/q$ increment of pressure coefficient across aileron nose seal (pressure below seal minus pressure above seal divided by dynamic pressure)

where

c chord of airfoil with surfaces neutral, feet

c_a chord of aileron aft of aileron hinge line, feet

c_t chord of tab aft of tab hinge line, feet

d_o airfoil section profile drag, pounds

h aileron section hinge moment, foot-pounds

h_t tab section hinge moment, foot-pounds

l airfoil section lift, pounds

m airfoil section pitching moment about quarter chord of airfoil, foot-pounds

n airfoil section normal force, pounds

q dynamic pressure of air stream ($\frac{1}{2}\rho V^2$), pounds per square foot

V free-stream velocity, feet per second

In addition to the preceding, the following symbols are employed:

α_o angle of attack for airfoil of infinite aspect ratio, degrees

δ_a aileron deflection with respect to the airfoil, degrees

δ_t tab deflection with respect to the aileron, degrees

b wing span of assumed airplane, feet

p rate of roll, radians per second

d increment above the normal profile of the upper and lower surface ordinates of the modified aileron profiles at $0.5c_a$

V_i indicated airspeed, miles per hour

c_{h_α} $=(\partial c_h/\partial\alpha)_{\delta_a=\delta_t=0}$ (measured through $\alpha=0°$)

$c_{h_{\delta_a}}$ $=(\partial c_h/\partial\delta_a)_{\alpha=\delta_t=0}$ (measured through $\delta_a=0°$)

$c_{h_{\delta_t}}$ $=(\partial c_h/\partial\delta_t)_{\alpha=\delta_a=0}$ (measured through $\delta_t=0°$)

$c_{h_{t_\alpha}}$ $=(\partial c_{h_t}/\partial\alpha)_{\delta_a=\delta_t=0}$ (measured through $\alpha=0°$)

$c_{h_{t_{\delta_a}}}$ $=(\partial c_{h_t}/\partial\delta_a)_{\alpha=\delta_t=0}$ (measured through $\delta_a=0°$)

$c_{h_{t_{\delta_t}}}$ $=(\partial c_{h_t}/\partial\delta_t)_{\alpha=\delta_a=0}$ (measured through $\delta_t=0°$)

c_{l_α} $=(\partial c_l/\partial\alpha)_{\delta_a=\delta_t=0}$ (measured through $\alpha=0°$)

$c_{l_{\delta_a}}$ $=(\partial c_l/\partial\delta_a)_{\alpha=\delta_t=0}$ (measured through $\delta_a=0°$)

$c_{l_{\delta_t}}$ $=(\partial c_l/\partial\delta_t)_{\alpha=\delta_a=0}$ (measured through $\delta_t=0°$)

The subscripts outside the parentheses represent the factors held constant during the measurement of the parameters.

The lift coefficient, profile-drag coefficient, and pitching-moment coefficient have been corrected for tunnel-wall effects. Section profile drag was determined by measurement of loss of momentum in the wing wake. A comparison of force-test and pressure-distribution measurements of section lift coefficient and section pitching-moment coefficient indicated that the end plates had no effect on these coefficients with the control surfaces neutral. No corrections have been applied to. section hinge-moment coefficients and no end-plate correction has been applied to Δc_l. Because of possible tip losses, it is believed that the measured aileron effectiveness is slightly low and rates of roll computed from these data will be conservative. By comparison of these data with section data on a similar airfoil, it is estimated that the decrease in the value of Δc_l due to this effect is not more than 12 percent.

TABLE I.—NACA 66, 2–216 ($a=0.6$) AIRFOIL

[Stations and ordinates are given in percent of the airfoil chord]

Upper surface		Lower surface	
Station	Ordinate	Station	Ordinate
0	0	0	0
0.371	1.243	0.629	−1.112
0.607	1.501	0.893	−1.319
1.091	1.886	1.409	−1.608
2.317	2.615	2.683	−2.127
4.794	3.701	5.206	−2.860
7.284	4.563	7.716	−3.441
9.781	5.308	10.219	−3.934
14.788	6.500	15.212	−4.702
19.806	7.428	20.194	−5.290
24.832	8.155	25.168	−5.741
29.862	8.700	30.138	−6.080
34.897	9.098	35.103	−6.312
39.936	9.356	40.064	−6.462
44.978	9.471	45.022	−6.523
50.023	9.431	49.977	−6.483
55.073	9.224	54.927	−6.336
60.141	8.800	59.859	−6.048
65.191	8.084	64.809	−5.574
70.198	7.068	69.802	−4.866
75.181	5.889	74.819	−4.037
80.148	4.585	79.852	−3.107
85.106	3.265	84.894	−2.177
90.061	1.937	89.939	−1.235
95.021	0.762	94.979	−0.432
100	0	100	0
Leading-edge radius=1.575		Trailing-edge radius=0.0625	

MODEL AND APPARATUS

The airfoil used in these tests was constructed of laminated mahogany to the NACA 66,2–216 ($a=0.6$) profile of 4-foot chord and 5-foot span. The airfoil ordinates are given in table I. The aft 0.35 chord of the airfoil was made removable to allow the testing of ailerons of various chords. A solid trailing-edge section was constructed and this section and the main airfoil were equipped with a single row of pressure orifices built into the upper and lower surfaces of the airfoil at the midspan section.

The ailerons were constructed of laminated mahogany and had a radius nose with a nose-gap seal of dental rubber dam. The aileron ordinates for the thickened and thinned profiles are given in table II and ordinates for the thickened and beveled trailing-edge profiles are given in table III. The ordinates of the normal-profile aileron are the same as the corresponding ordinates of the NACA 66,2–216 ($a=0.6$) airfoil. The details of the ailerons and the modifications tested are shown in figures 1, 2, and 3. The method of determining the profile of thickened and beveled trailing edges is described in the appendix. Since, as shown in figure 3, beveling the trailing edge was necessarily accompanied by a definite amount of thickening, the profiles so
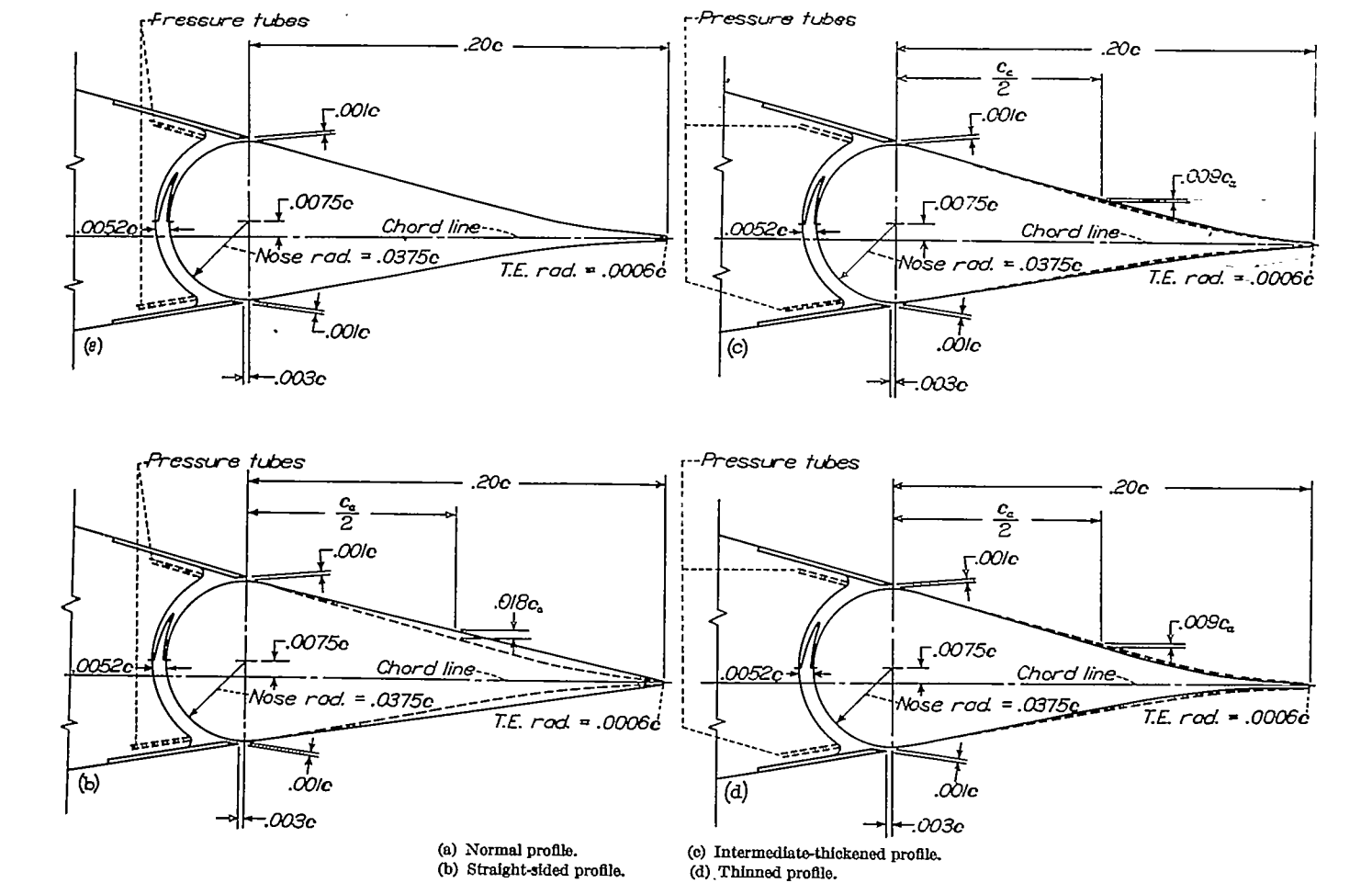
(a) Normal profile.
(b) Straight-sided profile.
(c) Intermediate-thickened profile.
(d) Thinned profile.

FIGURE 1.—Profile variations on the 0.20-chord, sealed gap, plain aileron

(a) Normal profile.
(b) Straight-sided profile.
(c) Intermediate-thickened profiler
(d) Thinned profile.
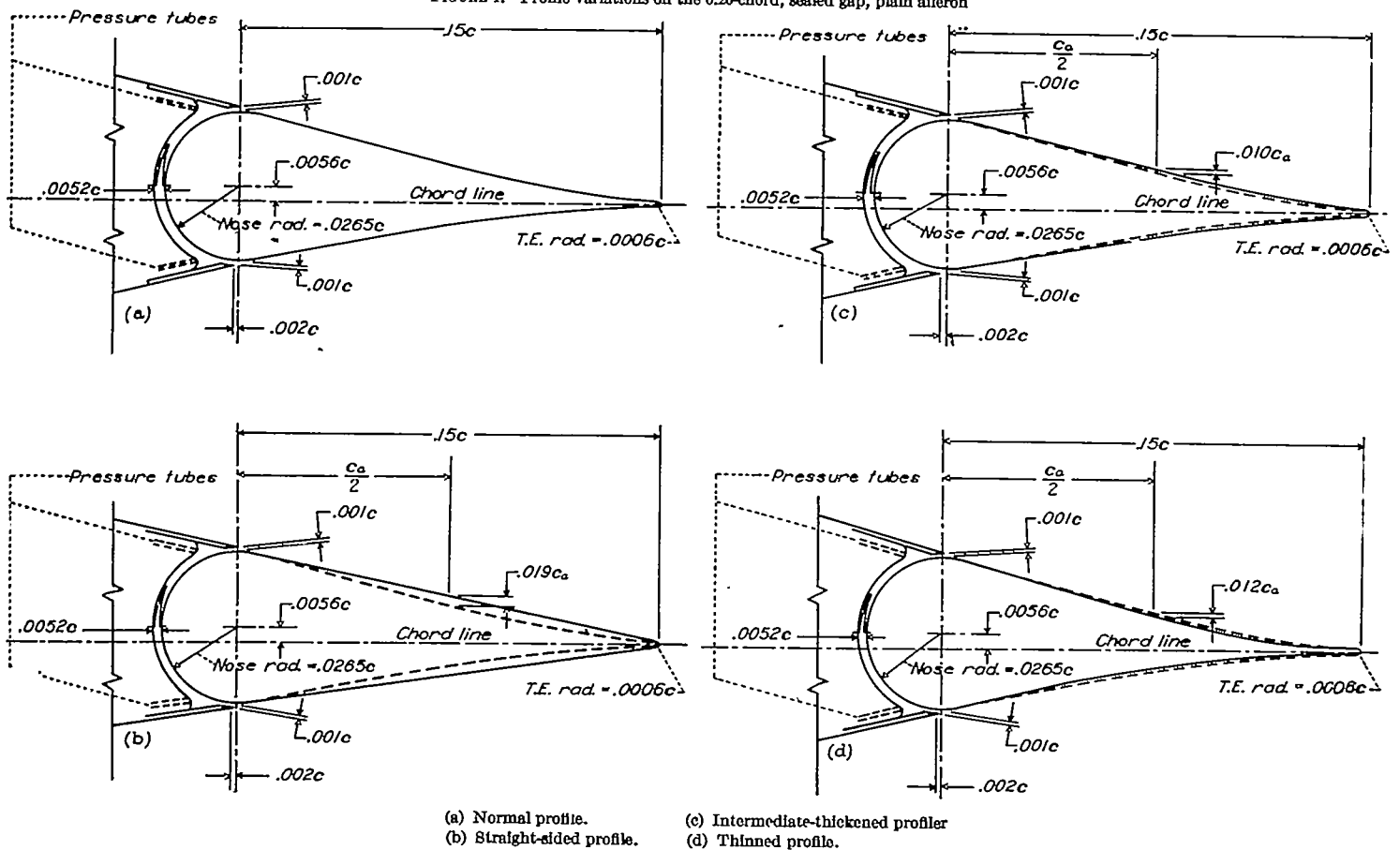
FIGURE 2.—Profile variations on the 0.15-chord, sealed gap, plain aileron.

(a) 0.40c_a bevel.   (c) 0.20c_a bevel.
(b) 0.30c_a bevel.   (d) 0.10c_a bevel.
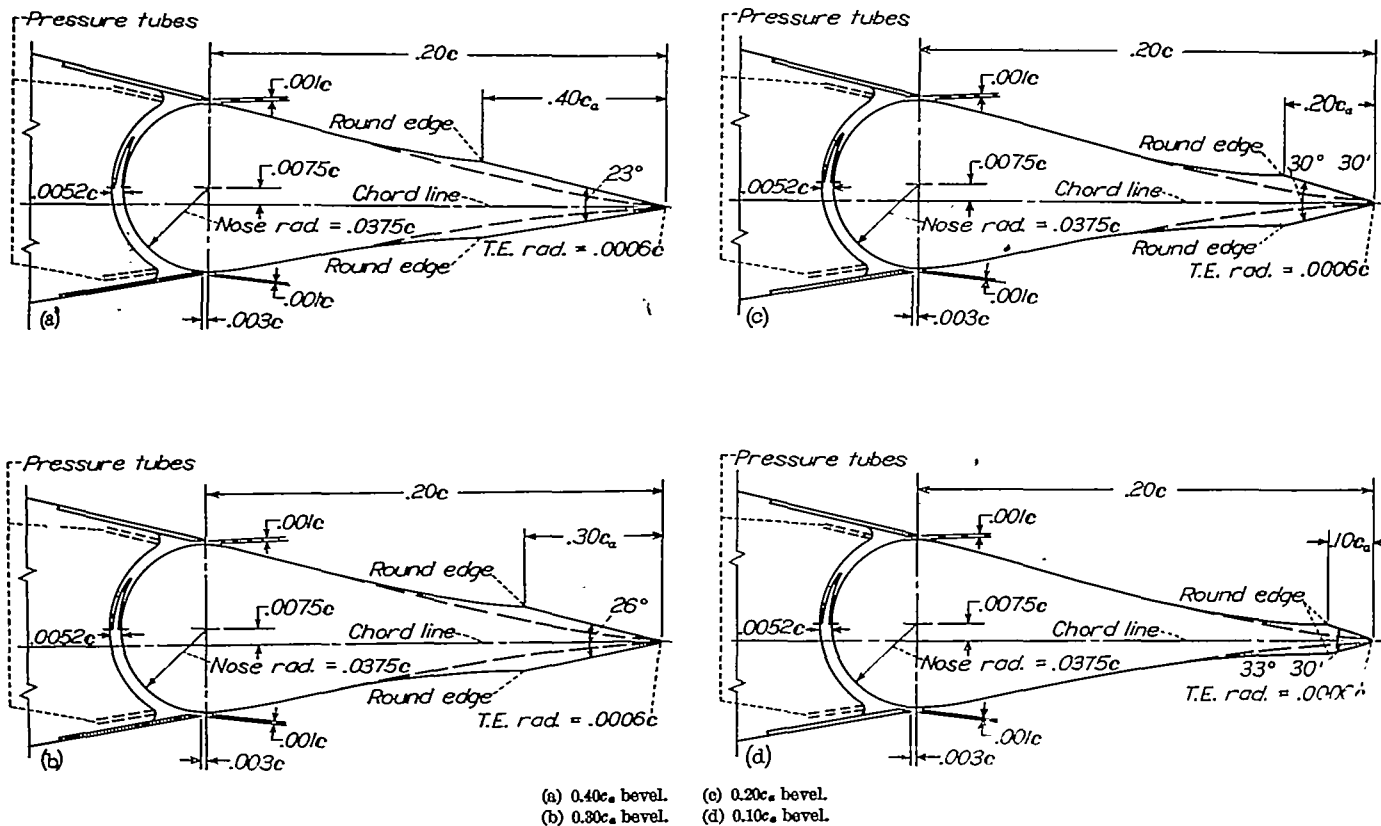
FIGURE 3.—Thickened and beveled trailing edges on 0.20-chord, plain ailerons.

modified are for simplicity hereafter referred to as beveled trailing-edge ailerons and beveling the trailing edge is understood to mean thickening and beveling as shown by the figure.

TABLE II.—ORDINATES OF THE NORMAL PROFILE AILERONS AND THE AILERONS OF THICKENED AND THINNED PROFILES

[Stations given are wing stations and ordinates are in percent of the airfoil chord]

Station	Normal profile		Straight-sided profile		Intermediate thickened profile		Thinned profile	
	Upper	Lower	Upper	Lower	Upper	Lower	Upper	Lower
0.20c Ailerons (T. E. radius=0.0625)								
81.25	4.27	−2.85	4.27	−2.85	4.27	−2.85	4.27	−2.85
83.33	3.77	−2.45	3.80	−2.55	3.78	−2.50	3.73	−2.40
85.42	3.21	−2.07	3.33	−2.24	3.27	−2.16	3.15	−1.99
87.50	2.65	−1.67	2.88	−1.93	2.76	−1.80	2.53	−1.54
89.58	2.08	−1.28	2.40	−1.61	2.24	−1.45	1.93	−1.11
91.67	1.54	−0.91	1.93	−1.30	1.73	−1.11	1.35	−0.72
93.75	1.06	−0.58	1.44	−0.99	1.25	−0.79	0.88	−0.38
95.83	0.63	−0.33	0.98	−0.68	0.80	−0.50	0.50	−0.16
97.92	0.31	−0.17	0.51	−0.36	0.41	−0.26	0.24	−0.07
100	0	0	0	0	0	0	0	0
0.15c Ailerons (T. E. radius=0.0625)								
87.50	2.65	−1.67	2.71	−1.75	2.68	−1.71	2.61	−1.60
89.58	2.08	−1.28	2.26	−1.48	2.17	−1.38	2.00	−1.17
91.67	1.54	−0.92	1.82	−1.19	1.69	−1.06	1.39	−0.76
93.75	1.06	−0.58	1.38	−0.90	1.22	−0.75	0.85	−0.38
95.83	0.63	−0.33	0.92	−0.60	0.78	−0.47	0.45	−0.16
97.92	0.31	−0.17	0.48	−0.33	0.40	−0.25	0.21	−0.07
100	0	0	0	0	0	0	0	0

Tabs of 0.20-aileron chord were tested on 0.20-chord normal profile and straight-sided profile ailerons. The tabs were full span constructed of steel in four sections to minimize the spanwise bending. The tabs had a radius nose and an unsealed nose gap of 0.0008 c. The ordinates of

the tabs were the same as the corresponding ordinates of the ailerons. Details of the tabs are shown in figures 4 and 5.
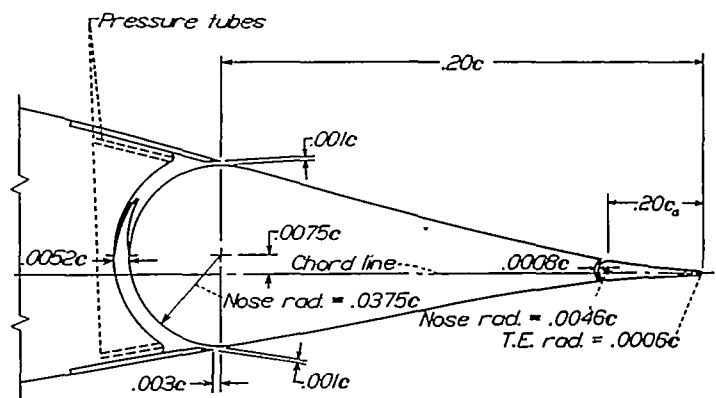
FIGURE 4.—The 0.20 aileron chord tab on the normal-profile aileron.
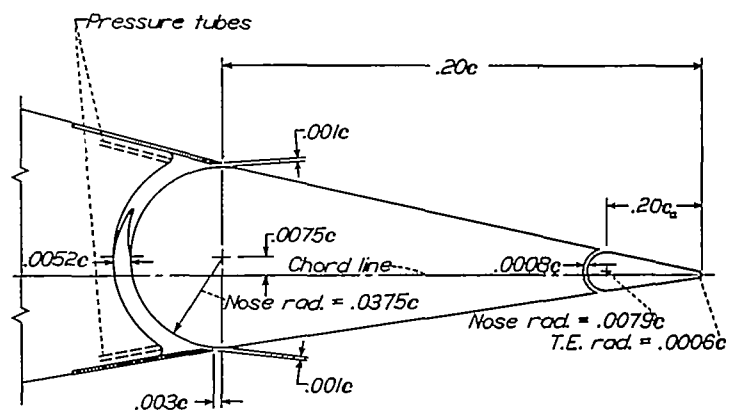
FIGURE 5.—The 0.20 aileron chord tab on the straight-sided profile aileron.

TABLE III.—ORDINATES OF BEVELED PROFILE AILERONS

[Stations given are wing stations and ordinates are in percent of the airfoil chord]

0.40c_a bevel			0.30c_a bevel			0.20c_a bevel			0.10c_a bevel		
Station	Upper	Lower	Station	Upper	Lower	Station	Upper	Lower	Station	Upper	Lower
81.25	4.27	−2.85	81.25	4.27	−2.85	81.25	4.27	−2.85	81.25	4.27	−2.85
83.33	3.77	−2.45	83.33	3.77	−2.45	83.33	3.77	−2.45	83.33	3.77	−2.45
85.42	3.21	−2.07	85.42	3.21	−2.07	85.42	3.21	−2.07	85.42	3.21	−2.07
87.50	2.71	−1.75	87.50	2.68	−1.72	87.50	2.65	−1.67	87.50	2.65	−1.67
89.58	2.29	−1.48	89.58	2.23	−1.44	89.58	2.10	−1.33	89.58	2.08	−1.28
91.67	2.01	−1.41	91.67	1.88	−1.25	91.67	1.67	−1.15	91.67	1.56	−0.98
92.00	2.00	−1.40	93.75	1.65	−1.24	93.75	1.38	−1.05	93.75	1.13	−0.79
			94.00	1.64	−1.23	96.00	1.27	−0.98	95.83	0.83	−0.66
									98.00	0.73	−0.58
Straight line from this station tangent to T. E. radius of 0.062			Straight line from this station tangent to T. E. radius of 0.062			Straight line from this station tangent to T. E. radius of 0.062			Straight line from this station tangent to T. E. radius of 0.062		

TEST INSTALLATION

The airfoil was mounted vertically in the test section of the Ames 7- by 10-foot wind tunnel No. 1 as shown in the photograph of figure 6. End plates were attached to the 5-foot-span section. Fairings of the same airfoil section as the wing were fastened to the tunnel floor and ceiling turntables and were used to shield the connections between the model and balance frame. These fairings were not equipped with ailerons. Provisions were made for changing the angle of attack and the aileron angle while the tunnel was in operation. Aileron and tab hinge moments were measured by means of electrical resistance-type strain gages which were mounted on members restraining the torque tubes of the surfaces from rotation.

FIGURE 6.—The NACA 66, 2-216 (a=0.6) airfoil equipped with the 0.20-chord plain aileron of normal profile.

TESTS

For each of the aileron-profile and trailing-edge modifications, two series of tests were made. The first series obtained aileron characteristics at the highest Reynolds number obtainable (9,000,000) at five angles of attack (−4°, −2°, 0°, 2°, and 4°). A second series at angles of attack of 0°, 4°, 8°, and 12° was made at a reduced Reynolds number (3,800,000). With the aileron neutral, section characteristics were obtained at a Reynolds number of 8,200,000. Section profile-drag coefficients were obtained with the aileron neutral, at the ideal lift coefficient (c_i=0.21) over a Reynolds number range of 3,000,000 to 10,000,000.

For the tab investigations the characteristics were obtained for each of the two aileron profiles at a Reynolds number of 9,000,000 for angles of attack of −4°, −2°, 0°, 2°, and 4°. These data covered a range of aileron deflections of ±20° and a range of tab deflections of ±25°. Similar data were obtained at angles of attack of 8° and 12° at test Reynolds numbers of 6,700,000 and 5,500,000, respectively. With the aileron neutral, section characteristics were obtained for tab deflections from −25° to 25° at a Reynolds number of 8,200,000.

RESULTS AND DISCUSSION

BASIC SECTION DATA

The basic section data may be utilized to predict the section characteristics of ailerons with any amount of internal nose balance by means of the equation

$$(c_h)_B = c_h + \frac{\Delta P}{q}\left(\frac{B^2 - R^2}{2}\right)$$

where

$(c_h)_B$ aileron section hinge-moment coefficient of aileron with sealed internal nose balance

c_h aileron section hinge-moment coefficient of plain aileron

B nose balance (expressed as fraction of c_a)

R nose radius of plain aileron (expressed as fraction of c_a)

While the basic data are useful for purposes of aileron design the prediction and comparison of the effects of aileron profile modification may be more conveniently demonstrated by means of section parameters. For this purpose plots showing the relation of various coefficients and parameters to other independent variables have been prepared. These plots together with the other summary figures prepared for the purposes of discussion are presented in figures 7 to 29. The basic section data are included in figures 30 to 64. For ease of discussion the effects of aileron profile modification, thickened and beveled trailing edges, and tabs will be discussed separately.
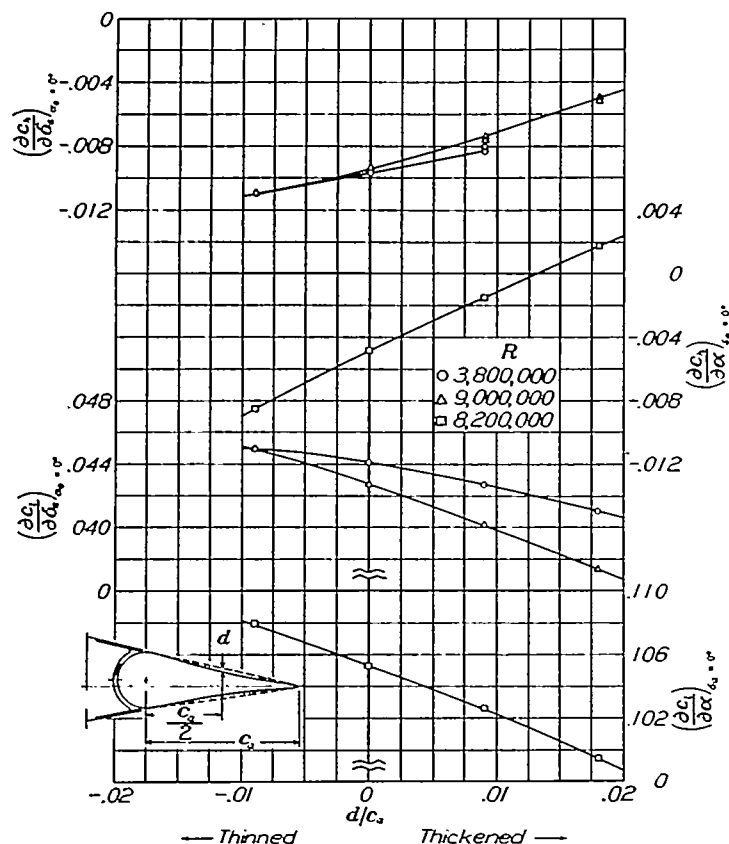
FIGURE 7.—The effect of modifications of the aileron profile on the section parameters of an NACA 66, 2-216 ($a=0.6$) airfoil equipped with a 0.20-chord, sealed gap, plain aileron.
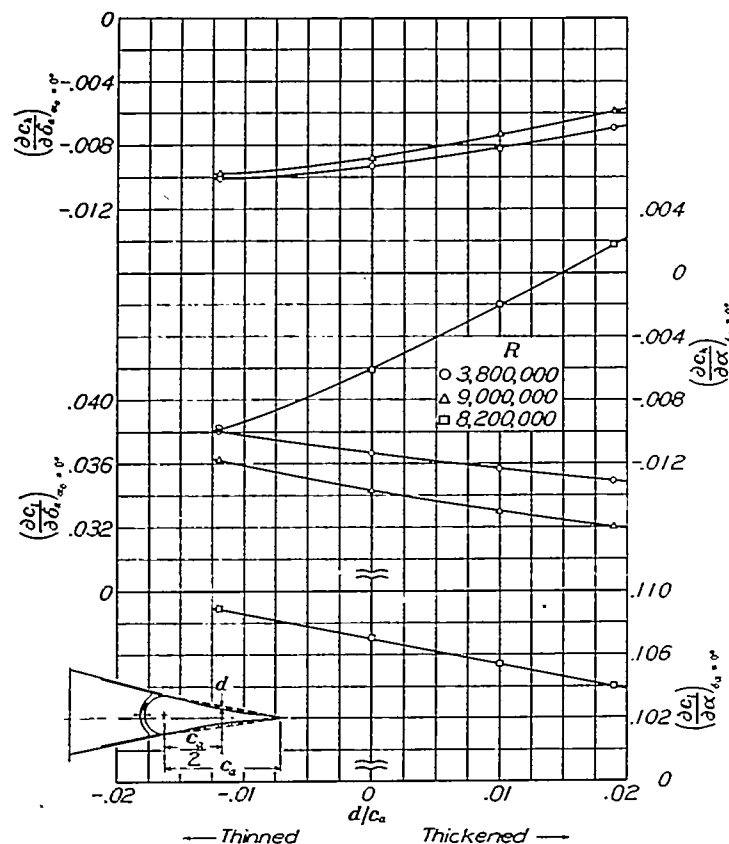

FIGURE 8.—The effect of modifications of the aileron profile on the section parameters of an NACA 66, 2-216 ($a=0.6$) airfoil equipped with a 0.15-chord, sealed gap, plain aileron.

AILERON PROFILE MODIFICATIONS

Aileron effectiveness.—The effect of the profile variations on the aileron-effectiveness parameter $c_{l_{\delta_a}}$ is shown in figures 7 and 8. Thickening the aileron profile reduced the effectiveness, and thinning the profile increased it, the change being very nearly a linear function of d.

Aileron profile had a similar influence on effectiveness at the higher aileron deflections where the flow over the aileron had separated. Examination of the basic data of figures 31 to 38 indicates that the differences due to profile modification decreased at the higher angles of attack, there being only a minor variation in effectiveness at an angle of attack of 12° for the various aileron profiles.

To determine the effect of control-surface profile on the aileron effectiveness of a typical installation, these data have been applied to the prediction of the aileron control characteristics of a typical pursuit airplane. The airplane data necessary for the calculations are presented in table IV. The calculations have been made assuming zero sideslip of the airplane and no torsional deflection of the wing. The effect of aileron profile on the wing lift-curve slope has been included in determination of c_{l_p} the damping-moment coefficient due to rolling. The calculated variation of $pb/2V$ with total aileron deflection for the various aileron profiles is presented in figures 9 and 10 for indicated airspeeds of 300 and 120 miles per hour. Examination of these figures reveals that the total aileron deflection necessary to produce a given $pb/2V$ at low speeds is little influenced by aileron profile. Thus, the size and the total deflection for an installation of given effectiveness will be unchanged by control-surface profile modifications.

TABLE IV.—CHARACTERISTICS OF ASSUMED AIRPLANES

	Pursuit	Medium Bomber
Wing:		
Area, square feet	275	600
Span, feet	41.5	80
Aspect ratio	6.23	8.0
Taper ratio	3:1	2.5:1
Section	66, 2-216 ($a=0.6$)	66, 2-216 ($a=0.6$)
Ailerons:		
Span	From 0.50b/2 to tip	From 0.50b/2 to tip
Chord	0.20c	0.20c
Deflection	±15°	±15°
Airplane:		
Wing loading, pounds per square foot	33.7	50
Aileron differential	1:1	1:1
Stick travel, inches	±8	
Control wheel travel		±180°
Control wheel diameter, inches		15

Aileron hinge moments.—The aileron hinge-moment parameters c_{h_α} and $c_{h_{\delta_a}}$ are plotted in figures 7 and 8 as functions of d. These figures indicate that both of these parameters are inversely proportional to d. The value of $(\partial c_h/\partial \alpha)_{\delta_a}$ varied with angle of attack and aileron deflection. At small angles of attack and zero aileron deflection, there was an approximate linear variation of $(\partial c_h/\partial \alpha)_{\delta_a=0}$ with d. At angles of attack greater than 6°, $(\partial c_h/\partial \alpha)_{\delta_a}$ has an approximately constant value of -0.010 irrespective of aileron profile.

The data of figures 7 and 8 have been plotted in figures 11 and 12 as hinge-moment parameters against lift parameters. These curves show the relative dependence of the
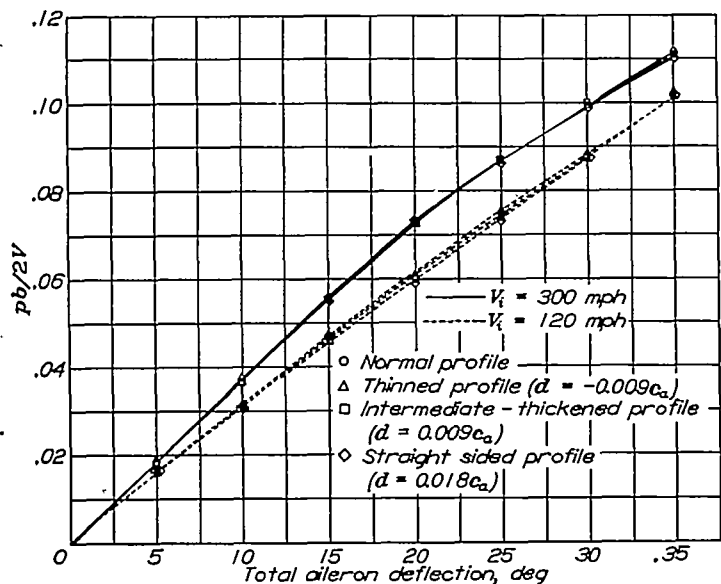
FIGURE 9.—The influence of profile on aileron effectiveness as applied to a typical pursuit airplane. 0.20-chord, sealed gap ailerons; equal up and down aileron deflection; assumed rigid wing and zero sideslip.
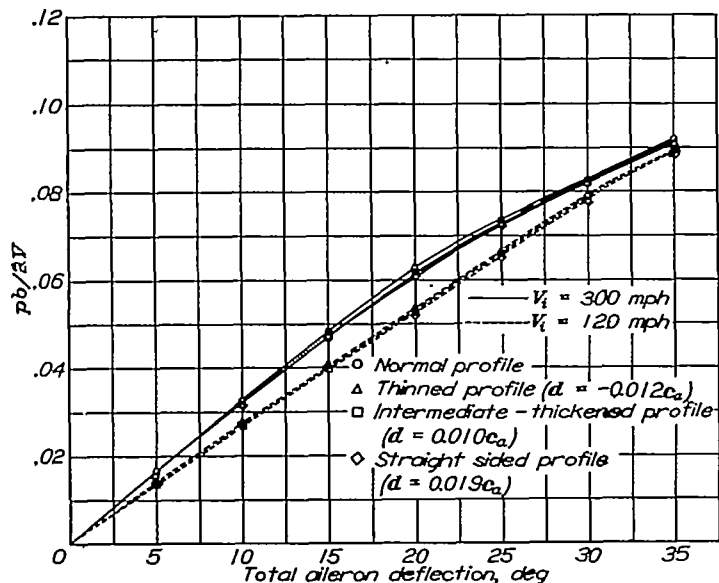

FIGURE 10.—The influence of profile on aileron effectiveness as applied to a typical pursuit airplane. 0.15-chord, sealed gap ailerons; equal up and down aileron deflection; assumed rigid wing and zero sideslip.

aileron hinge moments on the aileron effectiveness and on the slope of the wing-section lift curve, and indicate that any reduction in hinge moments by profile alteration is accompanied by a corresponding decrease in effectiveness.

Since the effect of aileron profile on $\Delta P/q$ was small, the hinge-moment coefficients of ailerons with internal nose balance will exhibit aileron profile effects similar to those observed on the plain ailerons. As separation occurs over the aileron at large deflections, there is an abrupt loss in P/q over the suction side of the control (side opposite the deflection). This loss accounts for the nonlinearity of the curves of $\Delta P/q$ against δ_a (figs. 31 to 38). It is this reduction in $\Delta P/q$ which causes the nonlinearity of hinge-moment curves of ailerons with large amounts of internal nose balance.

Aileron control forces.—The effect of modification of the aileron profile on aileron control characteristics may be evaluated from two considerations: the reduction in control force due to the profile modification when the aileron is designed with a given aerodynamic nose balance, and the reduction in nose balance due to the profile modification when the aileron is designed for a given control force.

Figures 13 and 14 illustrate the changes in control-force characteristics which result from small changes in aileron profile. The variation of stick force with $pb/2V$ for a typical pursuit airplane equipped with 0.20-chord ailerons with $0.534c_a$ internal nose balance is presented in these figures for indicated airspeeds of 300 and 120 miles per hour. At the higher speed, a decrease of $0.009c_a$ in the aileron ordinates at $0.5c_a$ reduces the $pb/2V$ obtainable with a 30-pound stick force from 0.08 to 0.056 and more than doubles the stick force
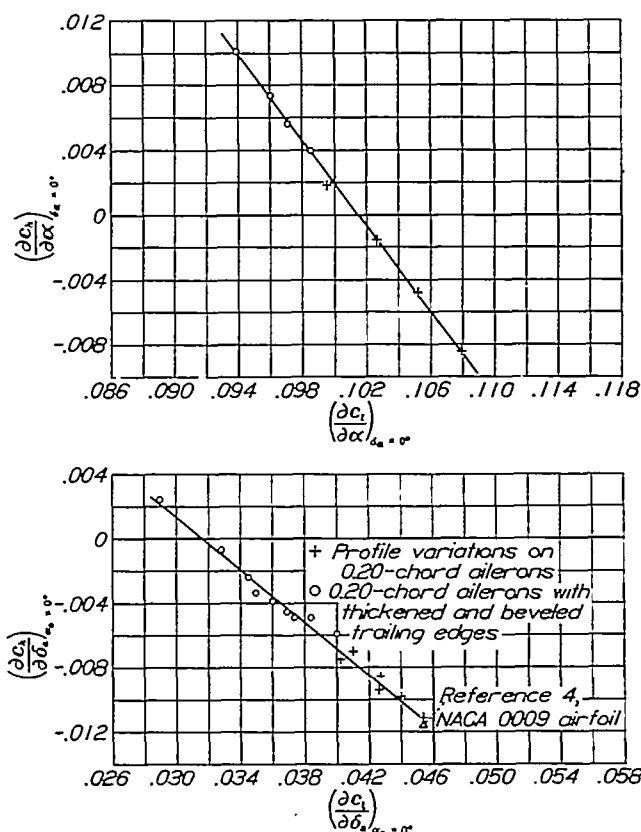
FIGURE 11.—The variation of hinge moment parameters with lift parameters for an NACA 66, 2-216 ($a=0.6$) airfoil equipped with a 0.20-chord, sealed gap, plain aileron.
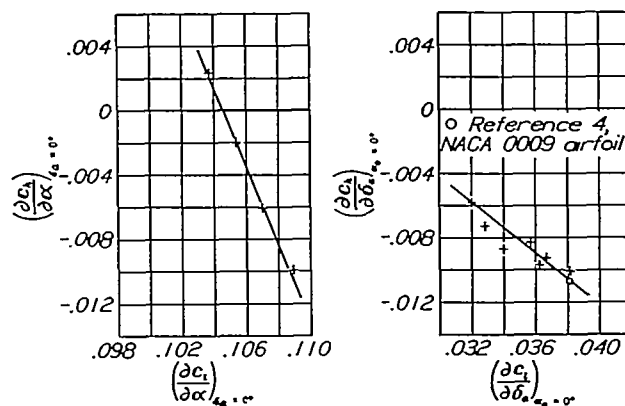
FIGURE 12.—The variation of hinge moment parameters with lift parameters for an NACA 66, 2-216 ($a=0.6$) airfoil equipped with a 0.15-chord, sealed gap, plain aileron.
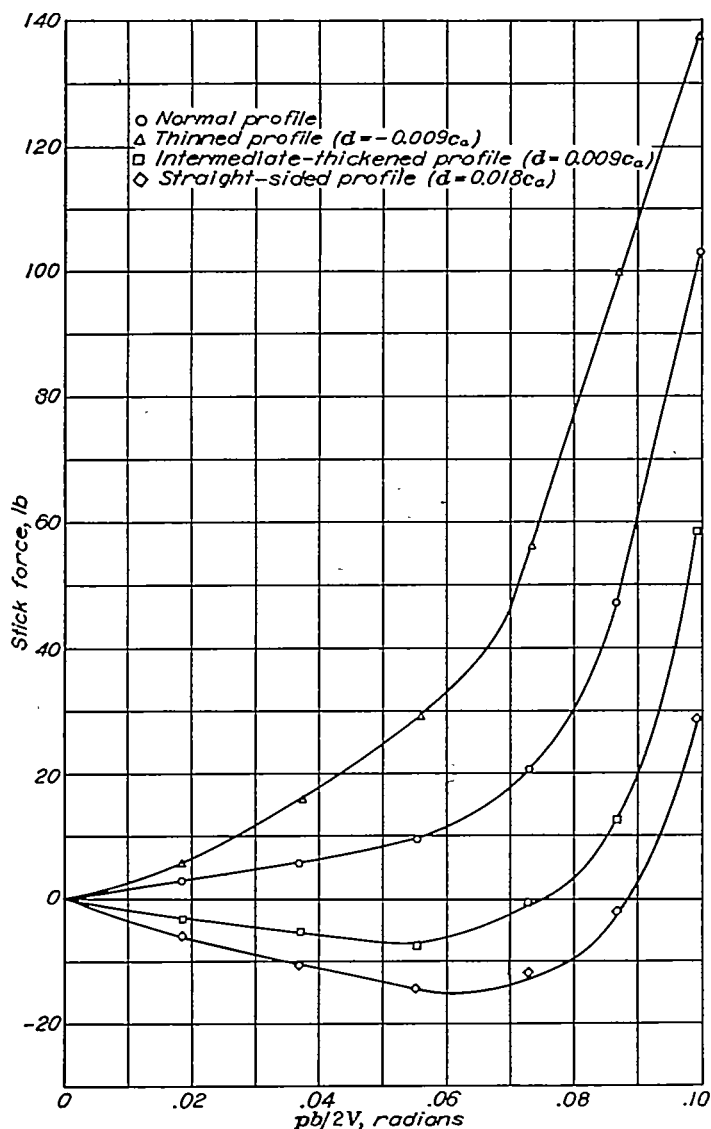
FIGURE 13.—The effect of modifications of the aileron profile on the aileron-control characteristics of a typical pursuit airplane equipped with 0.20-chord, sealed gap ailerons with $0.53c_a$ internal nose balance at an indicated airspeed of 300 mph.
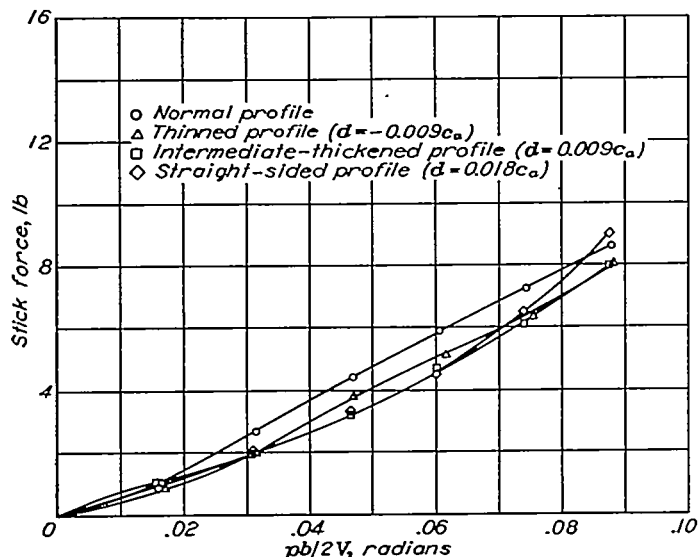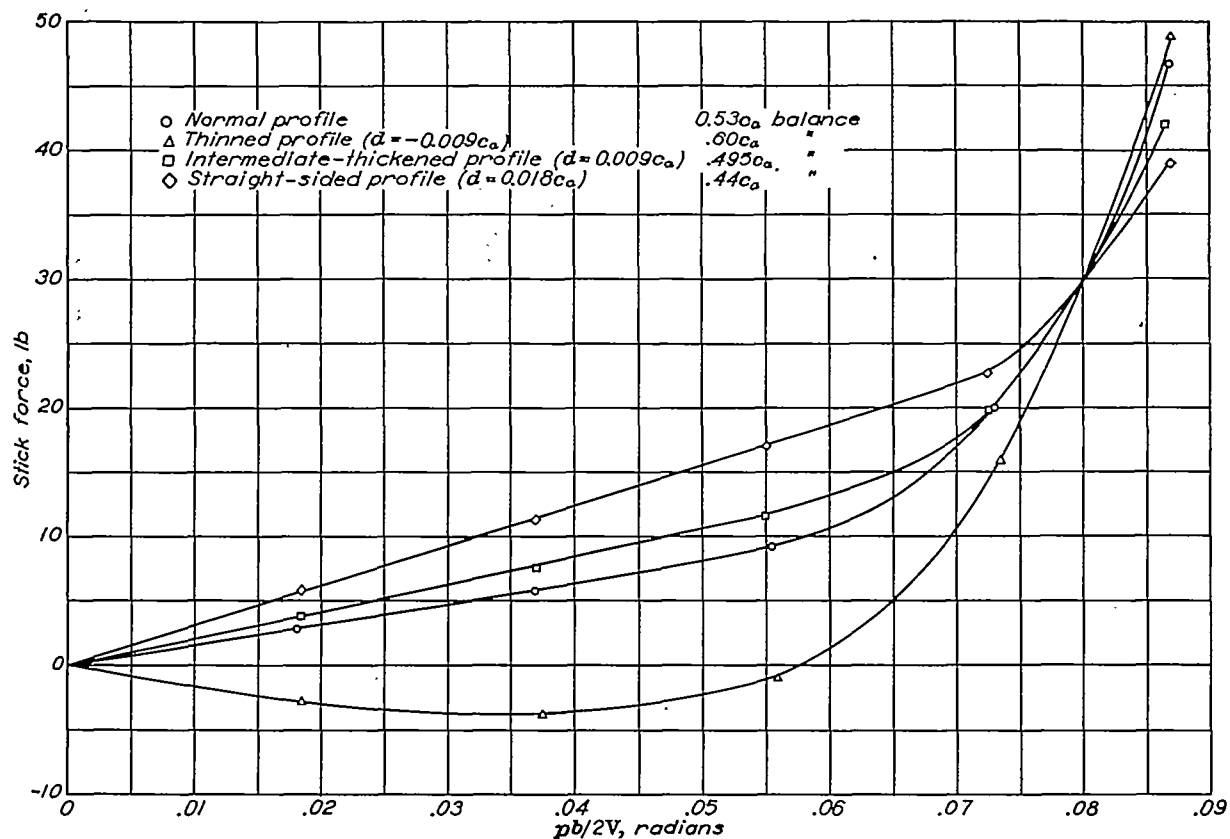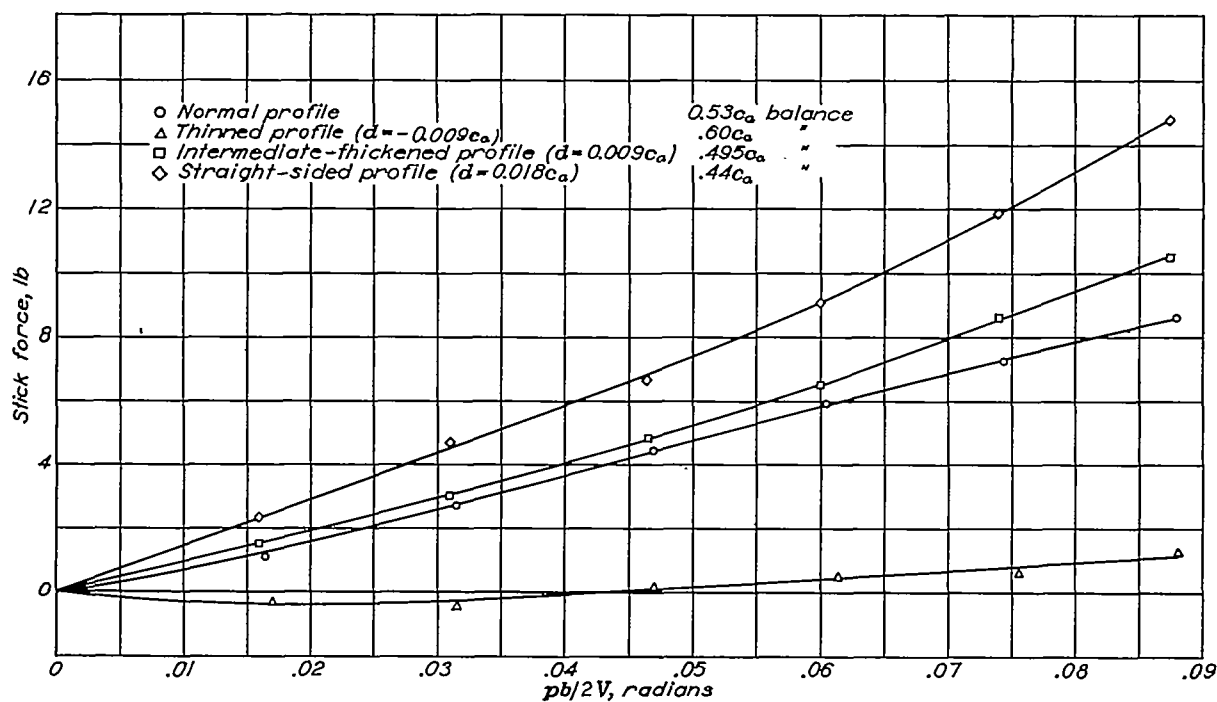

FIGURE 14.—The effect of modifications of the aileron profile on the aileron-control characteristics of a typical pursuit airplane equipped with 0.20-chord, sealed gap ailerons with $0.53c_a$ internal nose balance at an indicated airspeed of 120 mph.

for a $pb/2V$ of 0.08. Increasing the mid-chord ordinates of the aileron $0.009c_a$ changes the stick force from 8 pounds to an overbalance of 7 pounds at a $pb/2V$ of 0.05. Since results of overbalance are likely to prove catastrophic in a high-speed dive, due to the ailerons taking control, every effort should be made to maintain manufacturing tolerances and allowable surface deformations at a value which would preclude the occurrence of this condition.

The possible use of aileron profile changes to obtain desired stick-force characteristics is illustrated by figures 15 and 16. Control-force characteristics are shown for a typical pursuit airplane equipped with 0.20-chord ailerons. The airplane data necessary for the calculations are presented in table IV. Each aileron was assumed to have an internal nose balance such that a $pb/2V$ of 0.08 could be obtained with a 30-pound stick force at an indicated airspeed of 300 miles per hour. It will be observed that the thin-profile aileron which is closely enough balanced to satisfy the 30-pound stick-force limitation at high speed is overbalanced 4 pounds at a $pb/2V$ of 0.035. As the aileron profile is thickened, the control-force gradient becomes more positive, and the linear range of the gradient is extended to larger values of $pb/2V$. The primary problem of aileron-balance design is to make the control light enough at very high speed, while avoiding overbalance in any part of the deflection range, and retaining sufficient "feel" at low speeds. The danger of overbalance can be minimized by the attainment of a linear variation of control force with $pb/2V$ at high speeds. The nonlinearity of the hinge-moment curves of ailerons designed with internal nose balance prevents the realization of this ideal condition, but aileron profile offers a limited means of controlling the value and the linear range of this control-force gradient. These effects of aileron profile on control-force gradients are due mainly to two causes: the reduction in the amount of nose balance required by the thickened aileron profiles, with the consequent reduction in the nonlinearity of the hinge-moment curves of the balanced ailerons; and the presence of an unfavorable response characteristic (positive $(\partial c_h/\partial \alpha)_{\delta_a}$ at low aileron deflections (where an increase in stick force is desired), with favorable response at high aileron deflections (where a decrease in stick force is desired). This effect of response on control-force gradient is illustrated by figure 17 presenting the variation of $\Delta c_h'$ and $\Delta c_l'$ for the static condition and for the dynamic rolling condition of the assumed pursuit airplane.

The effect of aileron chord on the control-force characteristics can be obtained by a comparison of the 0.20-chord and 0.15-chord ailerons of normal and straight-sided profile. Figure 18 presents the variation of stick force with $pb/2V$ when the 0.15-chord and the 0.20-chord ailerons are each designed for a 30-pound stick force for a $pb/2V$ of 0.08 on the typical pursuit airplane at an indicated airspeed of 300 miles per hour. In all cases the 0.20-chord ailerons produce a more nearly linear variation of stick force with $pb/2V$ than can be acquired with the 0.15-chord aileron.

Lift.—The variation of c_{l_α} with d is shown in figures 7 and 8. These curves indicate that c_{l_α} varied approximately linearly with d, decreasing as d was increased.

FIGURE 15.—The effect of modifications of the aileron profile on the aileron-control characteristics of a typical pursuit airplane equipped with 0.20-chord, sealed gap ailerons with sufficient internal nose balance for a 30-pound high-speed stick force at a $pb/2V$ of 0.08. V_t=300 mph.
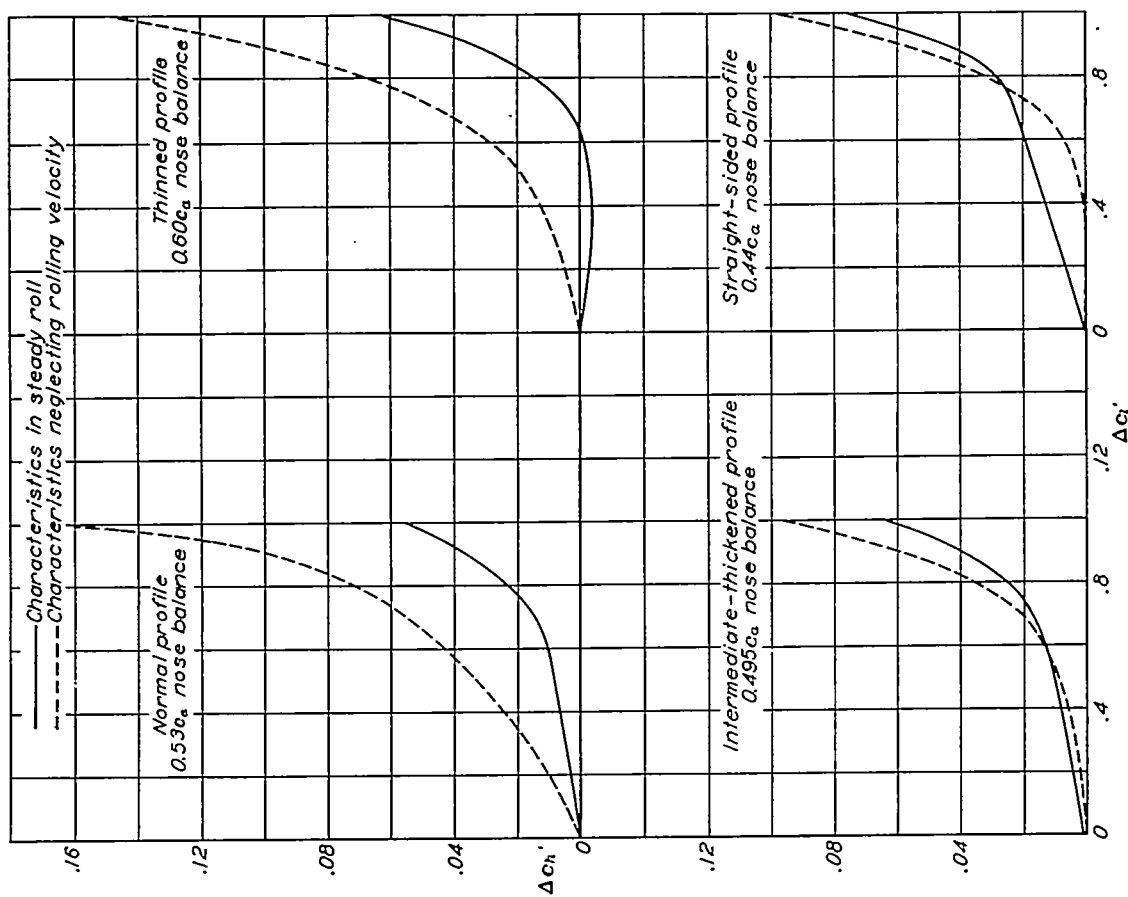

FIGURE 16.—The effect of modifications of the aileron profile on the aileron-control characteristics of a typical pursuit airplane equipped with 0.20-chord, sealed gap ailerons with sufficient internal nose balance for a 30-pound high-speed stick force at a $pb/2V$ of 0.08. V_t=120 mph.

FIGURE 17.—The variation of total hinge moment coefficient with section lift coefficient increment for various 0.20-chord aileron profiles, showing the effect of aileron profile on the response factor (variation of c_a due to rolling). $\alpha_0 = 0.01°$.
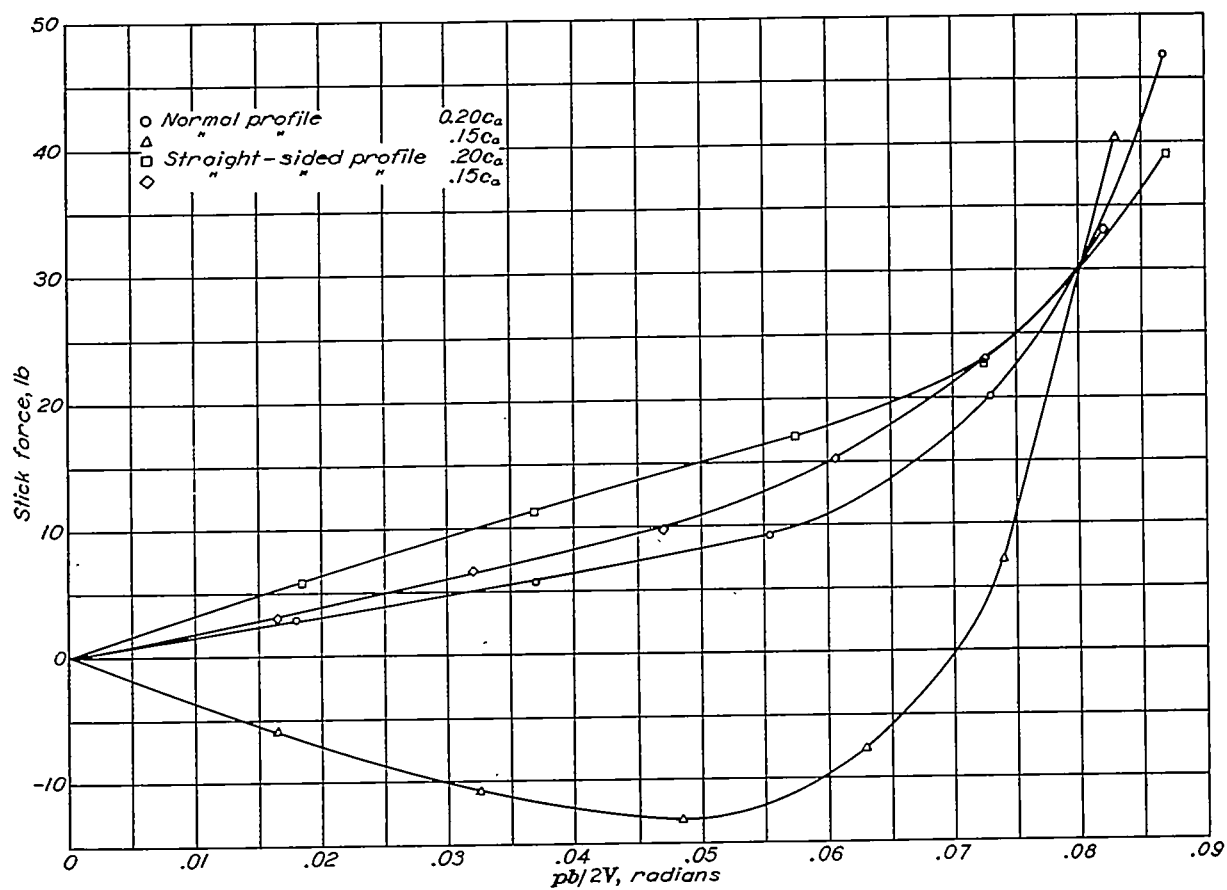
FIGURE 18.—The effect of aileron chord on the aileron-control characteristics of a typical pursuit airplane equipped with sealed gap ailerons with internal nose balance. $V_i = 300$ mph.

Pitching moment.—Thickening the aileron profile caused an increase in $(\partial c_m/\partial c_l)_{\delta_a=0}$ corresponding to a forward shift of the aerodynamic center. This is shown in figures 39 and 40.

Drag.—Figure 41 presents the variation of section profile-drag coefficient with Reynolds number at the ideal section lift coefficient ($c_i=0.21$). Thinning the aileron profile had no effect on the section profile-drag coefficient, but thickening the profile to straight-sided caused an increase in c_{d_0} of 0.0004 for the 0.20-chord aileron and 0.0002 for the 0.15–chord aileron.

Reynolds number.—Examination of figures 31 to 38 reveals that at small angles of attack, increasing Reynolds number resulted in a loss in $\Delta c_l'$, $\Delta c_h'$, and $\Delta P/q$. The magnitude of these effects of increasing Reynolds number is a function of d, increasing as d is increased. (See figs. 7 and 8.) At angles of attack beyond the low-drag range (greater than 2° and less than −1°), the effect of Reynolds number was considerably reduced. Measurements of the airfoil boundary-layer profiles indicated that these Reynolds number effects were caused by a forward movement of the transition point, with the aileron deflected, due to increasing Reynolds number. This forward movement of transition, resulting in a thickening of the boundary layer at the beginning of the pressure recovery, reduces the peak of the basic incremental lift and results in a less complete recovery, thus causing a decrease in effectiveness and $\Delta P/q$.

THICKENED AND BEVELED TRAILING EDGES

Aileron effectiveness.—The effect of the beveled trailing edge on the aileron effectiveness was similar to the effect of thickening the aileron profile. The effect of the bevel was to reduce the aileron effectiveness parameter $(\partial\alpha/\partial\delta_a)_{c_n}$ by about 10 percent.

Beveling the trailing edge had a similar influence on effectiveness at the higher aileron deflections, where the flow over the aileron has separated. Examination of figures 42 to 45 reveals that at an angle of attack of 12° there was only a minor variation in effectiveness due to beveling. The deleterious effects of trailing-edge bevel on aileron effectiveness were a maximum for the 0.20c_a bevel and decreased for both increasing and decreasing bevel lengths.

To determine the effect of beveled trailing edges on the aileron characteristics of typical installations, the data have been applied to the prediction of the aileron control characteristics of the pursuit airplane discussed in connection with profile modifications, and to the prediction of the control characteristics of a medium bomber. The airplane data necessary for the calculations are presented in table IV. The calculated variation of $pb/2V$ with total aileron deflection for the various bevels is presented in figures 19 and 20 for indicated airspeeds of 300 and 120 miles per hour. Examination of these figures reveals that the aileron effectiveness at low speeds was little influenced by aileron trailing-edge profile. Thus, as was the case for the profile modifications, the size and the total aileron deflection for an installation of given effectiveness would be unchanged by beveling of the aileron trailing edge.
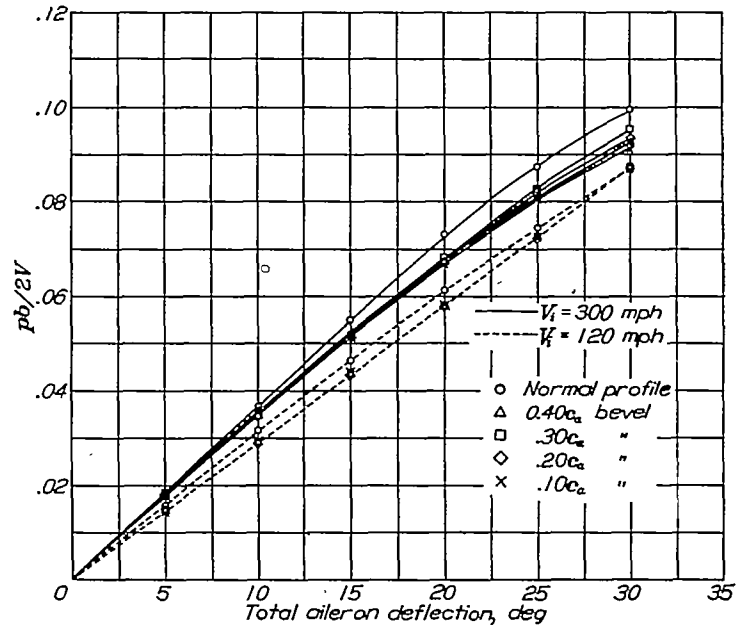
FIGURE 19.—Effect of beveled trailing edges on aileron effectiveness as applied to a typical pursuit airplane; 0.20-chord, sealed gap ailerons; equal up and down aileron deflection; assumed rigid wing and zero sideslip.
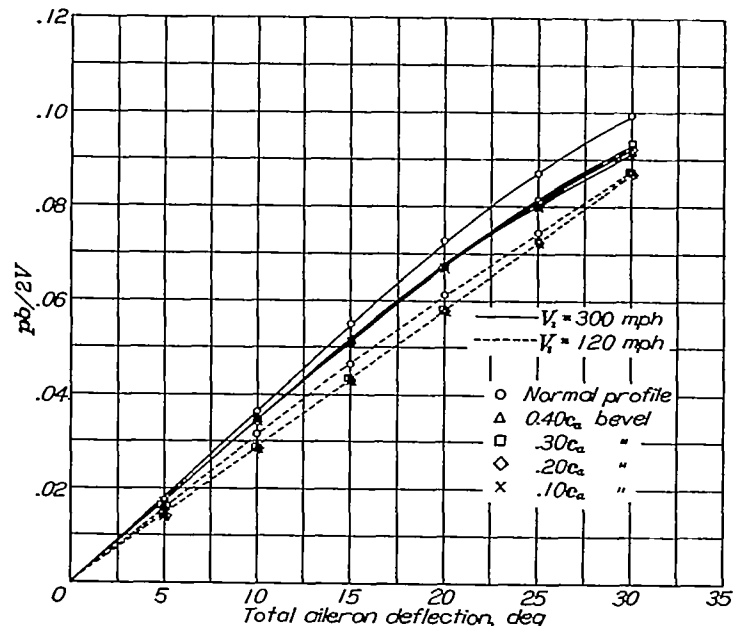
FIGURE 20.—Effect of beveled trailing edges on aileron effectiveness as applied to a typical medium bomber; 0.20-chord, sealed gap ailerons; equal up and down aileron deflection; assumed rigid wing and zero sideslip.

Aileron hinge moments.—As shown by figures 42 to 45, beveling the aileron trailing edge resulted in an algebraic increase in $c_{h_{\delta_a}}$. However, at large angles of attack, the effects of the bevel tend to disappear. Comparative curves of Δc_h against δ_a for the various bevel lengths are shown in figure 21. The balancing effect of the bevel increased with reduction in bevel length to an optimum value with the 0.20c_a bevel. For the shorter bevel, the balancing effect was lessened.

Unlike the thickened and thinned aileron profiles, the presence of the beveled trailing edge had a large effect on the angular range of linear hinge-moment characteristics. At $\alpha_0=0$, this range was reduced from 16° of total aileron deflection for the normal-profile aileron to 8° of total aileron
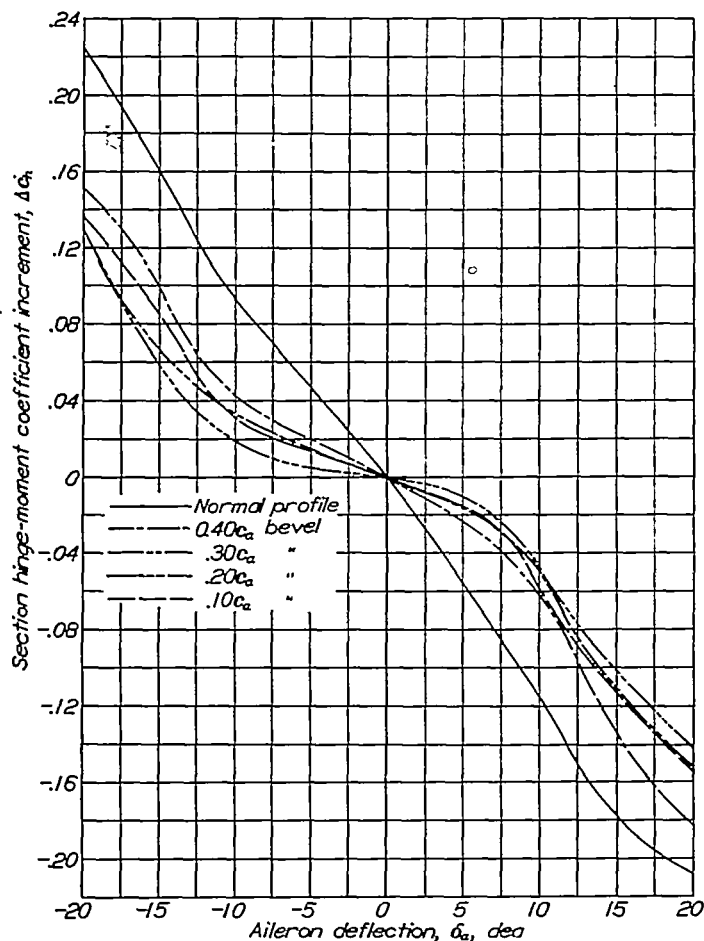
FIGURE 21.—Effect of beveled trailing edges on Δc_h against δ_a for 0.20-chord, sealed gap, plain ailerons on an NACA 66, 2-216 ($a=0.6$) airfoil at zero angle of attack. $R=9,000,000$.

deflection for the $0.20c_a$ bevel. This linear range was a minimum for the $0.20c_a$ bevel, and increased for both increasing and decreasing bevel lengths.

As in the case of the thickened and thinned profiles, the value of $(\partial c_h/\partial\alpha)_{\delta_a}$ varied with both angle of attack and aileron deflection. At small angles of attack and small aileron deflections, the beveled trailing edge caused a large algebraic increase in $(\partial c_h/\partial\alpha)_{\delta_a}$ (from -0.0049 for the normal-profile aileron to 0.010 for the $0.20c_a$ bevel). A positive value of $(\partial c_h/\partial\alpha)_{\delta_a}$ will induce an unfavorable response and will tend to increase the effective dihedral and the damping in roll, stick free. As the aileron angle was increased, $(\partial c_h/\partial\alpha)_{\delta_a}$ became negative (i. e., the response became favorable) for the beveled profiles at the aileron deflections at which separation occurred over the ailerons. At angles of attack greater than $6°$, $(\partial c_h/\partial\alpha)_{\delta_a=0}$ had a constant value of -0.010 irrespective of aileron profile.

To determine the effect of nose seal on the beveled trailing-edge profiles, tests at five angles of attack were made on the $0.20c_a$ beveled profile with a 0.25-inch (0.0052c) nose gap. The data obtained are shown in figure 46. In addition to the loss in effectiveness usually associated with this condition, the nose gap decreased the hinge moments at low aileron deflections and further decreased the angular range of linear-hinge-moment characteristics. Because of the decreased effectiveness, the unsealed beveled aileron is inferior

to the sealed beveled aileron as a means of reducing control forces.

The data for the beveled trailing-edge ailerons have been plotted in figure 11, together with the data for the thickened and thinned profiles, as hinge-moment parameters against lift parameters to show the relative dependence of the aileron hinge moments on the aileron effectiveness and on the slope of the wing section lift curve. The small deviation of the experimental points from the mean curves indicates that the relationships indicated are not influenced by the chordwise distribution of thickness of the control-surface profile. An experimental point is also presented from data obtained on an NACA 0009 airfoil (reference 4) which indicates that for the same effectiveness, similar hinge moments may be anticipated for ailerons on an NACA 66,2–216 ($a=0.6$) airfoil as are experienced on ailerons on an NACA 0009 airfoil. A similar agreement between the subject data and the NACA 0009 data did not exist for c_{h_α} against c_{l_α}.

The effect of the beveled trailing edge on $\Delta P/q$ was small and similar to the effect of thickening the aileron profile.

Aileron control forces.—Figures 22 to 25 illustrate the changes in control-force characteristics which result from a beveled trailing edge. The airplane data necessary for these calculations are presented in table IV. For the pursuit airplane, the ailerons were selected with $0.40c_a$ aerodynamic nose balance, and for the medium bomber no nose balance was used. At a $pb/2V$ of 0.08 at high speed, the $0.30c_a$ bevel caused a 70-pound reduction in stick force for the pursuit airplane and an 80-pound reduction in wheel force for the medium bomber. At low speeds the percent reduction in control force due to the bevel was less. This was caused by the previously mentioned reduction in bevel effect on hinge moments at large angles of attack. The effect of the trailing-edge bevel on the angular range of linear control characteristics is further emphasized by figures 22 and 24. While the variation of control force with $pb/2V$ was linear for the airplane equipped with normal-profile ailerons to a $pb/2V$ of 0.07, the linear range with the aileron with a $0.20c_a$ bevel (sealed) extended only to a $pb/2V$ of 0.035. The removal of the nose seal on the $0.20c_a$ bevel aileron further reduced this range to a $pb/2V$ of 0.02.

Figures 26 to 29 present the variation of control force with $pb/2V$ when each aileron had an assumed nose balance such that a $pb/2V$ of 0.08 could be attained with a stick force of 30 pounds at 300 miles per hour on the pursuit airplane and a wheel force of 80 pounds at 250 miles per hour on the medium bomber.

For the pursuit airplane under consideration, the $0.40c_a$, $0.20c_a$, and $0.10c_a$ beveled trailing-edge ailerons were overbalanced for moderate values of $pb/2V$ at $V_i=300$ miles per hour. This overbalance is a result of the reduced linear range of hinge-moment coefficient against aileron deflection due to the beveled trailing edge and the reduced effectiveness of the beveled profiles. Another contributing factor to the overbalance is the fact that the addition of the bevel caused a larger reduction in $\Delta P/q$ at large aileron deflection than it did at small aileron deflection. This difference increases the effectiveness of the internal balance at the aileron deflections corresponding to low rates of roll and thus
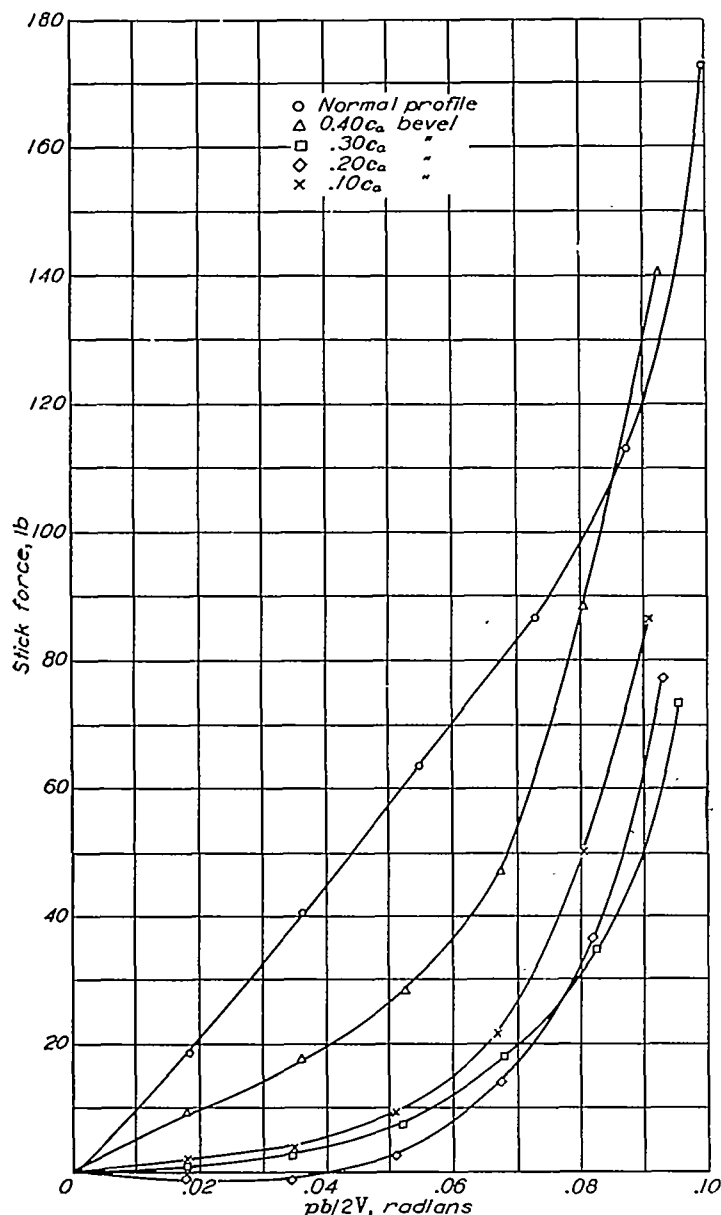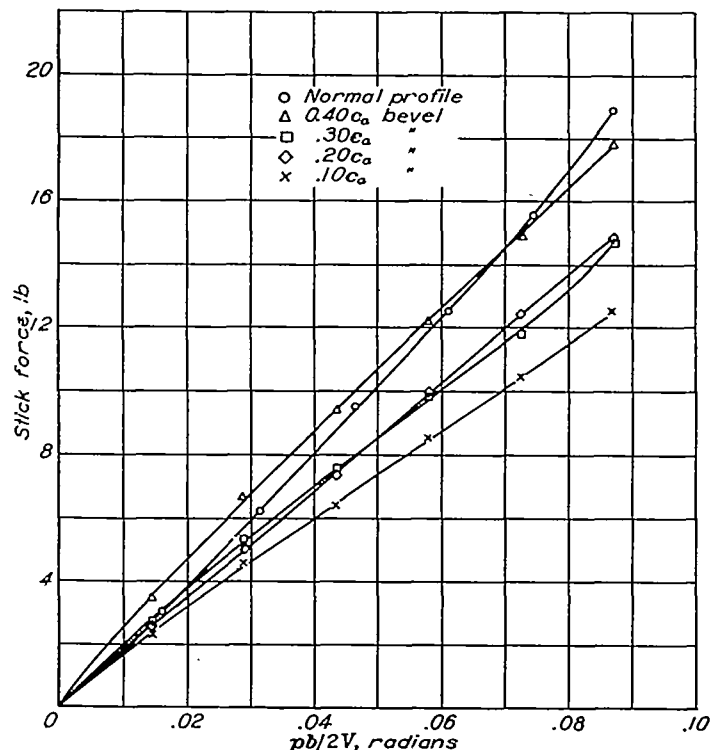
FIGURE 22.—Effect of beveled trailing edges on the aileron-control characteristics of a typical pursuit airplane equipped with 0.20-chord, sealed gap ailerons with 0.40c$_a$ internal nose balance at an indicated airspeed of 300 mph.
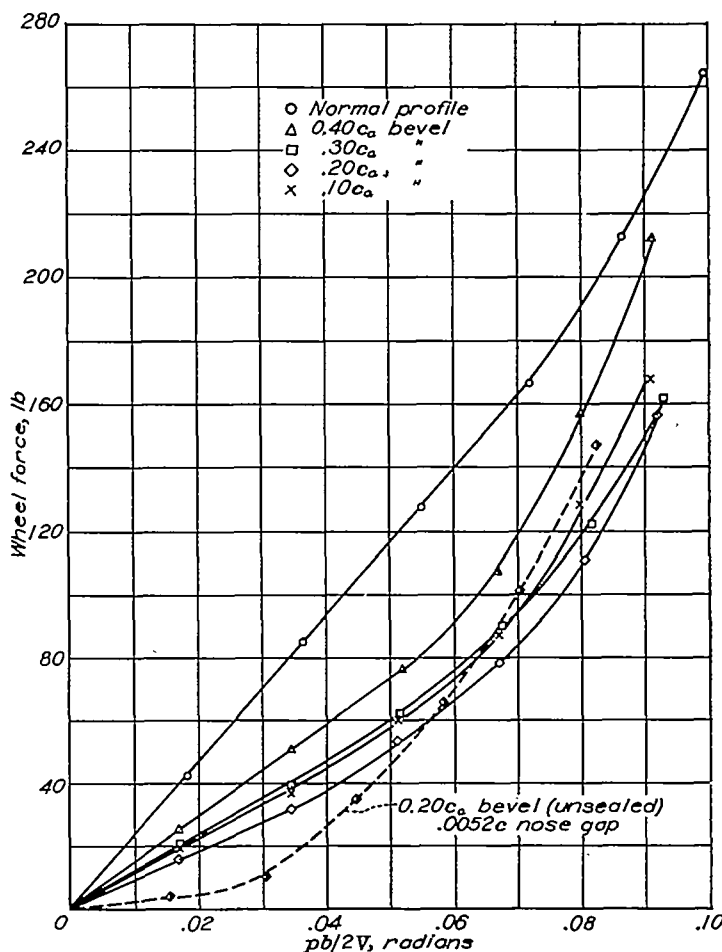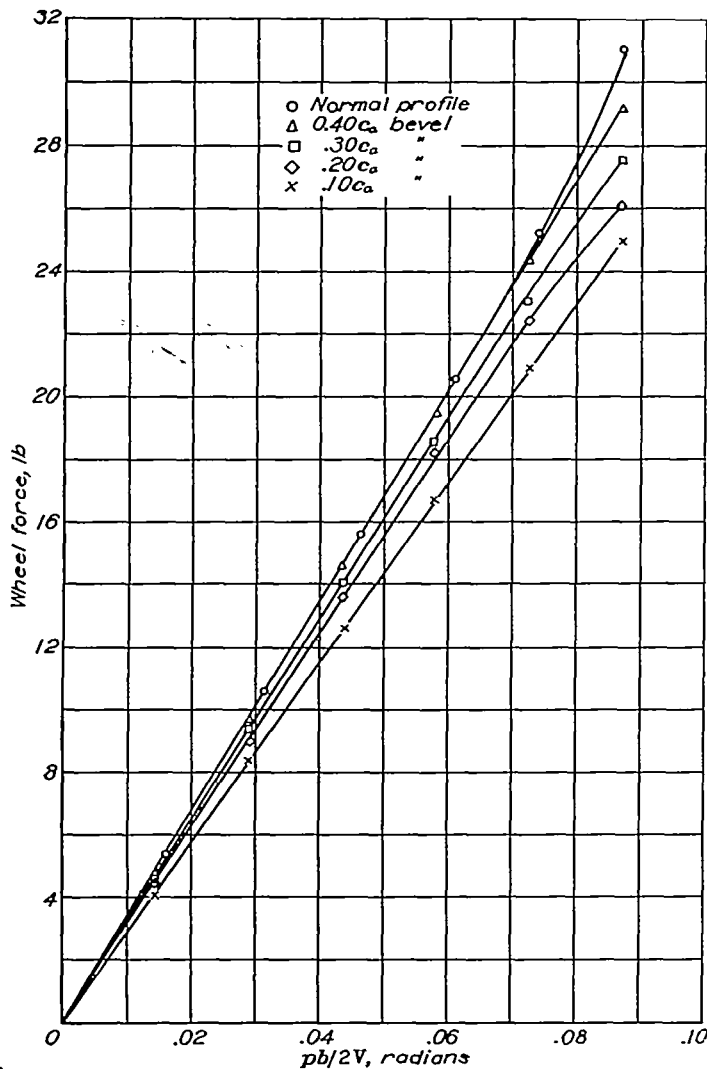

FIGURE 23.—Effect of beveled trailing edges on the aileron-control characteristics of a typical pursuit airplane equipped with 0.20-chord, sealed gap ailerons with 0.40c$_a$ internal nose balance at an indicated airspeed of 120 mph.

FIGURE 24.—Effect of beveled trailing edges on the aileron-control characteristics of a medium bomber equipped with 0.20-chord, sealed gap ailerons with no nose balance at an indicated airspeed of 250 mph.

contributes to the overbalance. These deleterious effects are partially compensated for by the reduced balance required with the beveled profiles and the presence of an unfavorable response at low aileron deflections and a favorable response at high aileron deflections, both factors tending to increase the linearity of stick force against $pb/2V$. While the ailerons with $0.30c_a$ bevel were not overbalanced, the variation of stick force with $pb/2V$ was not as nearly linear as was the gradient attainable with the normal-profile aileron.

When applied to the medium bomber, the bevel had an equally large effect on the wheel-force gradient and the nose balance required for a high-speed wheel force of 80 pounds for a $pb/2V$ of 0.08. When designed for this condition, the required nose balance varied from $0.455c_a$ for the normal-profile aileron to $0.296c_a$ for the aileron with $0.30c_a$ bevel. The effect on high-speed wheel-force gradient was such that the control force necessary to attain a $pb/2V$ of 0.06 varied

FIGURE 25.—Effect of beveled trailing edges on the aileron-control characteristics of a medium bomber equipped with 0.20-chord, sealed gap ailerons with no nose balance at an indicated airspeed of 100 mph.

from 54 pounds for the normal profile to 25 pounds for the $0.40c_a$ bevel profile. At low speeds the control force was increased due to the presence of the bevel. This effect is due to the reduced nose balance required of the beveled contours.

Lift.—Thickening and beveling the aileron trailing-edge profile caused a decrease in c_{l_α}. This is shown in figure 47. The effect was maximum for the 0.20 c_a bevel and decreased for both increasing and decreasing bevel lengths.

Pitching-moment.—Beveling the aileron trailing edge caused an increase in $(\partial c_m/\partial c_l)_{\delta_a=0}$ corresponding to a forward shift of the aerodynamic center. This is shown in figure 47.

Drag.—Figure 48 presents the variation of section profile drag coefficient with Reynolds number at the ideal lift coefficient ($c_l=0.21$). The presence of the aileron bevel caused an increase in c_{d_0} of 0.0001.

Reynolds number.—Examination of figures 42 to 45 and measurement of the airfoil boundary-layer profiles indicated that Reynolds number had an effect on the beveled aileron profiles similar to the effect noted for the thickened profiles. The result was a loss in $\Delta c_l'$, $\Delta c_h'$, and $\Delta P/q$. The magnitude

of these effects was a maximum for the 0.20 c_a bevel and decreased for both increasing and decreasing bevel lengths.

TABS

Basic section data for 0.20-aileron-chord tabs on 0.20-chord ailerons are presented in figures 49 to 56 for the normal profile aileron and in figures 57 to 64 for the straight-sided profile aileron. While the basic data are useful for purposes of design, the comparison of the effects of tabs may be more conveniently demonstrated by means of the section parameters. These parameters as obtained from the basic data are summarized in table V.

TABLE V.—SECTION PARAMETERS OF THE NACA 66,2–216 ($a=0.6$) AIRFOIL EQUIPPED WITH $0.20c$ PLAIN SEALED AILERONS AND $0.20c_a$ PLAIN UNSEALED TABS

Parameter	Reynolds number	Normal profile	Straight-sided profile
$\partial\alpha/\partial\delta_a$		−0.4055	−0.377
$(\partial c_f/\partial\alpha)_{\delta_a=\delta_t=0}$	8,200,000	.1053	.0905
$(\partial c_f/\partial\delta_a)_{\alpha_e=\delta_t=0}$	9,000,000	.0427	.0375
$(\partial c_f/\partial\delta_t)_{\alpha_e=\delta_a=0}$	9,000,000	.0105	.0085
$(\partial c_h/\partial\alpha)_{\delta_a=\delta_t=0}$	8,200,000	−.0048	.0017
$(\partial c_h/\partial\delta_a)_{\alpha_e=\delta_t=0}$	9,000,000	−.0090	−.0050
$(\partial c_h/\partial\delta_t)_{\alpha_e=\delta_a=0}$	9,000,000	−.0085	−.0075
$(\partial c_{h_t}/\partial\alpha)_{\delta_a=\delta_t=0}$	8,200,000	−.0028	−.0024
$(\partial c_{h_t}/\partial\delta_a)_{\alpha_e=\delta_t=0}$	9,000,000	−.0044	.0010
$(\partial c_{h_t}/\partial\delta_t)_{\alpha_e=\delta_a=0}$	9,000,000	−.0074	−.0039
$[\partial(\Delta P/q)/\partial\alpha]_{\delta_a=\delta_t=0}$	8,200,000	.009	.009
$[\partial(\Delta P/q)/\partial\delta_a]_{\alpha_e=\delta_t=0}$	9,000,000	.06	.06
$[\partial(\Delta P/q)/\partial\delta_t]_{\alpha_e=\delta_a=0}$	9,000,000	.0055	.003

Tab effectiveness.—The effectiveness of a tab as a means of reducing aileron hinge moments is measured by the parameter $\partial c_h/\partial\delta_t$ and by the ratio of this parameter to the parameter $\partial c_h/\partial\delta_a$. As shown by table V the value of $\partial c_h/\partial\delta_t$ is −0.0085 for the normal-profile aileron and −0.0075 for the straight-sided aileron. These values are comparable to values obtained for similar control surfaces on an NACA 0009 airfoil (reference 4). The value of the ratio $\dfrac{\partial c_h/\partial\delta_t}{\partial c_h/\partial\delta_a}$ is 0.89 for the normal-profile aileron as compared to 1.5 for the straight-sided aileron. This indicates that the tab on the straight-sided plain aileron is approximately 68 percent more effective than the tab on the normal-profile plain aileron. As might be expected, the tab on the normal-profile aileron remained effective to larger deflections than did the tab on the straight-sided aileron. It should be noted that previous results (reference 5) have indicated tabs to be more efficient with the tab gaps sealed; however, the effect of seals was not included in the present investigation.

Tab hinge moments.—The value of the tab hinge-moment parameter $\partial c_{h_t}/\partial\delta_t$ as shown in table V is −0.0074 for the tab on the normal-profile aileron as compared to −0.0039 for the tab on the straight-sided aileron. These values are of approximately the same ratio as the ratio of the aileron hinge-moment parameters $\partial c_h/\partial\delta_a$.

Applications of tabs.—It has been shown in reference 1 that fixed tabs in conjunction with a differential linkage offer a means for reducing aileron-operating forces. Such tabs do not appreciably influence the aileron effectiveness.

The results of reference 2 have indicated that the use of ailerons with simple or spring-linked balancing tabs would
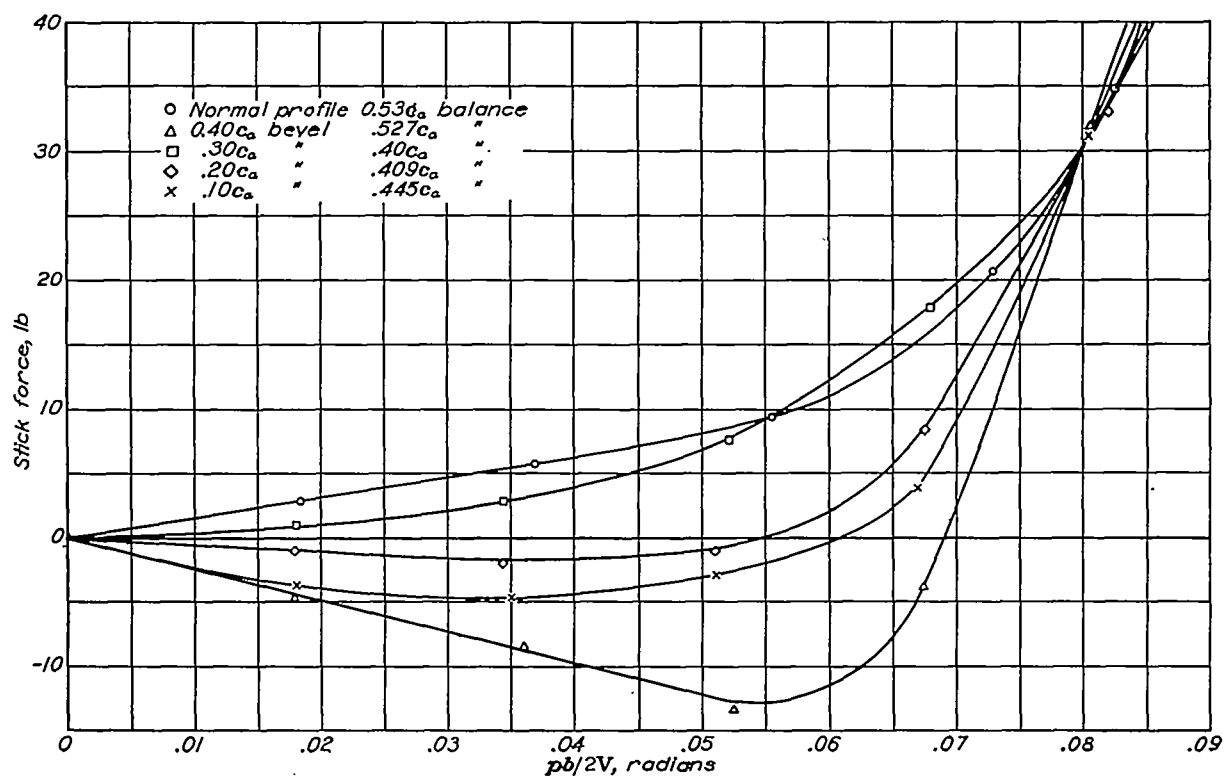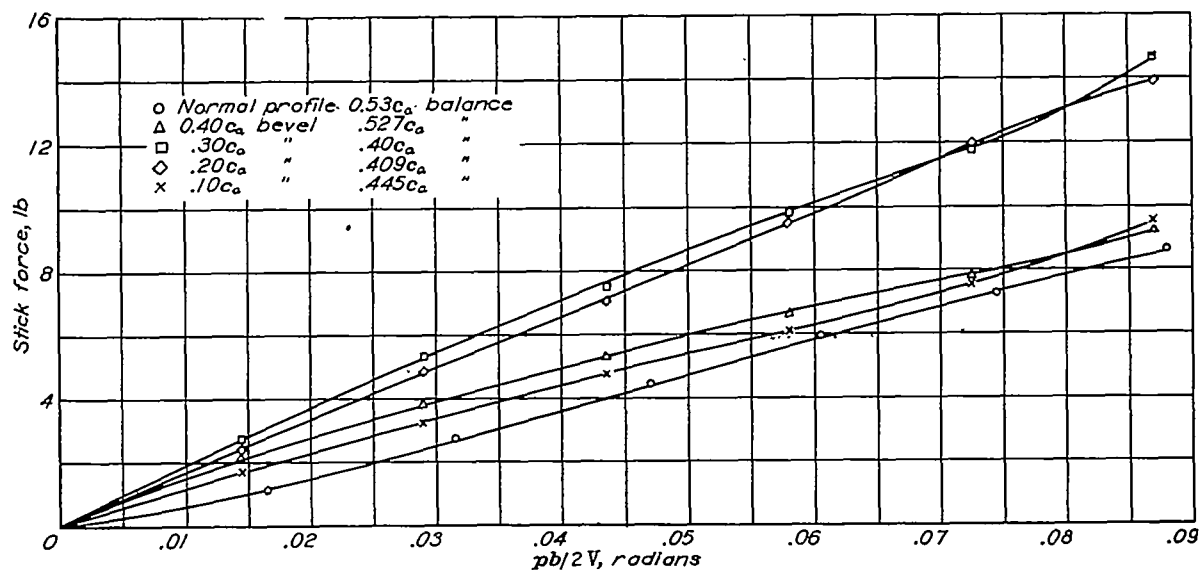
FIGURE 26.—Effect of beveled trailing edges on the aileron-control characteristics of a typical pursuit airplane equipped with 0.20-chord, sealed gap ailerons with sufficient internal nose balance for a 30-pound high-speed stick force at a $pb/2V$ of 0.08. V_r=300 mph.
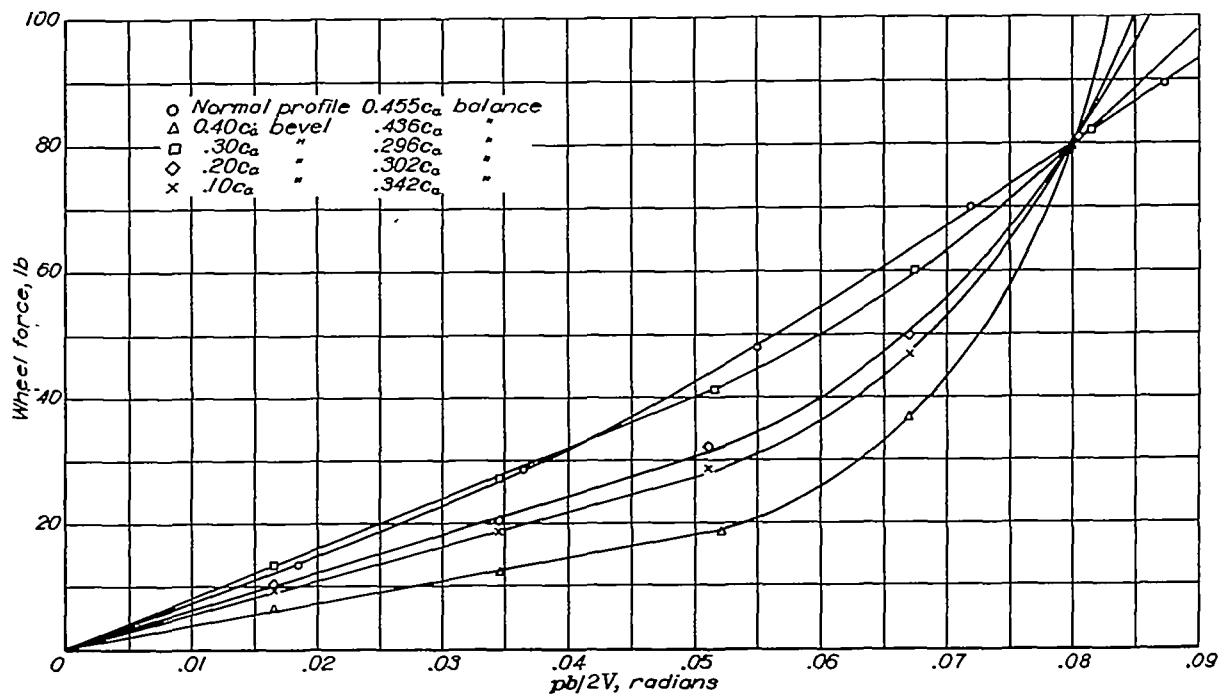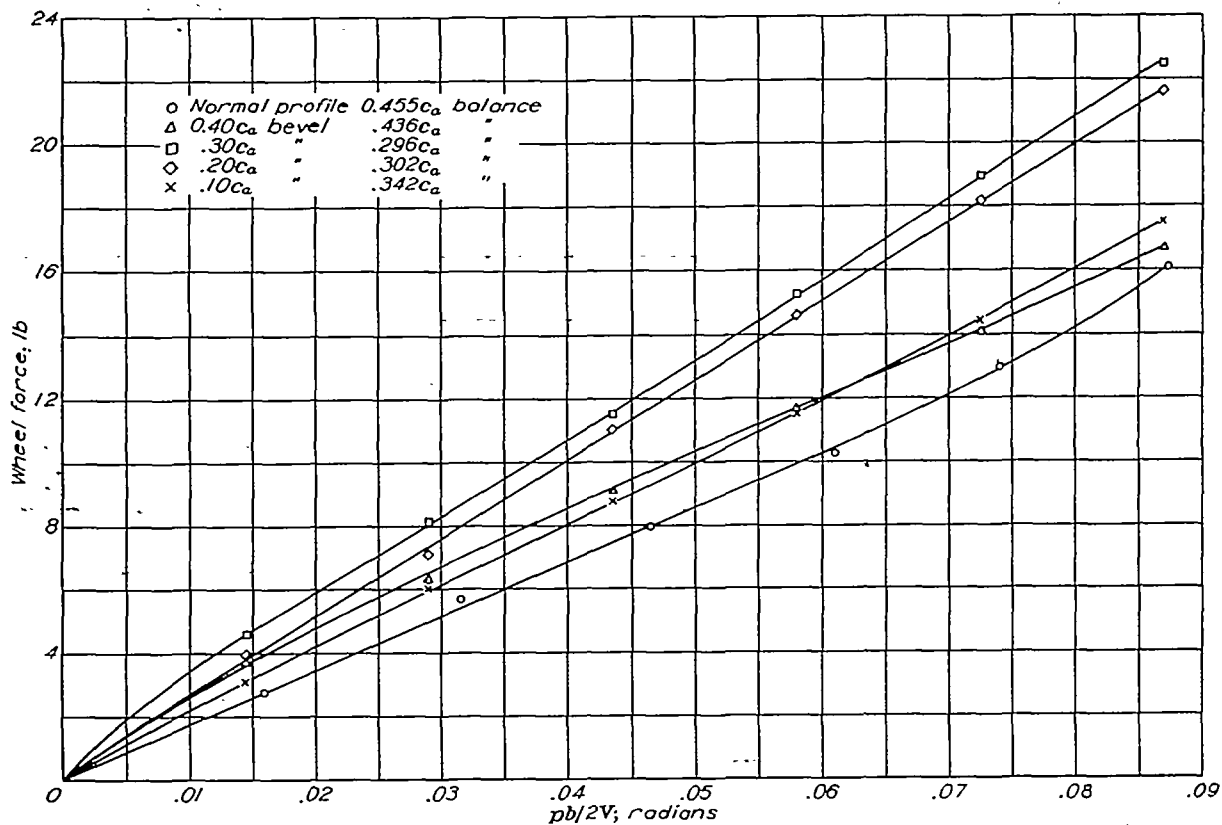

FIGURE 27.—Effect of beveled trailing edges on the aileron-control characteristics of a typical pursuit airplane equipped with 0.20-chord, sealed gap ailerons with sufficient internal nose balance for a 30-pound high-speed stick force at a $pb/2V$ of 0.08. V_r= 120 mph.

FIGURE 28.—Effect of beveled trailing edges on the aileron-control characteristics of a typical medium bomber equipped with 0.20-chord, sealed gap ailerons with sufficient internal nose balance for an 80-pound high-speed wheel force at a $pb/2V$ of 0.08. V_i= 250 mph.

FIGURE 29.—Effect of beveled trailing edges on the aileron-control characteristics of a typical medium bomber equipped with 0.20-chord, sealed gap ailerons with sufficient internal nose balance for an 80-pound high-speed wheel force at a $pb/2V$ of 0.08. V_i=100 mph.
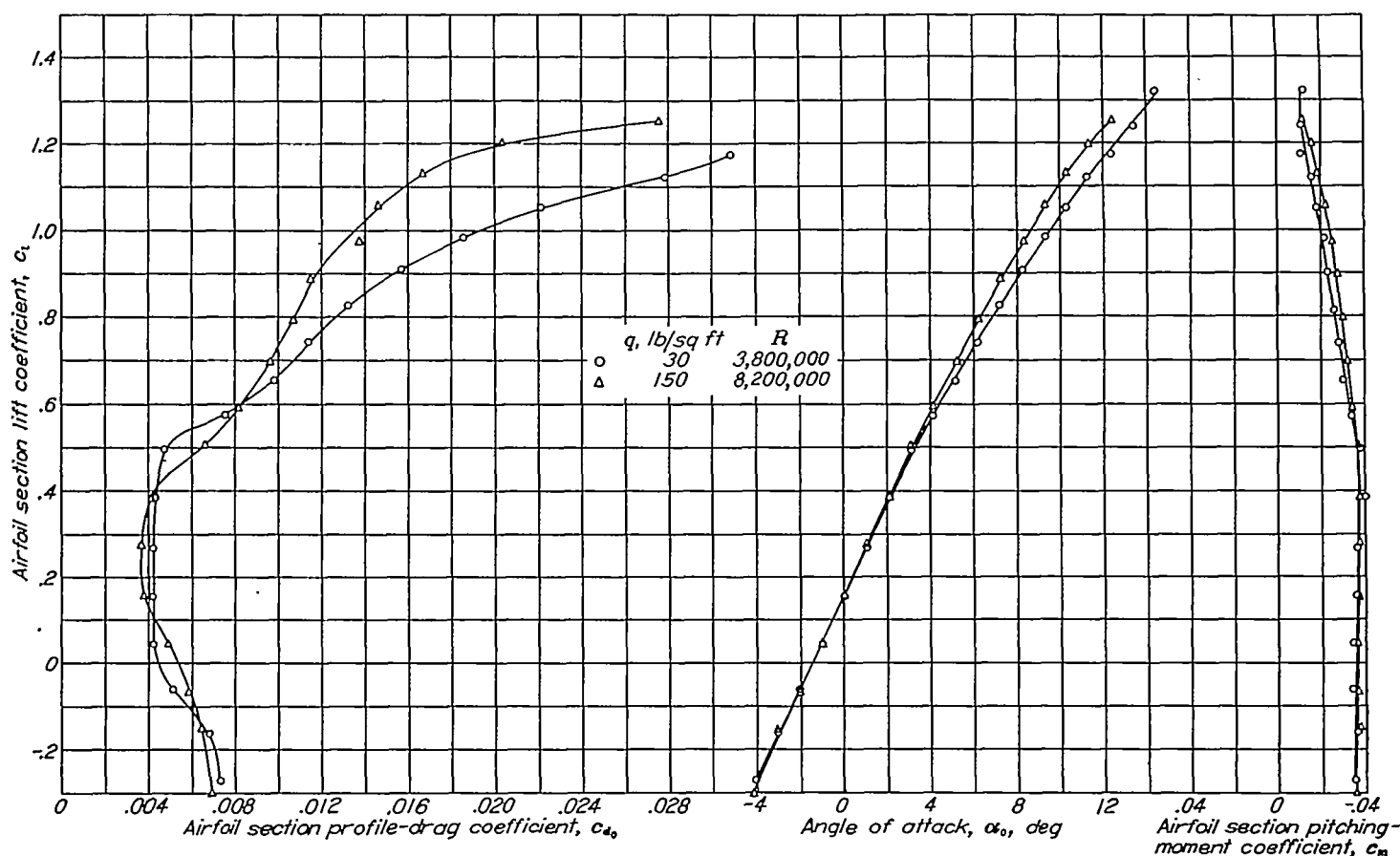
FIGURE 30.—Section aerodynamic characteristics of an NACA 66, 2-216 (a=0.6) airfoil.

reduce the high-speed control forces to considerably less than those experienced in the use of plain-sealed ailerons if the systems were designed for low maximum deflections. However, because the over-all effectiveness is less for an aileron and simple balancing-tab combination than for a plain aileron, the chord, the span, or the maximum deflection must be greater for the aileron-tab combination than for the plain aileron to produce a given maximum rate of roll.

The use of spring-linked tabs designed to give desirable force characteristics at large rates of roll at high speed would reduce the variation of control force with speed and would also cause an increase in rolling effectiveness for a given control deflection as the speed was reduced, relative to plain ailerons or ailerons with simple balancing tabs.

The basic tab data contained in figures 49 to 64 are sufficient for the application of tabs on a low-drag airfoil to any of the foregoing types of installations.

CONCLUSIONS

Results of tests of various aileron profile modifications and tabs on the characteristics of ailerons on the NACA 66, 2-216 (a=0.6) airfoil indicate the following conclusions:

1. Aileron profile offers a convenient means of adjusting the high-speed control force and the control-force gradients for conventional ailerons on a low-drag wing. Thickening the profile, which decreases the aileron hinge moments, also decreases the aileron effectiveness. Thinning the profile has the opposite effect. These effects of profile diminish as the angle of attack is increased, there being practically no effect at an angle of attack of 12°.

2. The necessity of fabricating aileron profiles to close tolerances is illustrated in that deviations of the order of ±0.005 aileron chord from the specified profile on the ailerons of a typical pursuit airplane can cause stick-force variations of ±20 pounds for a large rate of roll at an indicated airspeed of 300 miles per hour.

3. Of the aileron profile modifications included in this investigation, the aileron with the straight-sided profile displayed the most desirable force characteristics. The variation of high-speed control force with rate of roll was most nearly linear for this profile, thus minimizing the danger of aileron overbalance in high-speed flight. The ease of fabrication of a straight-sided profile is especially desirable when application is to be made to a low-drag airfoil with its characteristic cusped profile. The application of tabs to the straight-sided aileron offers no difficulties, the tab effectiveness being of the same order of magnitude as for the normal-profile installation. The increase in minimum section profile-drag coefficient caused by departure from the optimum cusped profile is only of the order of 10 percent.

No consideration has been given in this report to the effects of compressibility. Tests have indicated that Mach number effects can be minimized by maintaining the trailing-edge angle of the control surface at as small an angle as possible. It is thus possible that at very high Mach numbers the normal-profile aileron may be superior to the aileron of straight-sided profile.

AMES AERONAUTICAL LABORATORY,
    NATIONAL ADVISORY COMMITTEE FOR AERONAUTICS,
    MOFFETT FIELD, CALIF.

APPENDIX

The method of determining the thickened and beveled profiles is outlined below:

1. At the chordwise station defining the bevel, a perpendicular was erected.

2. With the intersection of the mean line of the normal profile and the perpendicular as a center, a circle was constructed.

3. The radius of the circle r was such that the intersection of lines drawn from the hinge center of the aileron and the trailing edge of the aileron intersected on the perpendicular at 10° at a distance r from the mean line.

4. With these intersections defining their centers two circles of radius r were constructed and tangent lines drawn from these circles to the trailing-edge radius.

5. The forward profile was a free fairing for $0.40c_a$ at which point normal profile was regained.

6. The intersection of this fairing and the bevel was slightly rounded but no attempt was made to fix this radius of curvature.

This method of construction was favored because it was assumed that the action of the bevel was similar to that of a balancing tab and it was desired to maintain every variable constant except the length of the bevel. The aileron profile forward of the bevel was faired into the normal profile to eliminate the abrupt change in profile at the hinge line which would result if straight-sided surfaces were used.

Construction of beveled trailing edge ailerons.
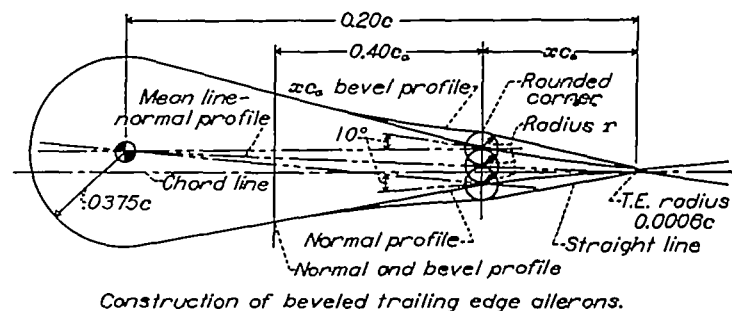
REFERENCES

1. Soulé, H. A., and Hootman, James A.: A Flight Investigation of the Reduction of Aileron Operating Force by Means of Fixed Tabs and Differential Linkage, with Notes on Linkage Design. NACA TN No. 653, 1938.

2. Rogallo, F. M., and Purser, Paul E: Wind-Tunnel Investigation of a Plain Aileron with Various Trailing-Edge Modification on a Tapered Wing. III–Ailerons with Simple and Spring-Linked Balancing Tabs. NACA ARR, Jan. 1943.

3. Morgan, M. B., Morris, D. E., and Bethwaite, C. F.: Flight Tests of Spring Tab Ailerons on a Spitfire. R. & M. No. 2029, British A. R. C., 1942.

4. Ames, Milton B., Jr., and Sears, Richard I.; Determination of Control-Surface Characteristics from NACA Plain-Flap and Tab Data. NACA Rep. No. 721, 1941.

5. Imlay, Frederick H., and Bird, J. D.: Wind-Tunnel Tests of Hinge-Moment Characteristics of Spring-Tab Ailerons. NACA ARR No. 4A26, 1944.

(a) $R=9,000,000.$

(b) $R=3,800,000.$
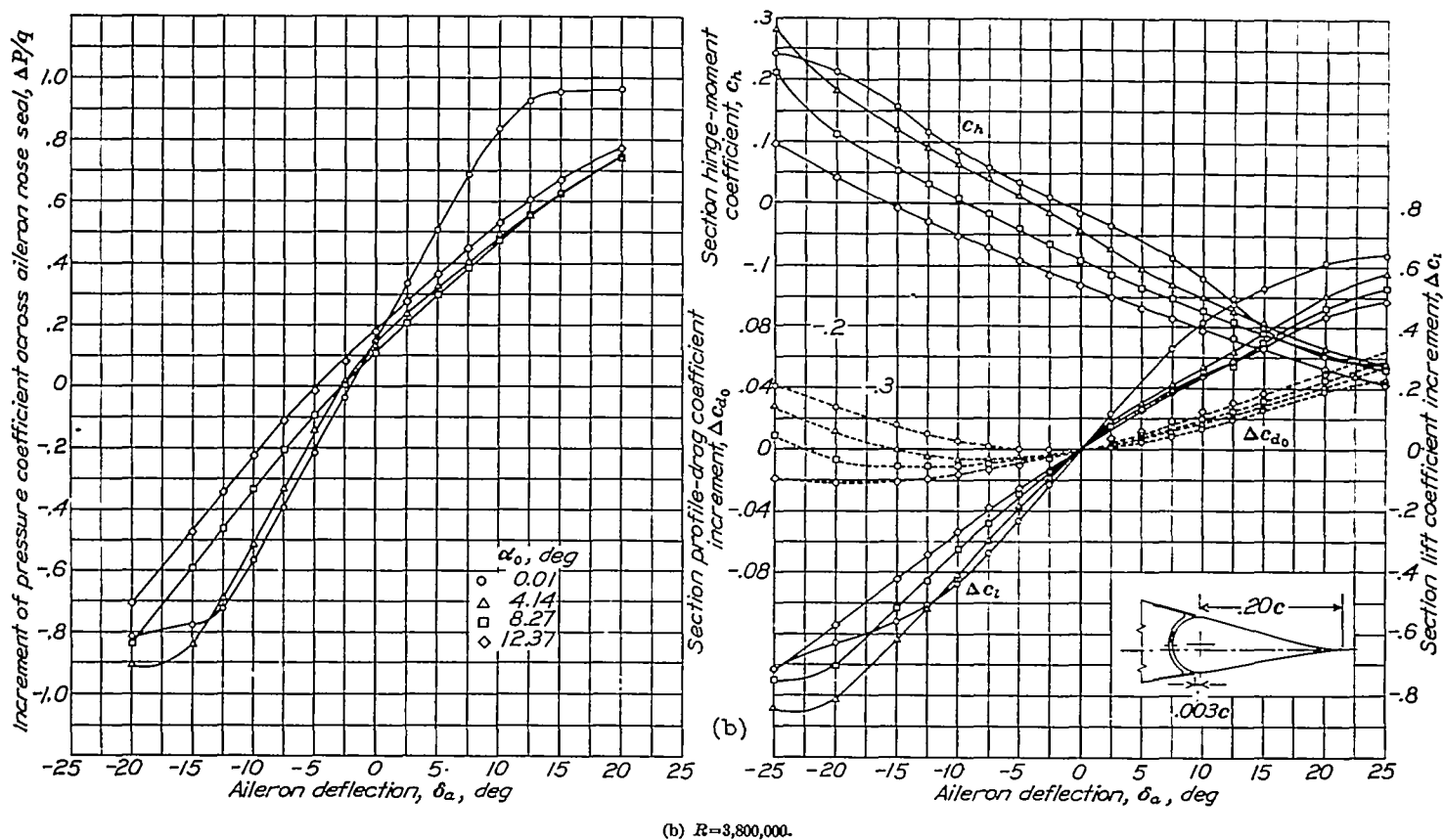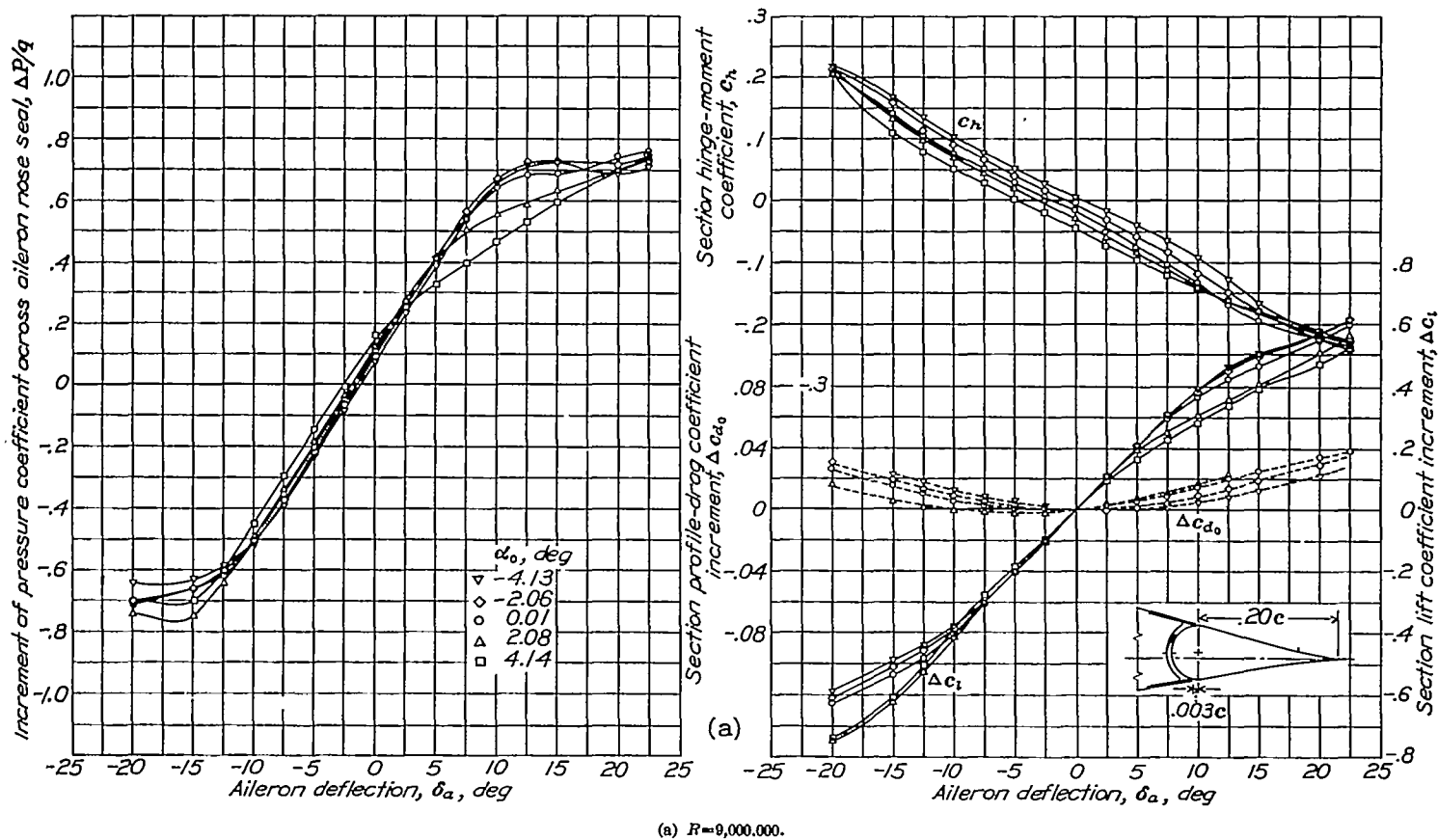
FIGURE 31.—Section aerodynamic characteristics of an NACA 66, 2–216 ($a=0.6$) airfoil equpped with a 0.20-chord. sealed gap, plain aileron of normal profile.
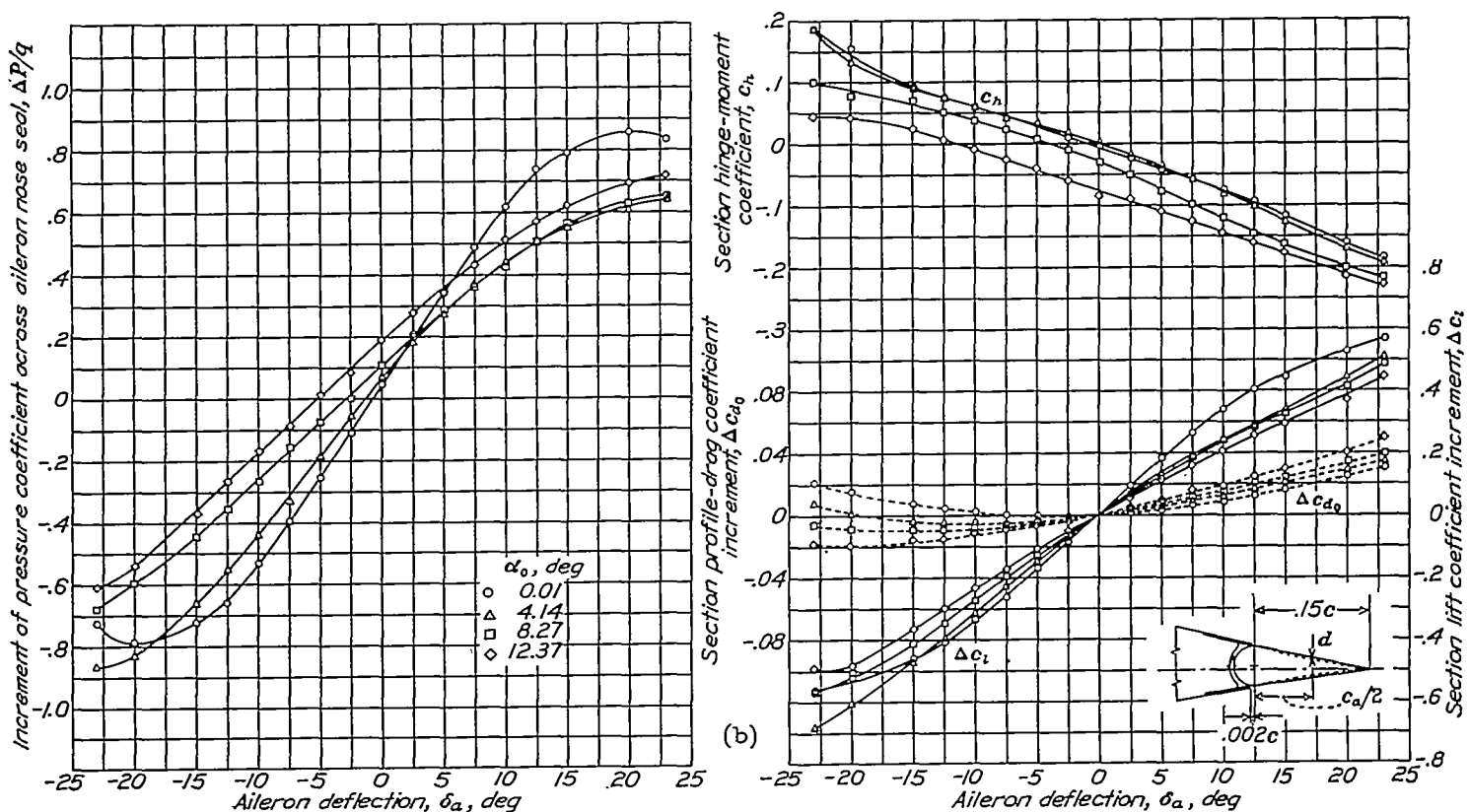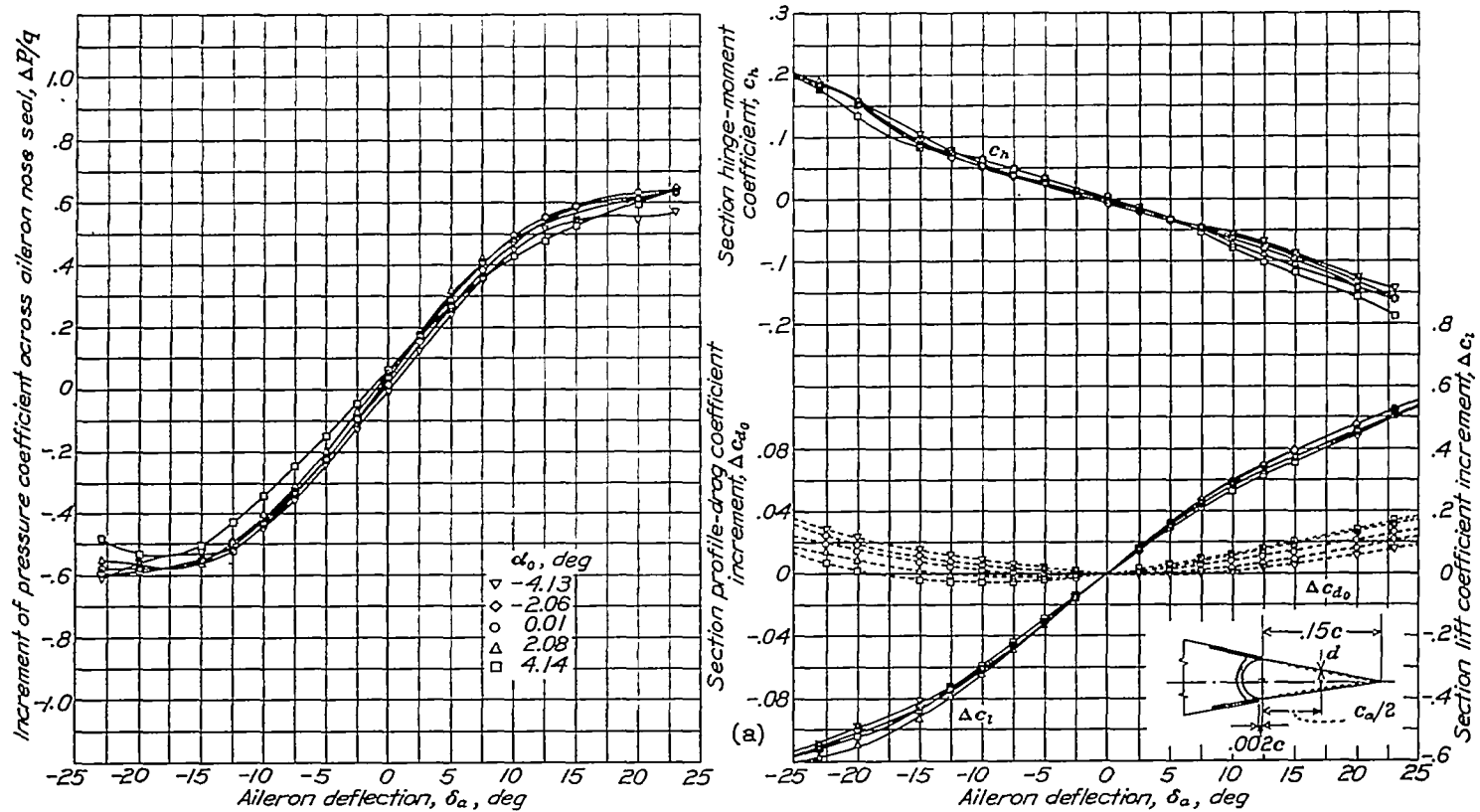
(a) $R=9,000,000$
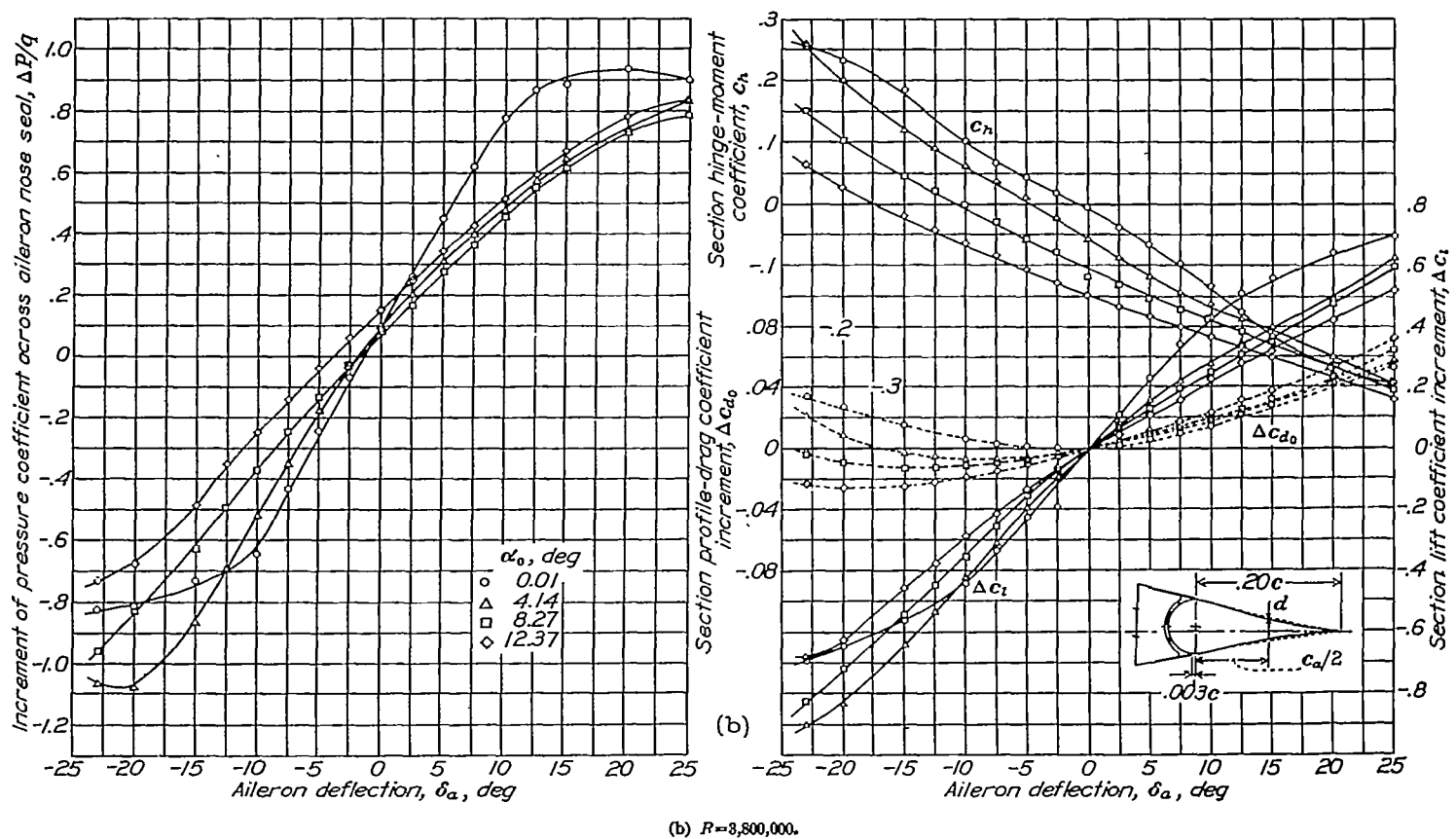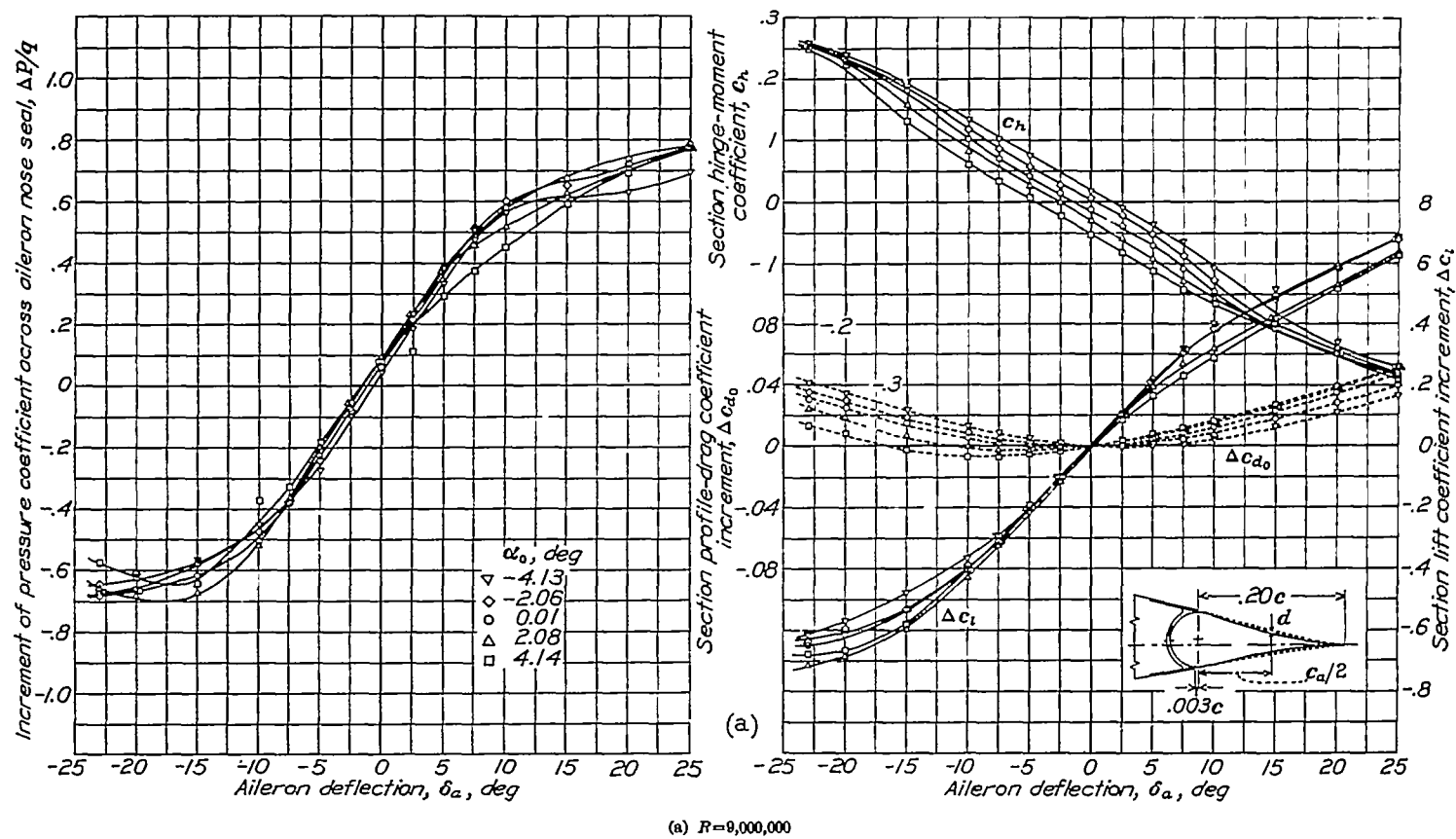
(b) $R=3,800,000$.

FIGURE 32.—Section aerodynamic characteristics of an NACA 66, 2-216 ($a=0.6$) airfoil equipped with a 0.20-chord, sealed gap, plain aileron of thinned profile. $d=-0.009c_a$.
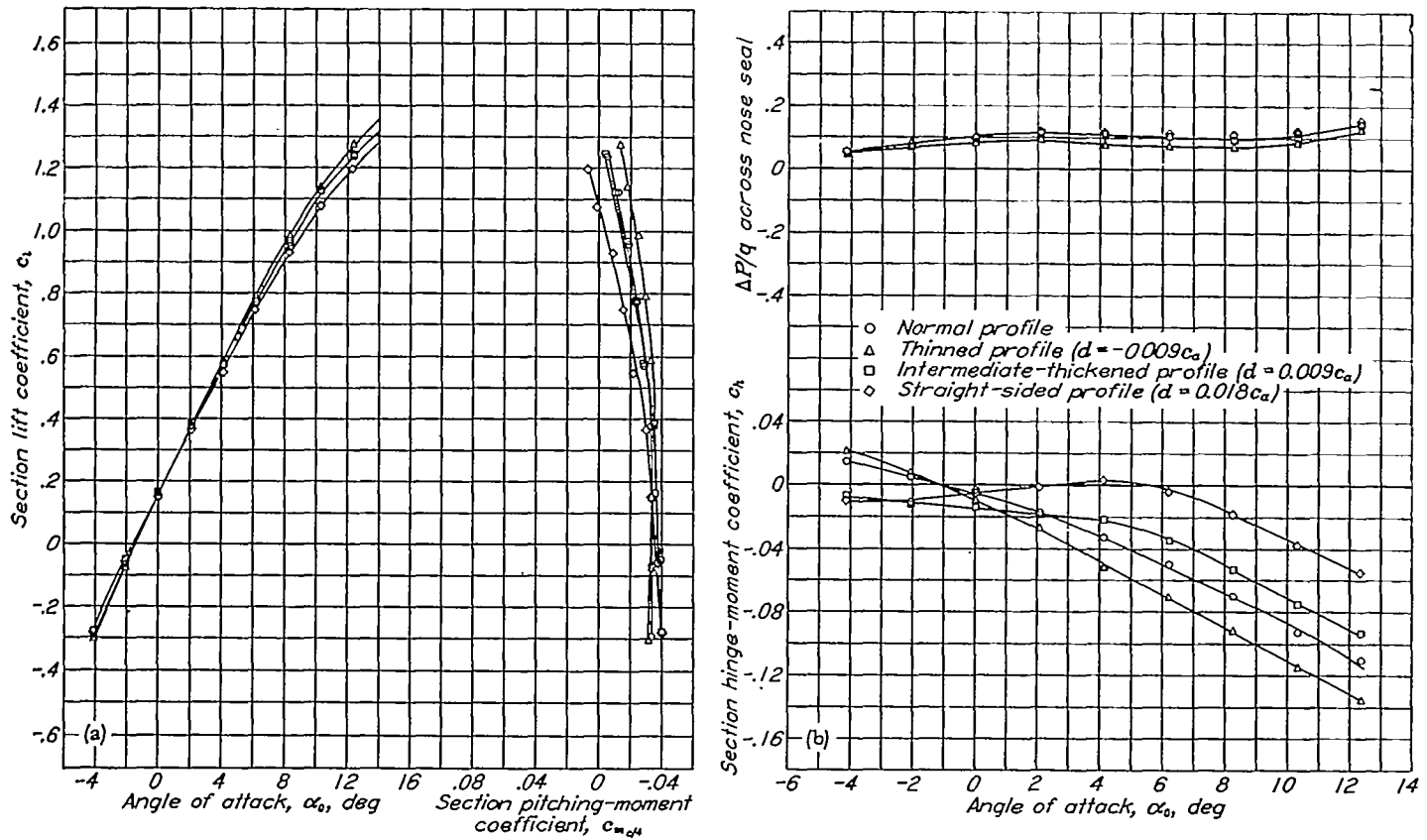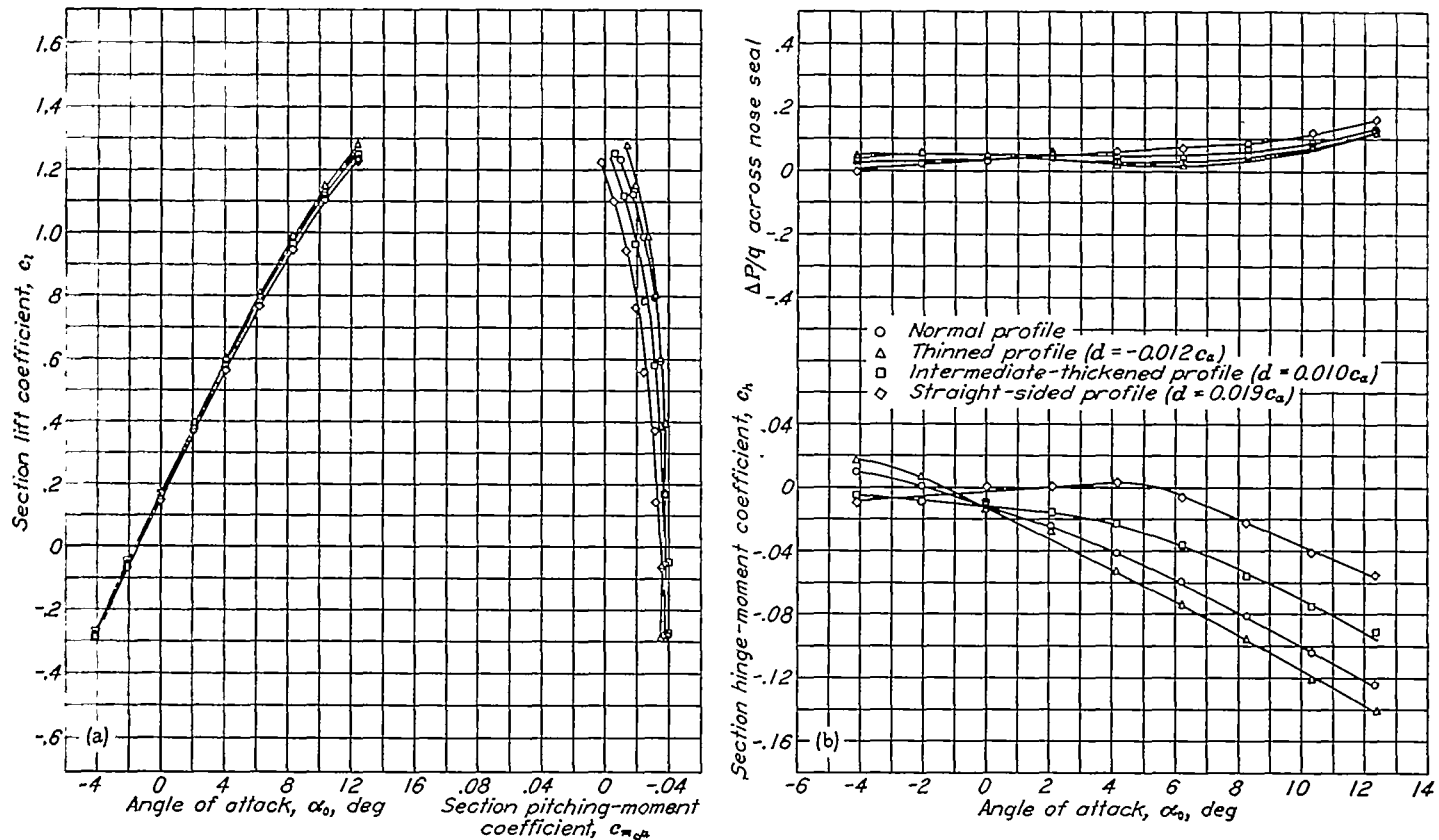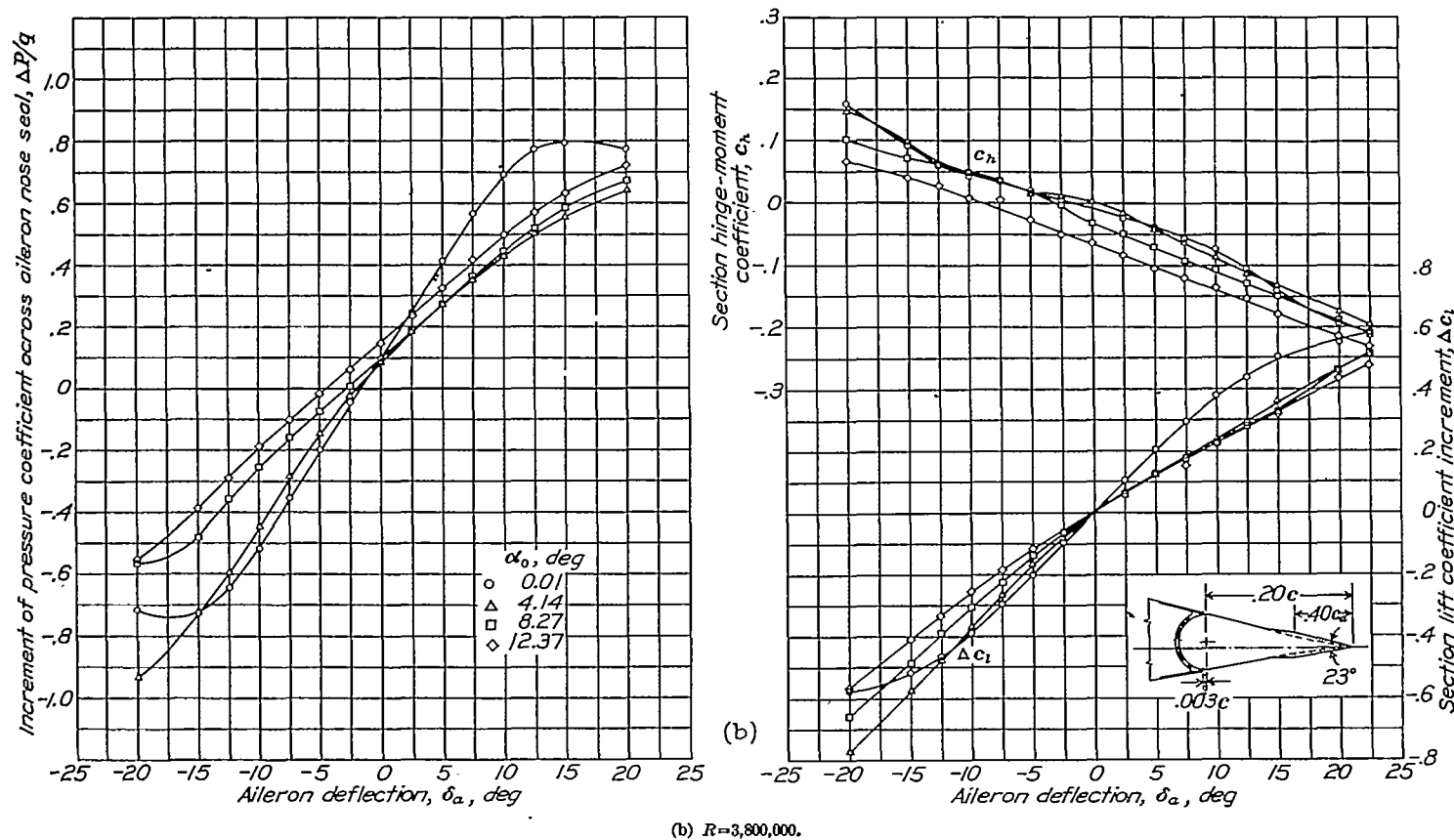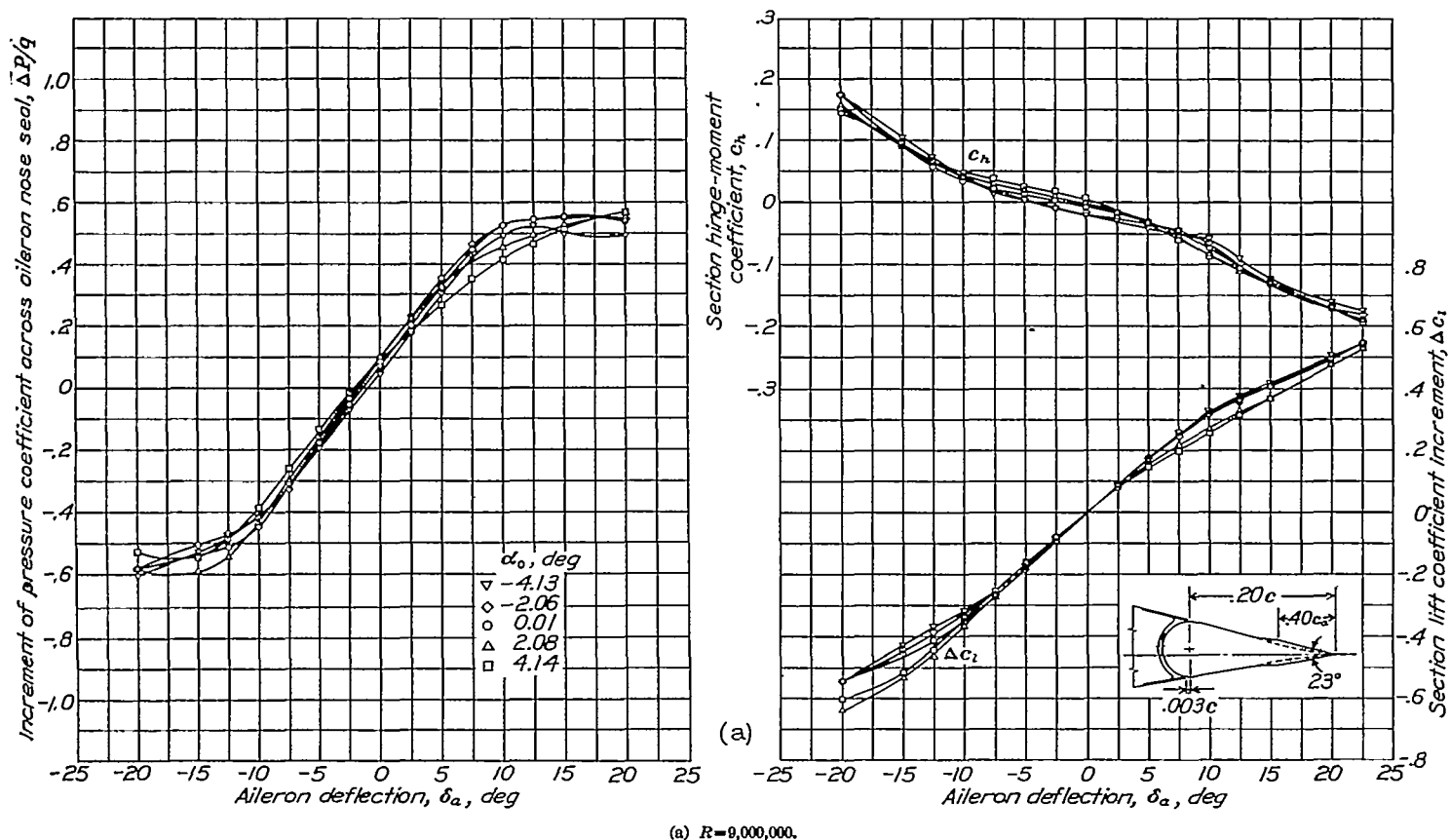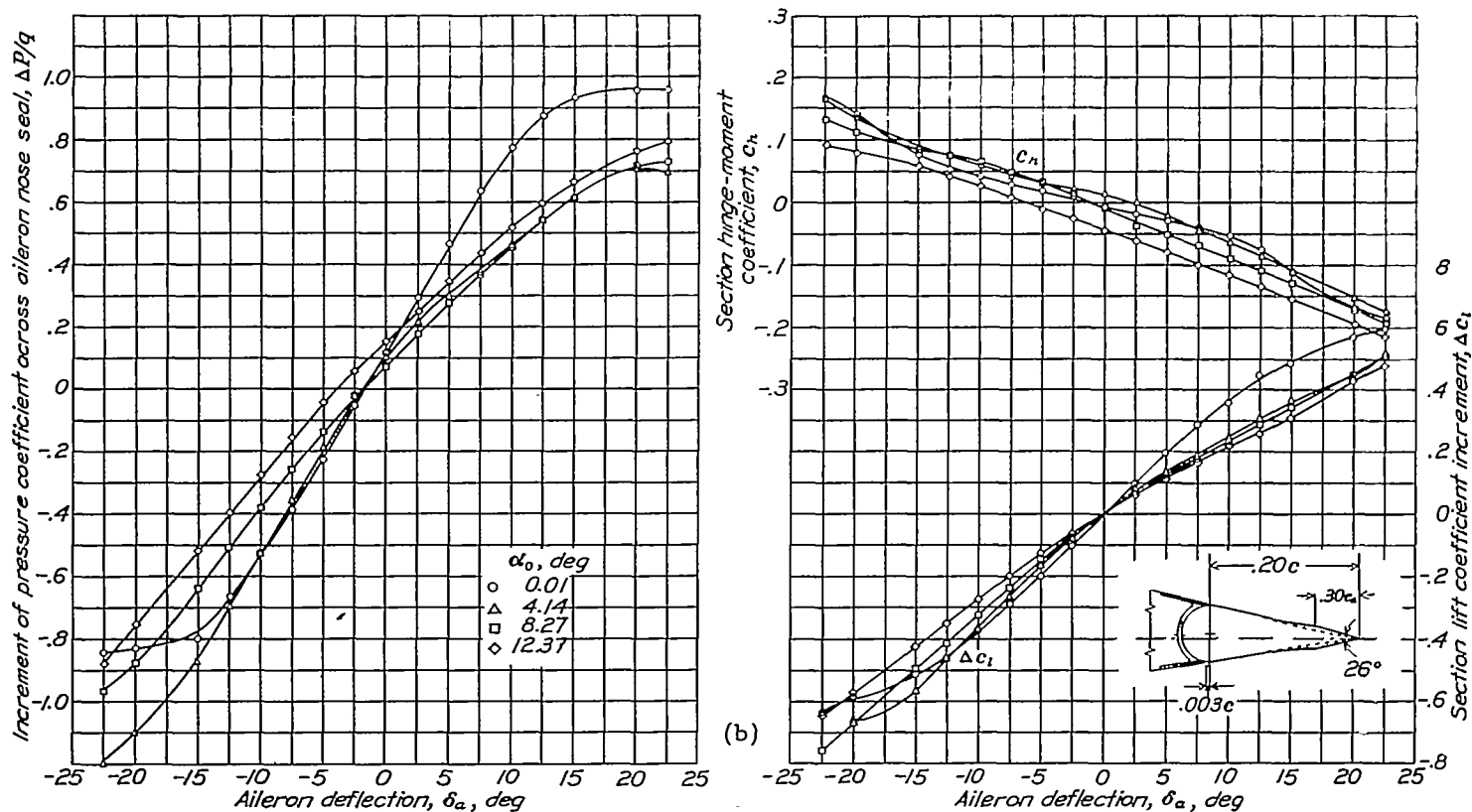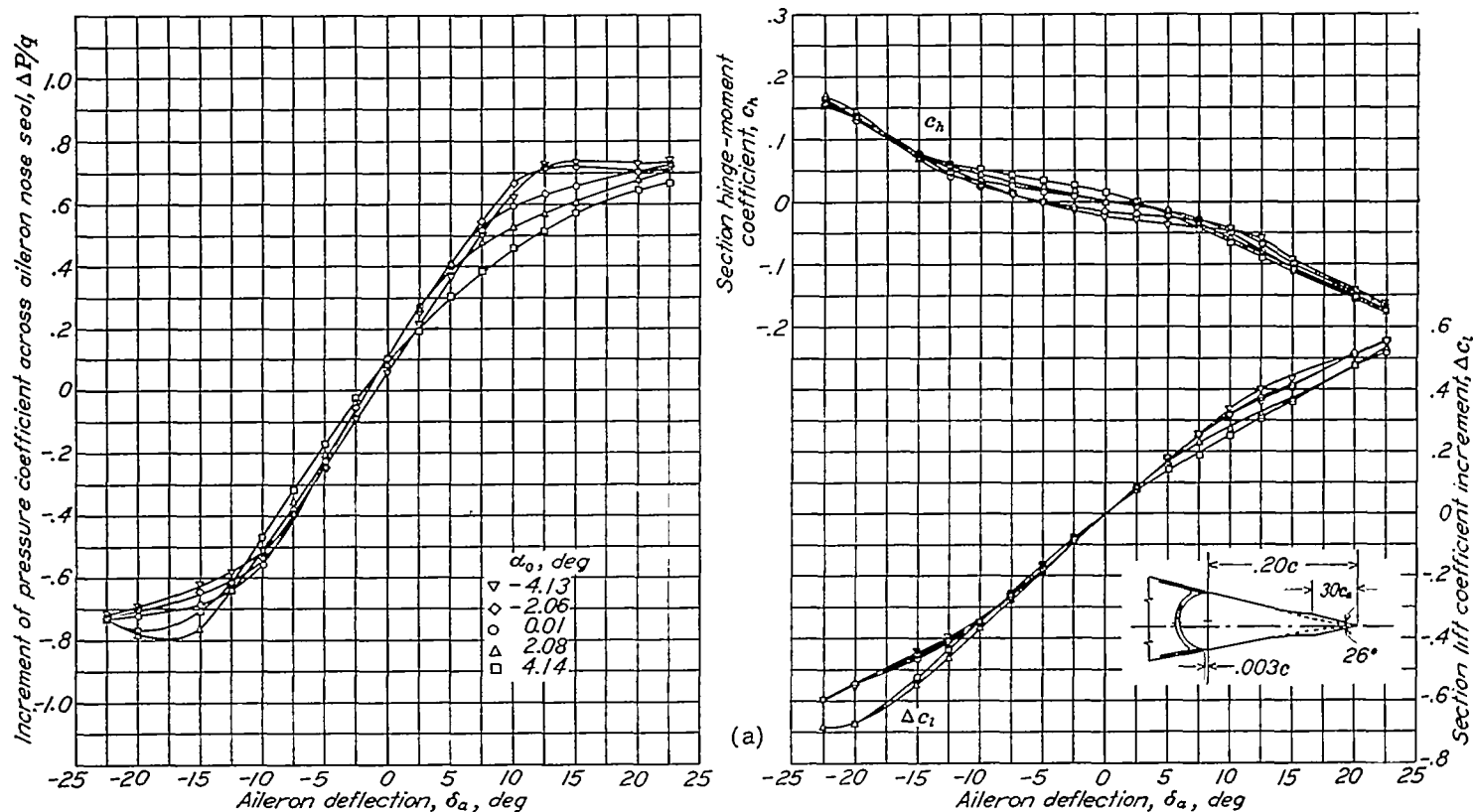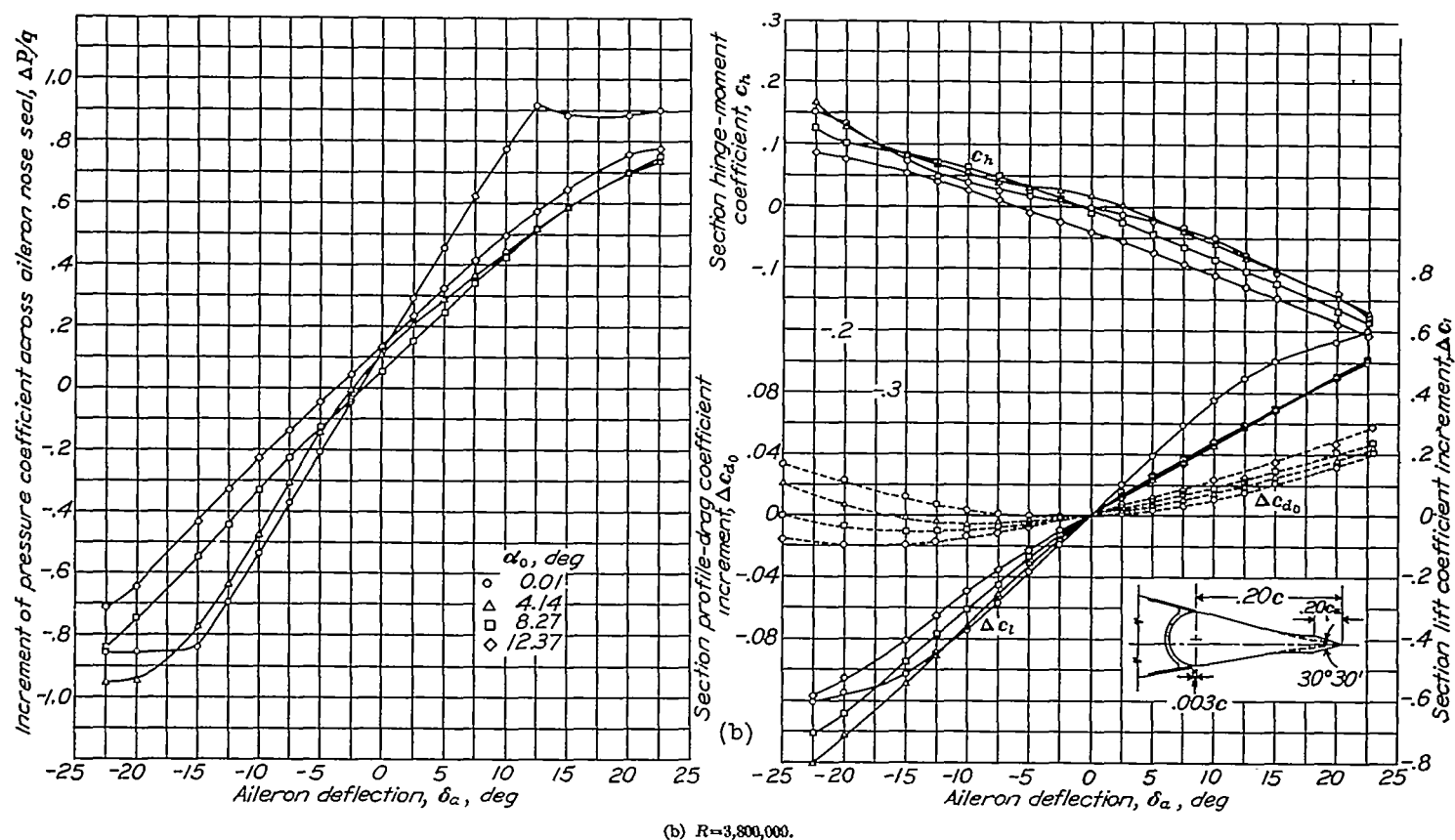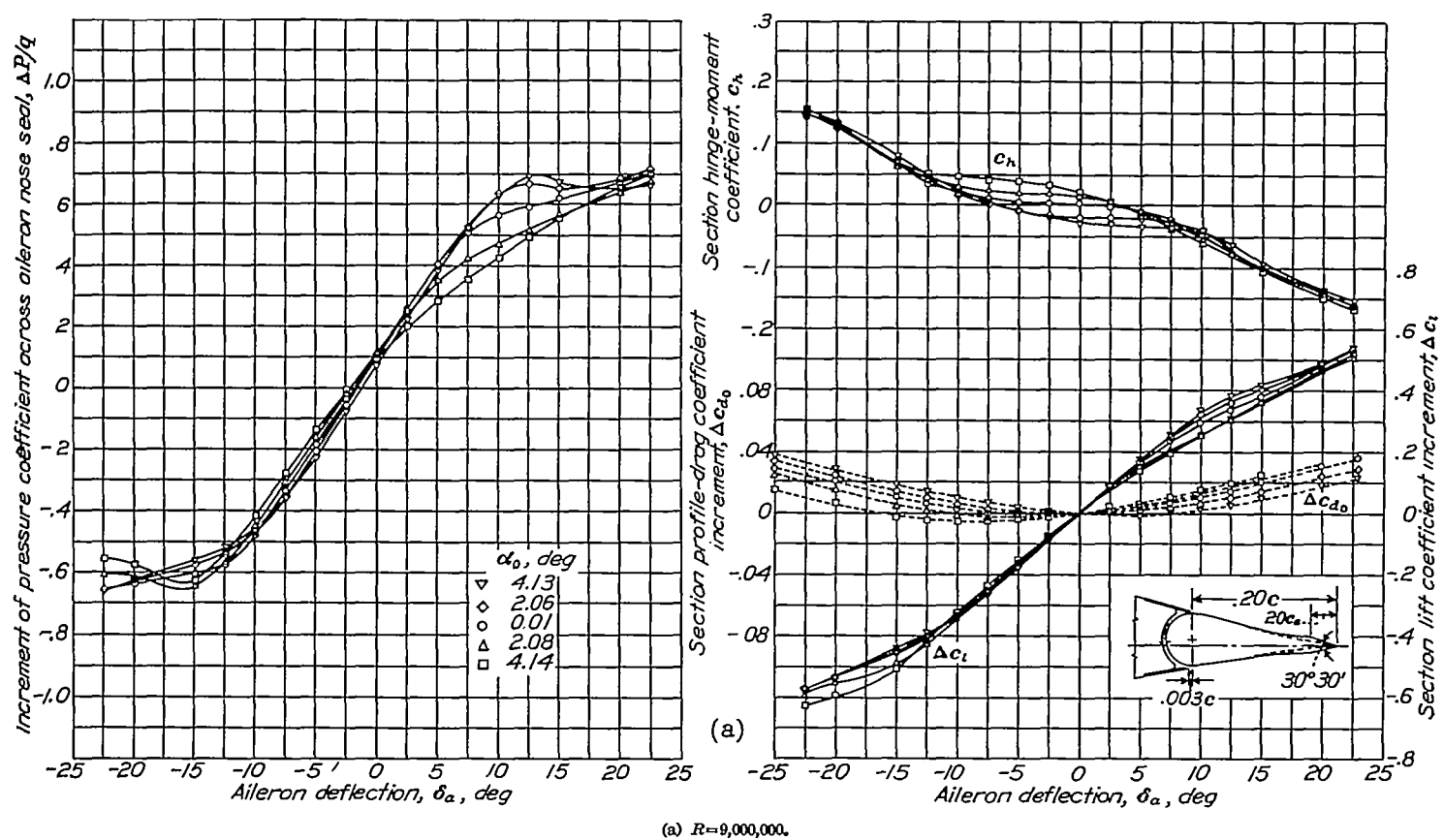
(a) $R = 9,000,000$.
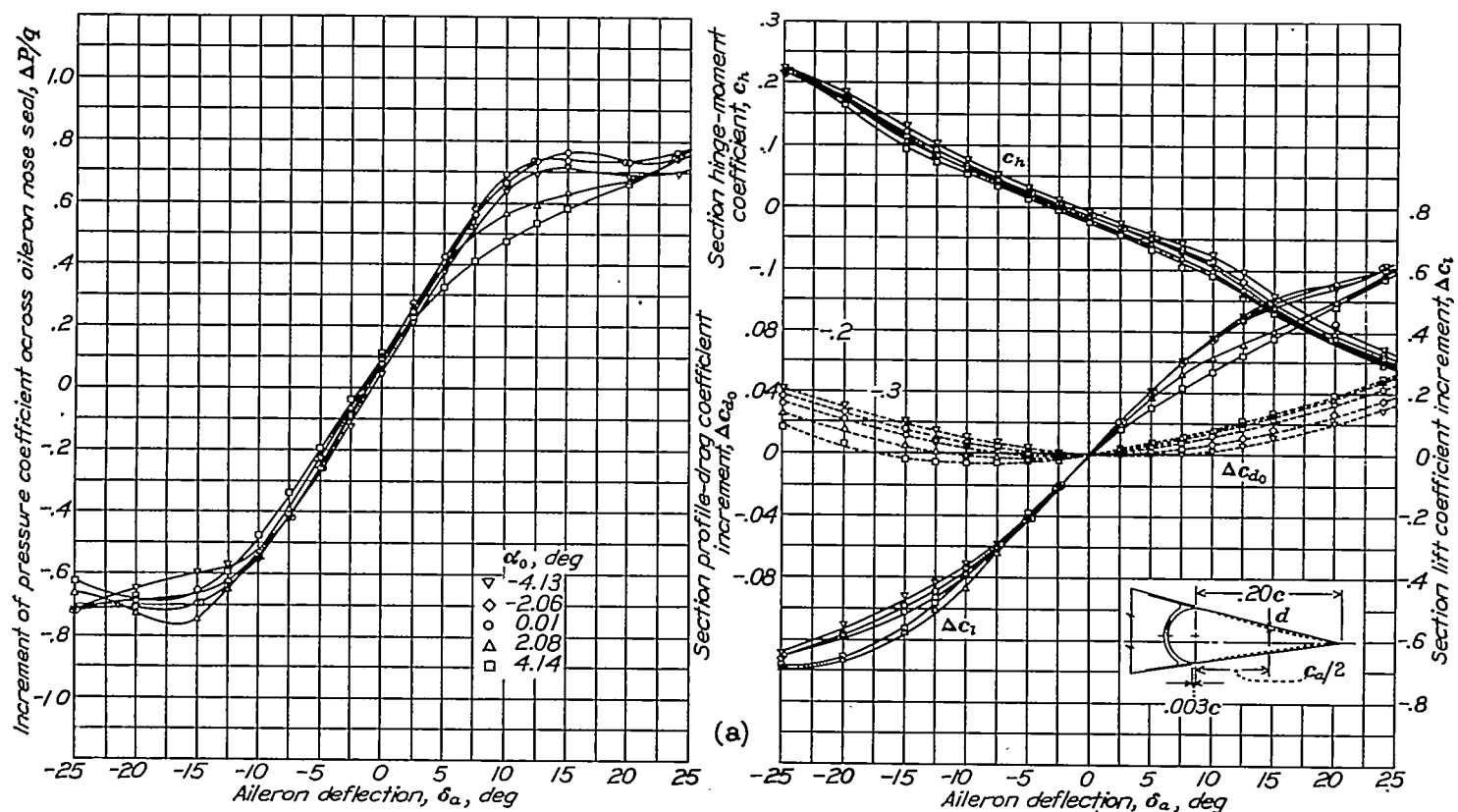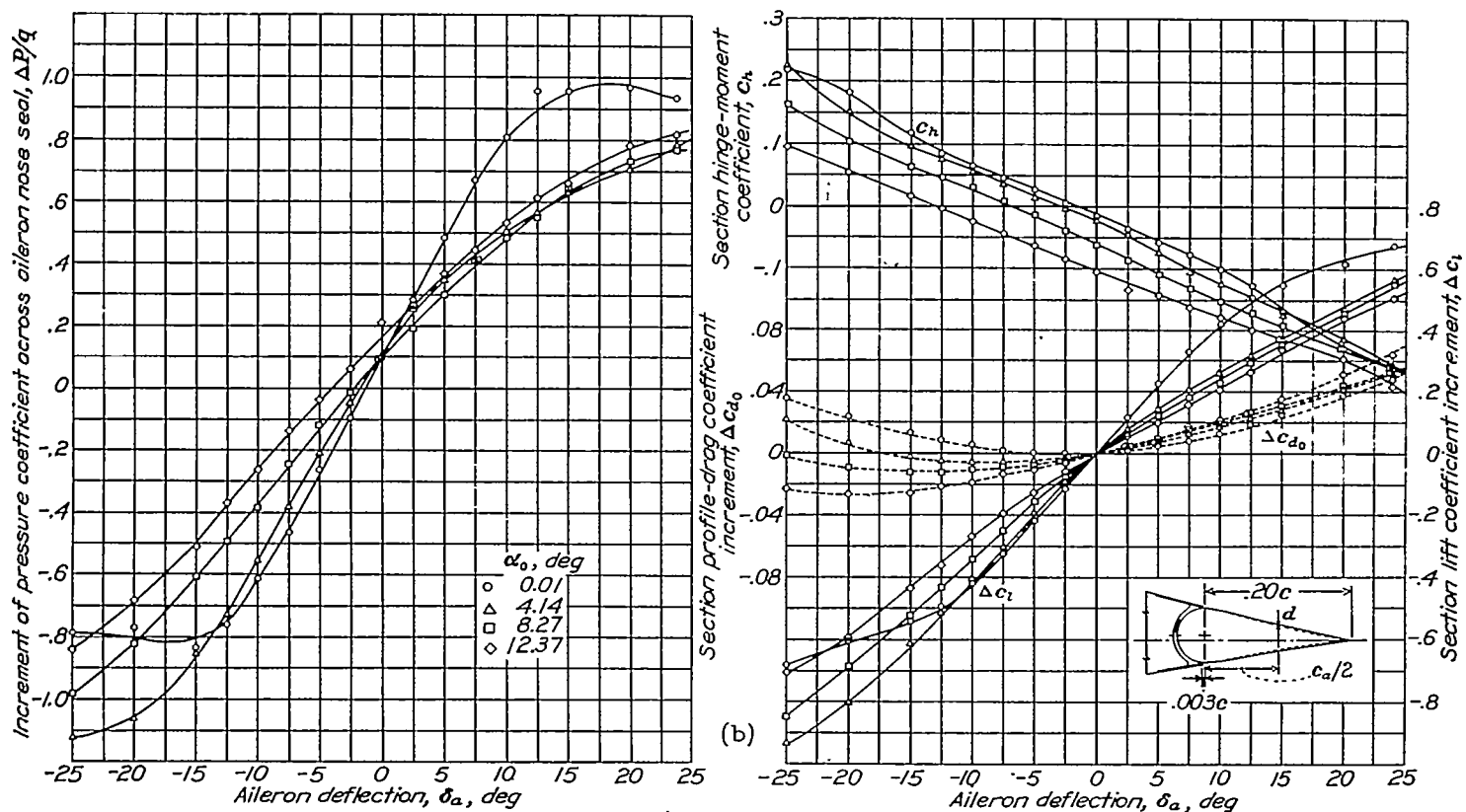
(b) $R = 3,800,000$

FIGURE 33.—Section aerodynamic characteristics of an NACA 66, 2–216 ($a = 0.6$) airfoil equipped with a 0.20-chord, sealed gap, plain aileron of intermediate-thickened profile. $d = 0.009c_a$.

(a) $R=9,000,000$.

(b) $R=5,500,000$ to $7,800,000$.
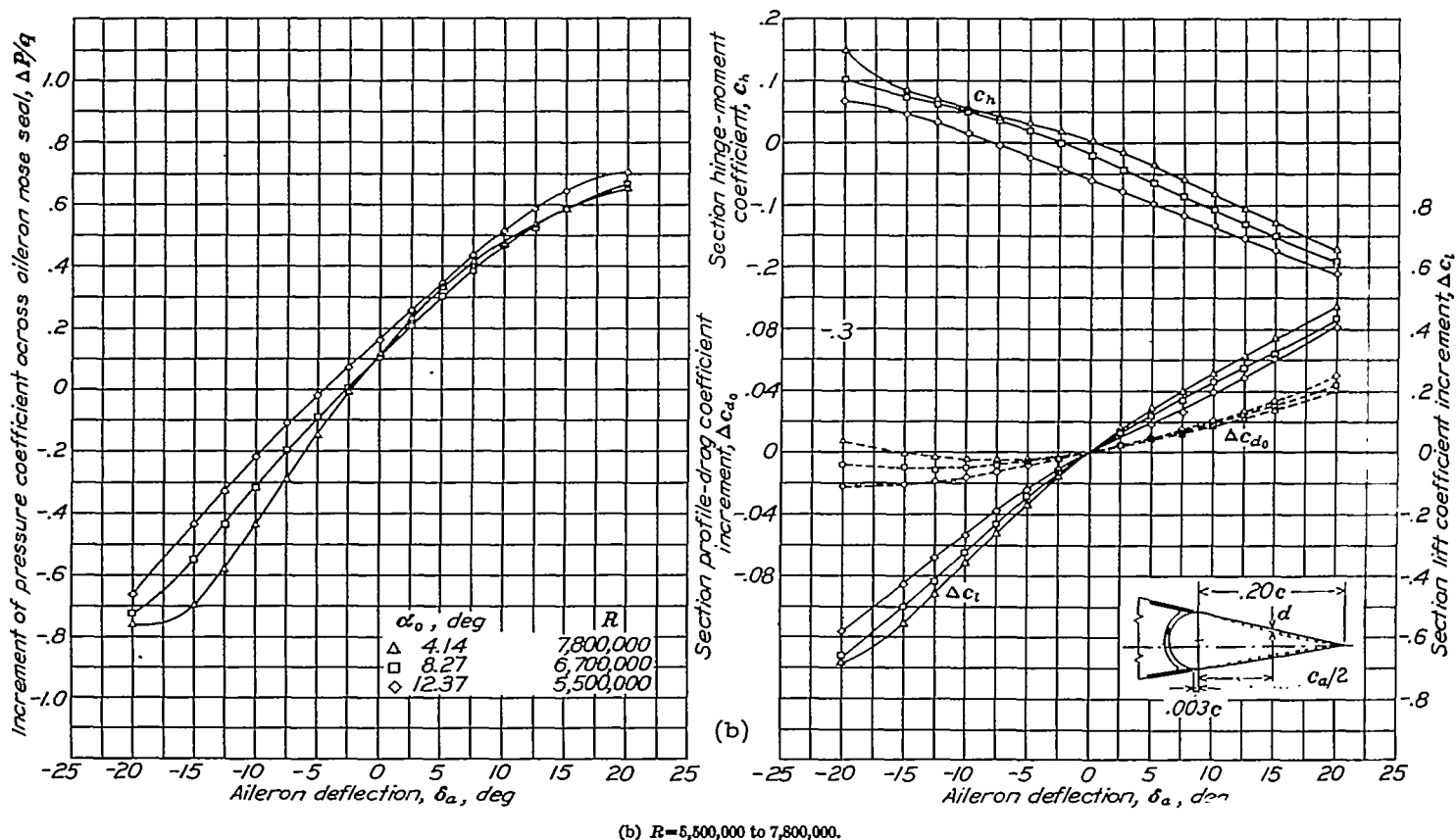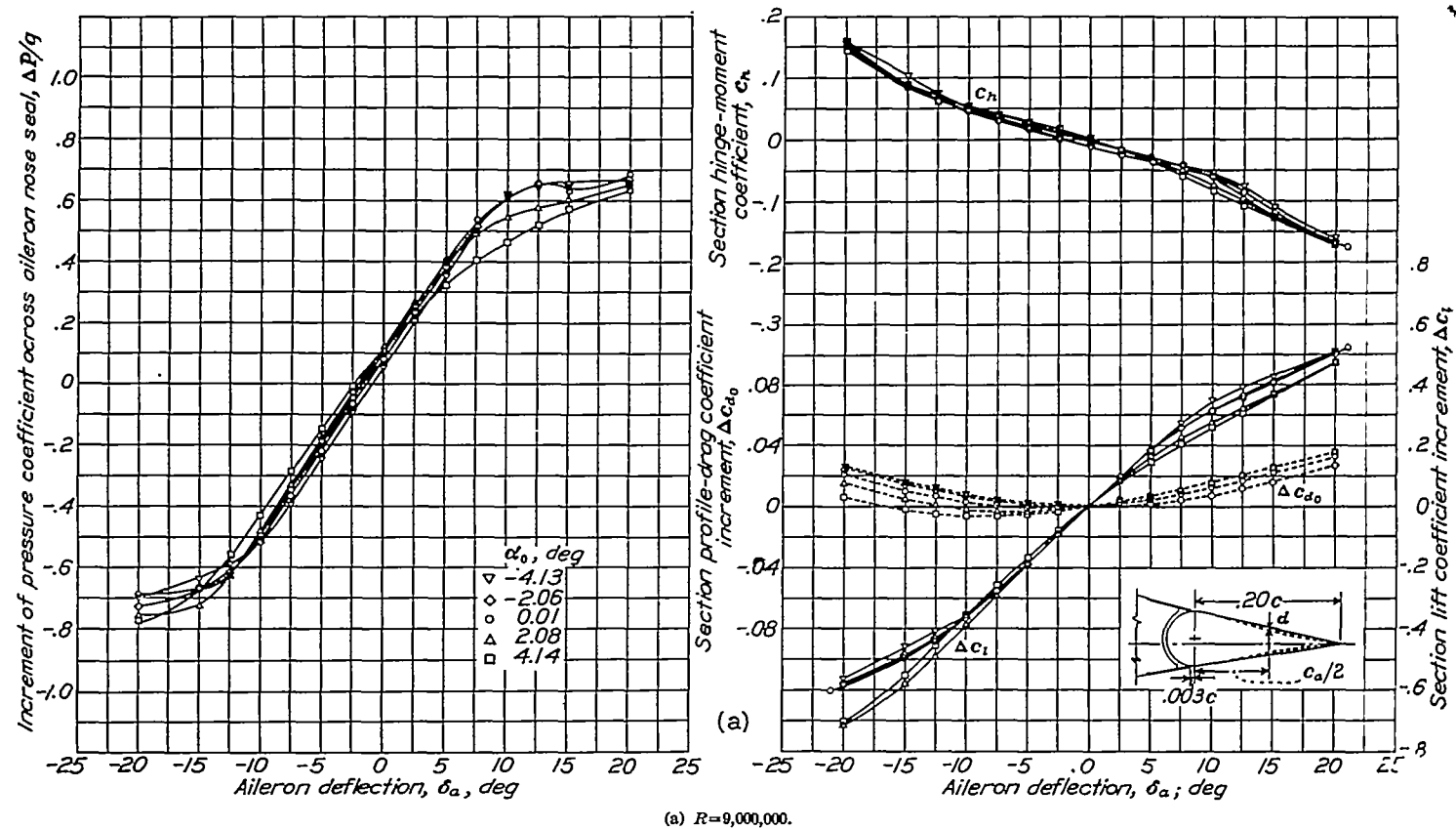
FIGURE 34.—Section aerodynamic characteristics of an NACA 66, 2-216 ($a=0.6$) airfoil equipped with a 0.20-chord, sealed gap, plain aileron of straight-sided profile. $d=0.018c_a$.
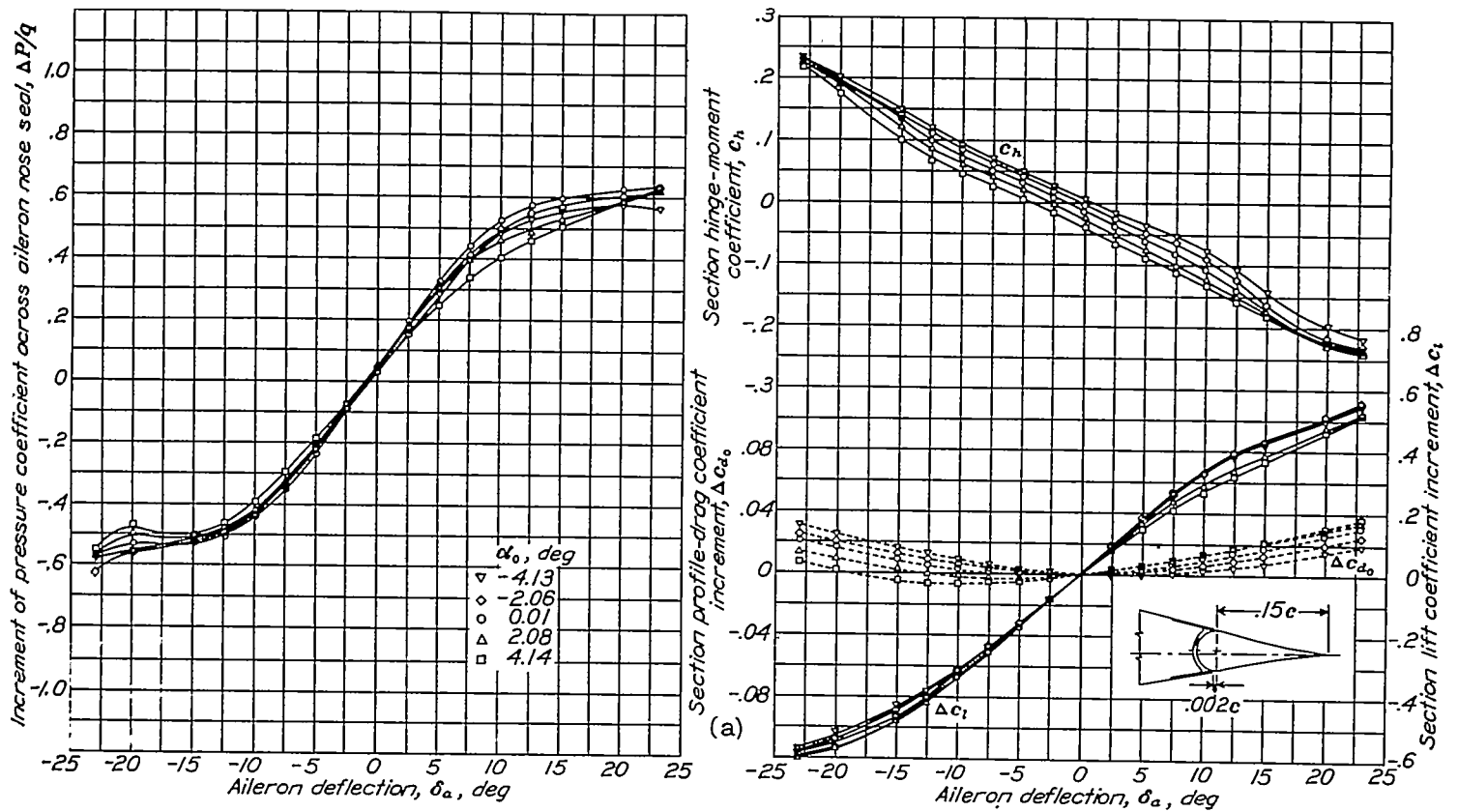
(a) $R = 9{,}000{,}000$.
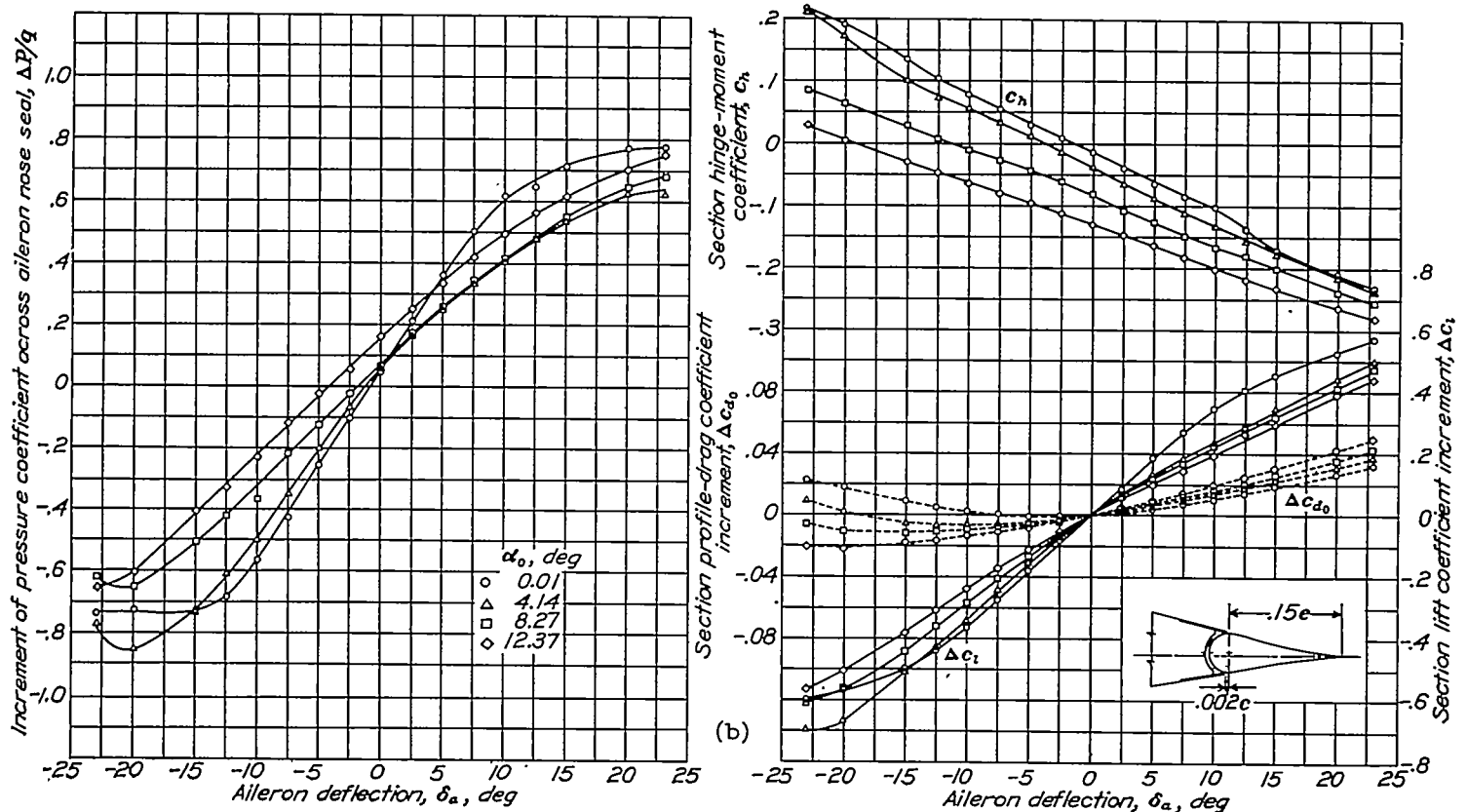
(b) $R = 3{,}800{,}000$.

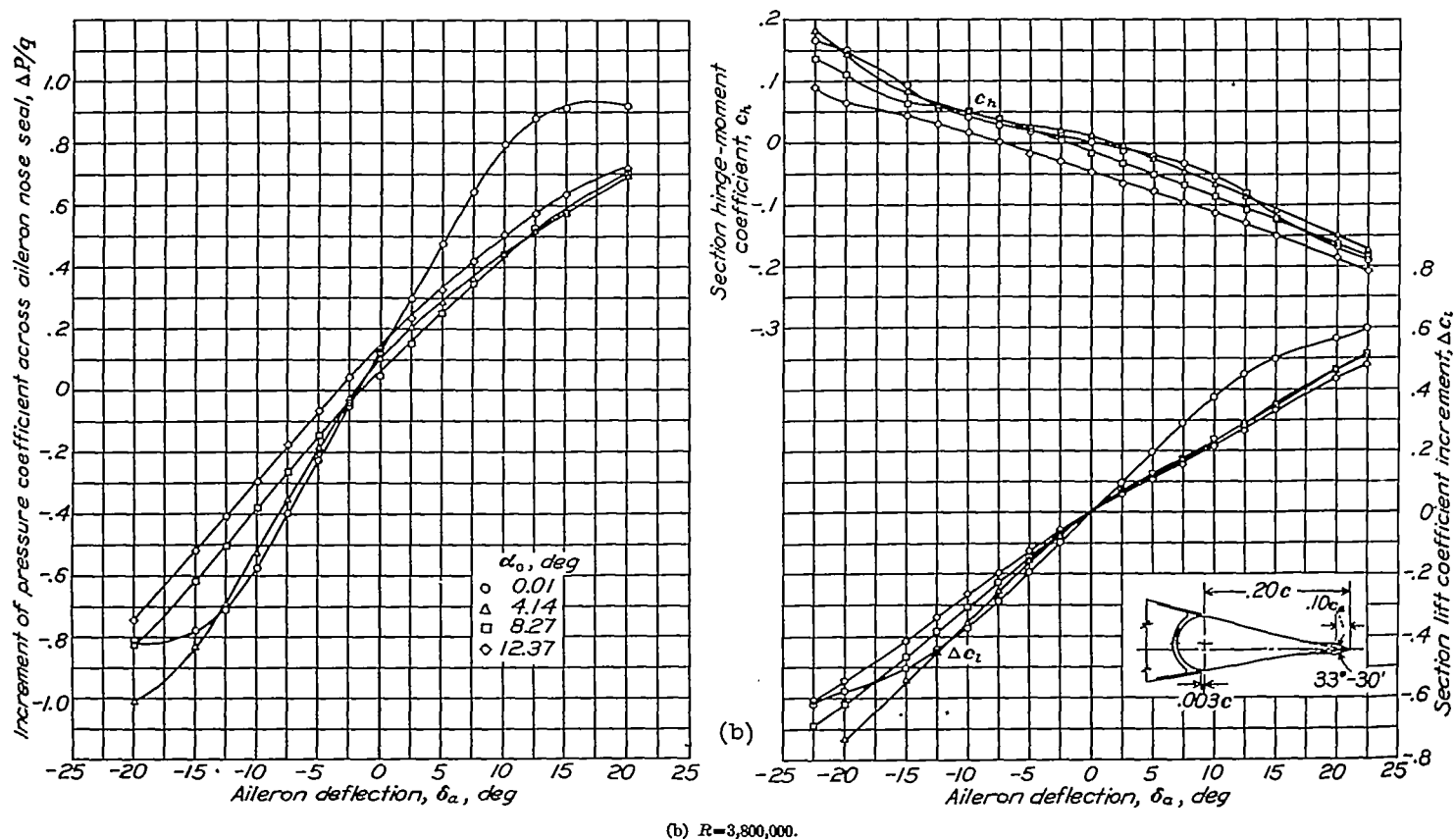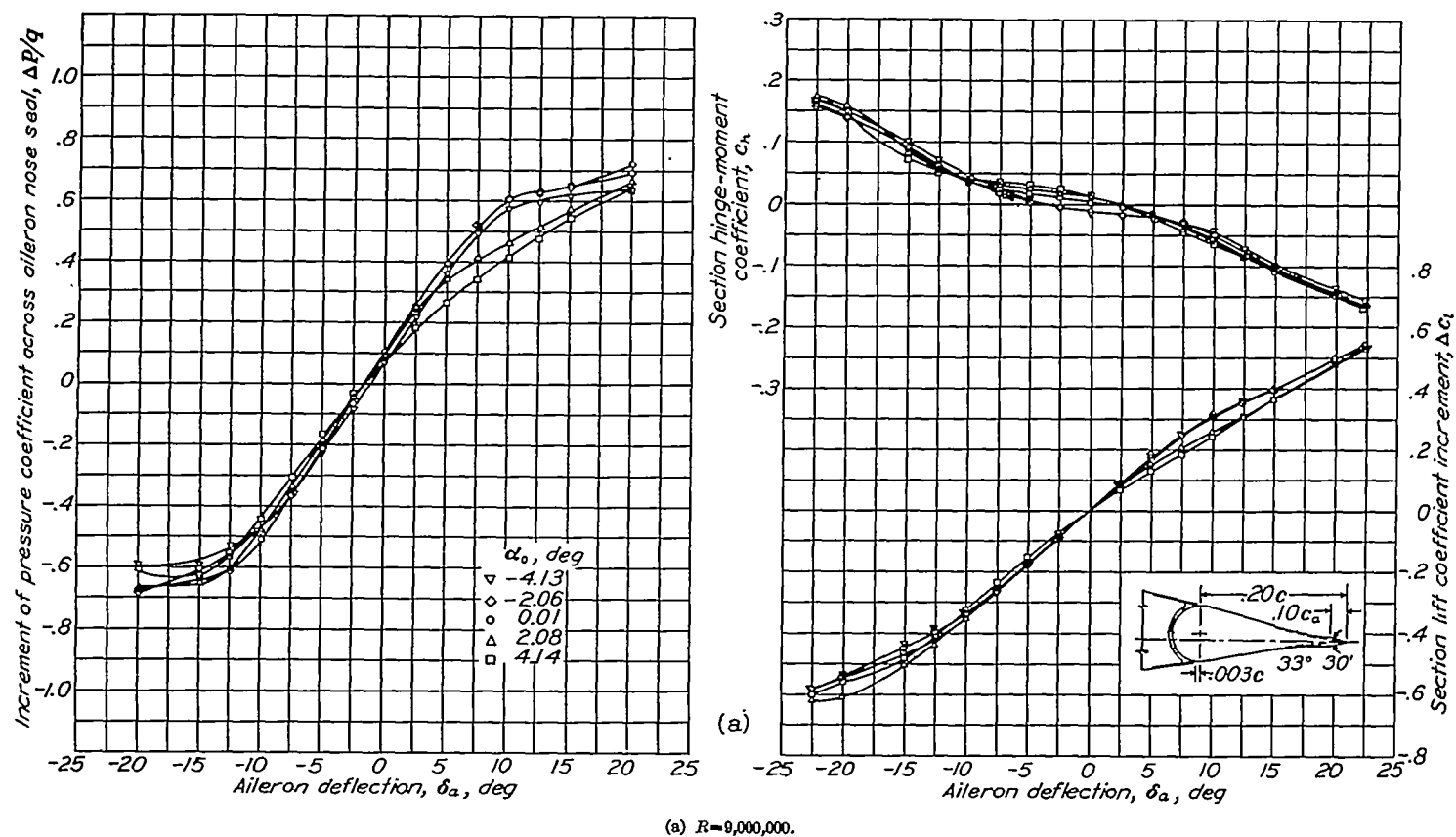FIGURE 35.—Section aerodynamic characteristics of an NACA 66, 2-216 ($a=0.6$) airfoil equipped with a 0.15-chord, sealed gap, plain aileron of normal profile.

(a) $R=9,000,000$.

(b) $R=3,800,000$.
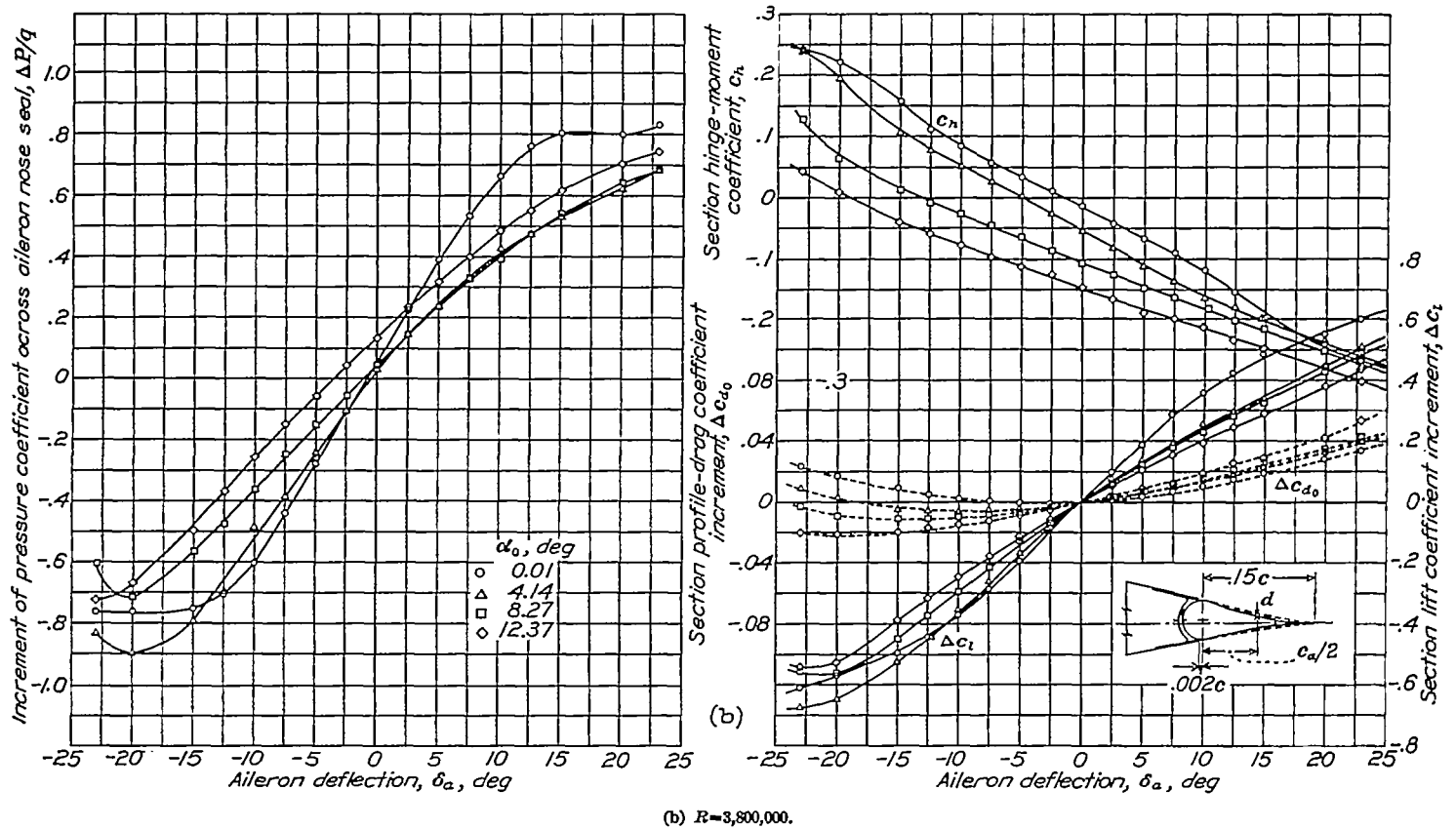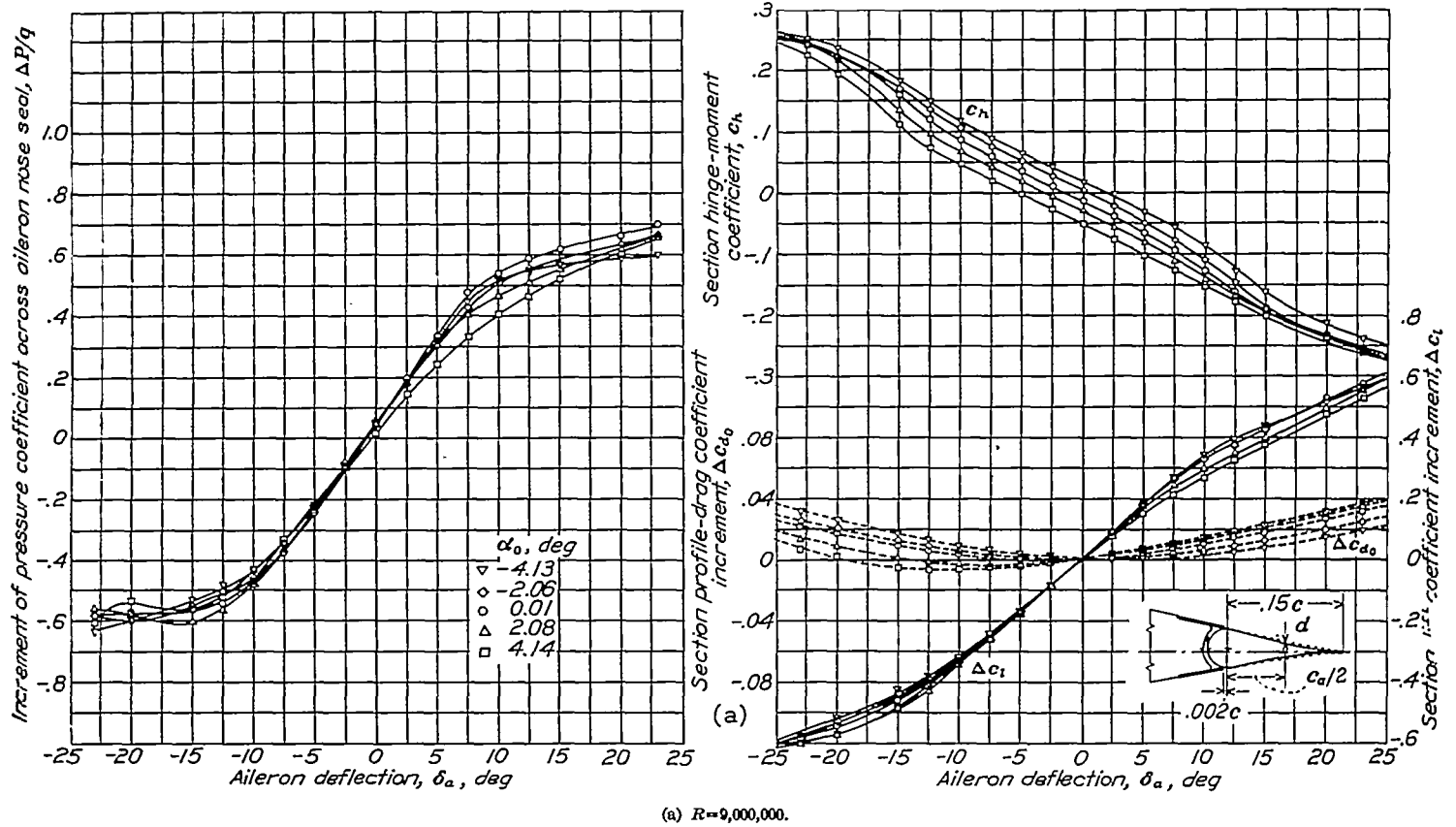
FIGURE 36.—Section aerodynamic characteristics of an NACA 66, 2-216 ($a=0.6$) airfoil equipped with a 0.15-chord, sealed gap, plain aileron of thinned profile. $d=-0.012c_a$.
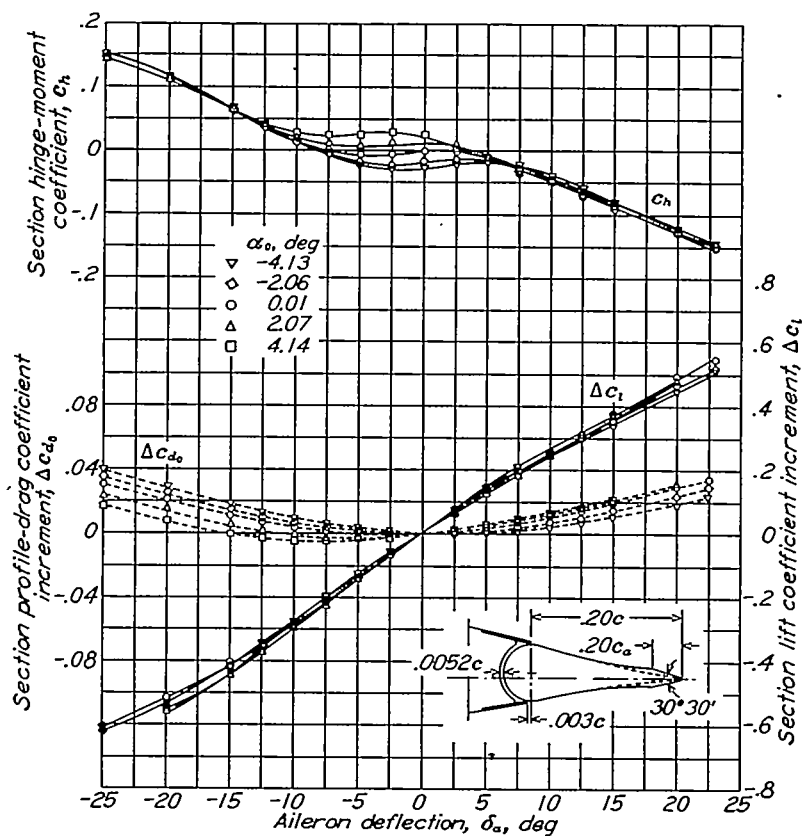
(a) $R = 9,000,000$.

(b) $R = 3,800,000$.
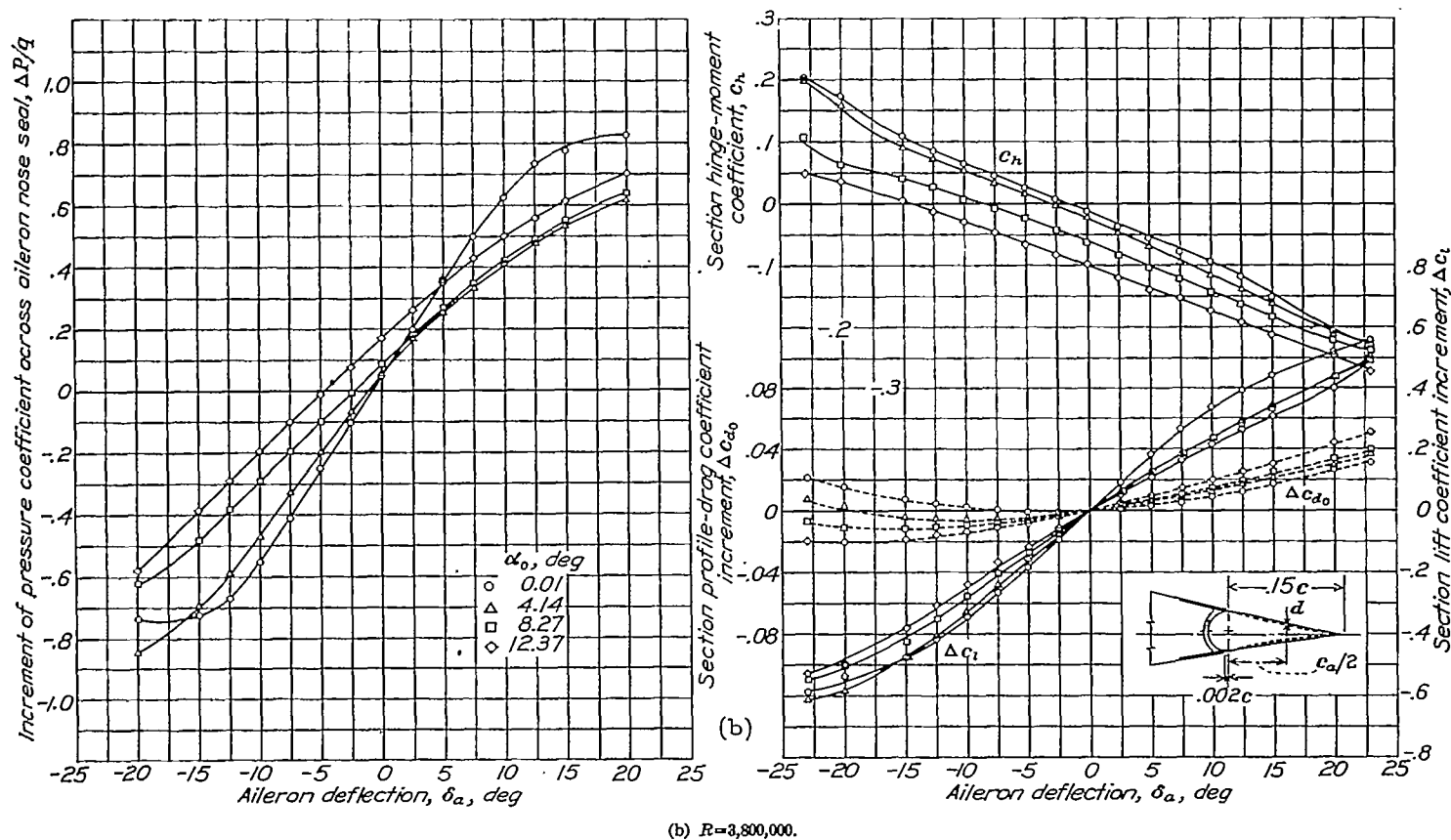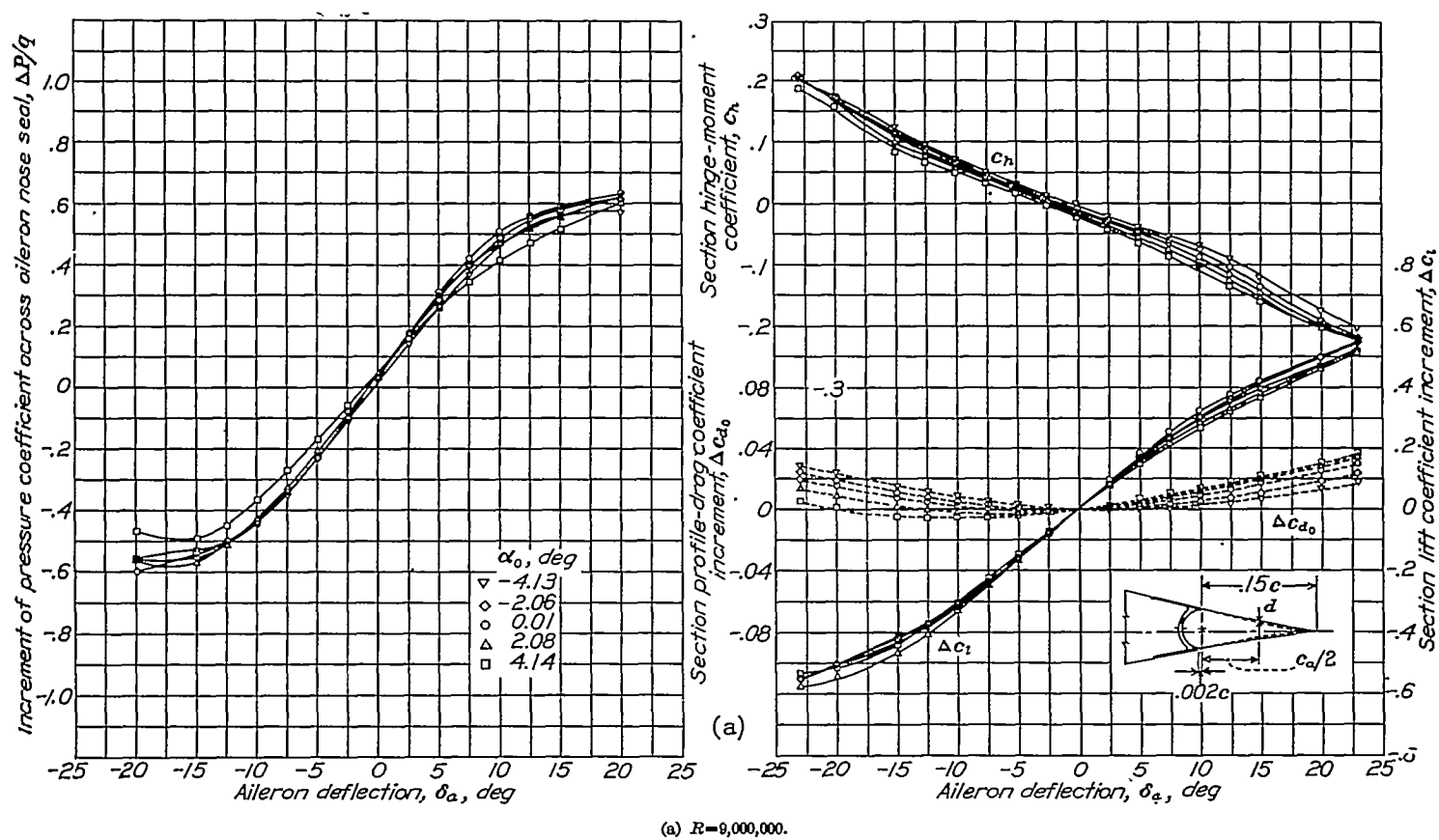
FIGURE 37.—Section aerodynamic characteristics of an NACA 66, 2-216 ($a=0.6$) airfoil equipped with a 0.15-chord, sealed gap, plain aileron of intermediate-thickened profile. $d=0.010c_a$.

(a) $R=9,000,000$.

(b) $R=3,800,000$.

FIGURE 38.—Section aerodynamic characteristics of an NACA 66, 2-216 ($a=0.6$) airfoil equipped with a 0.15-chord, sealed gap, plain aileron of straight-sided profile. $d=0.019c_a$.

FIGURE 39.—The effect of modifications of the aileron profile on the section aerodynamic characteristics of an NACA 66, 2-216 (a=0.6) airfoil equipped with a 0.20-chord, sealed gap, plain aileron. Aileron undeflected. R=8,200,000.
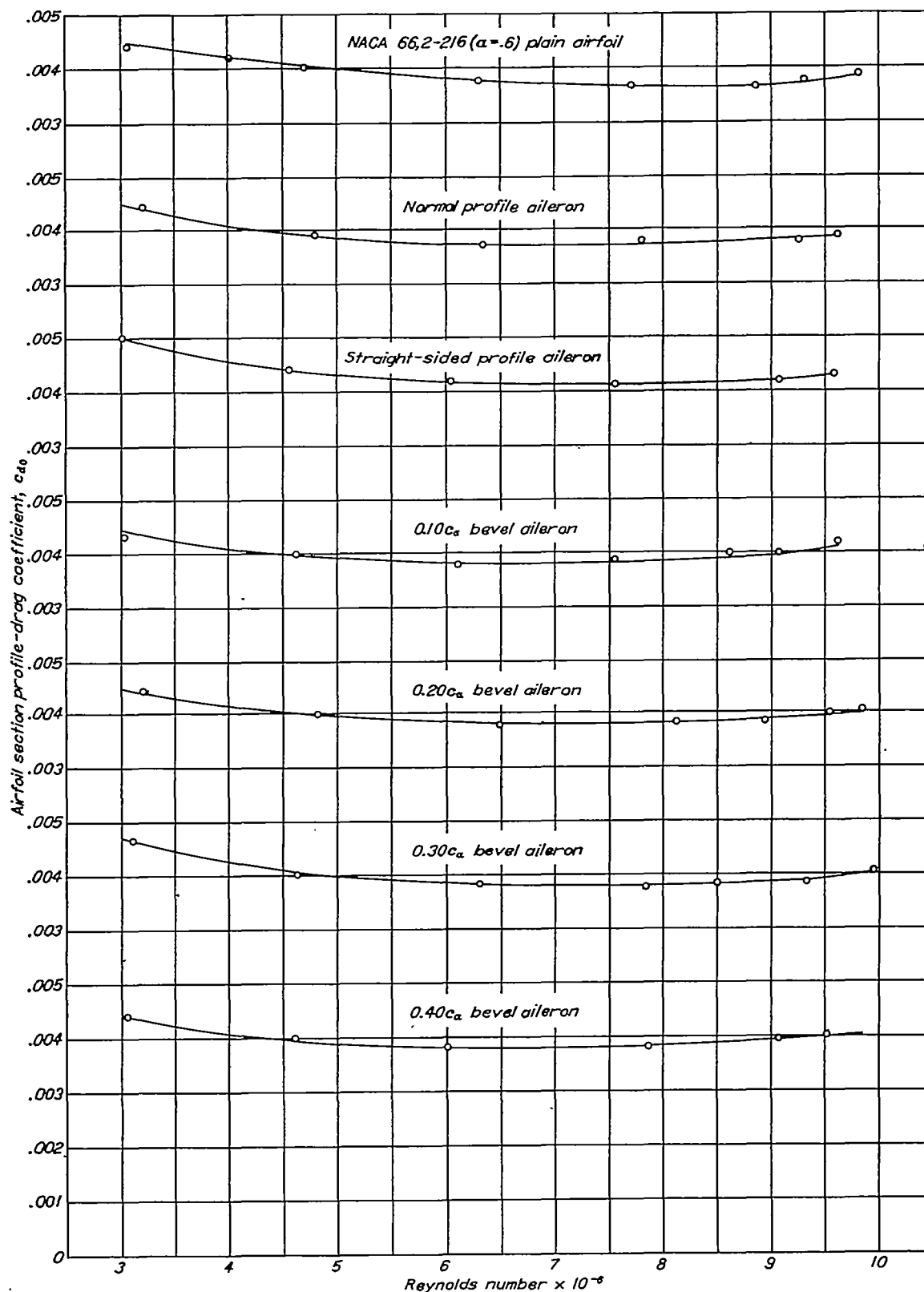

FIGURE 40.—The effect of modifications of the aileron profile on the section aerodynamic characteristics of an NACA 66, 2-216 (a=0.6) airfoil equipped with a 0.15-chord, sealed gap, plain aileron. Aileron undeflected. R=8,200,000.

NACA 66,2-216 (a=.6) plain airfoil

0.20-chord normal profile aileron

o   0.20-chord aileron (d = -0.009c_a)
Δ   .15- "   "   (d = -0.012c_a)
      Thinned profile aileron

o   0.20-chord aileron (d = 0.018c_a)
Δ   .15- "   "   (d = 0.019c_a)
      Straight-sided profile aileron

Airfoil section profile-drag coefficient, c_{d_0}

Reynolds number × 10^{-6}
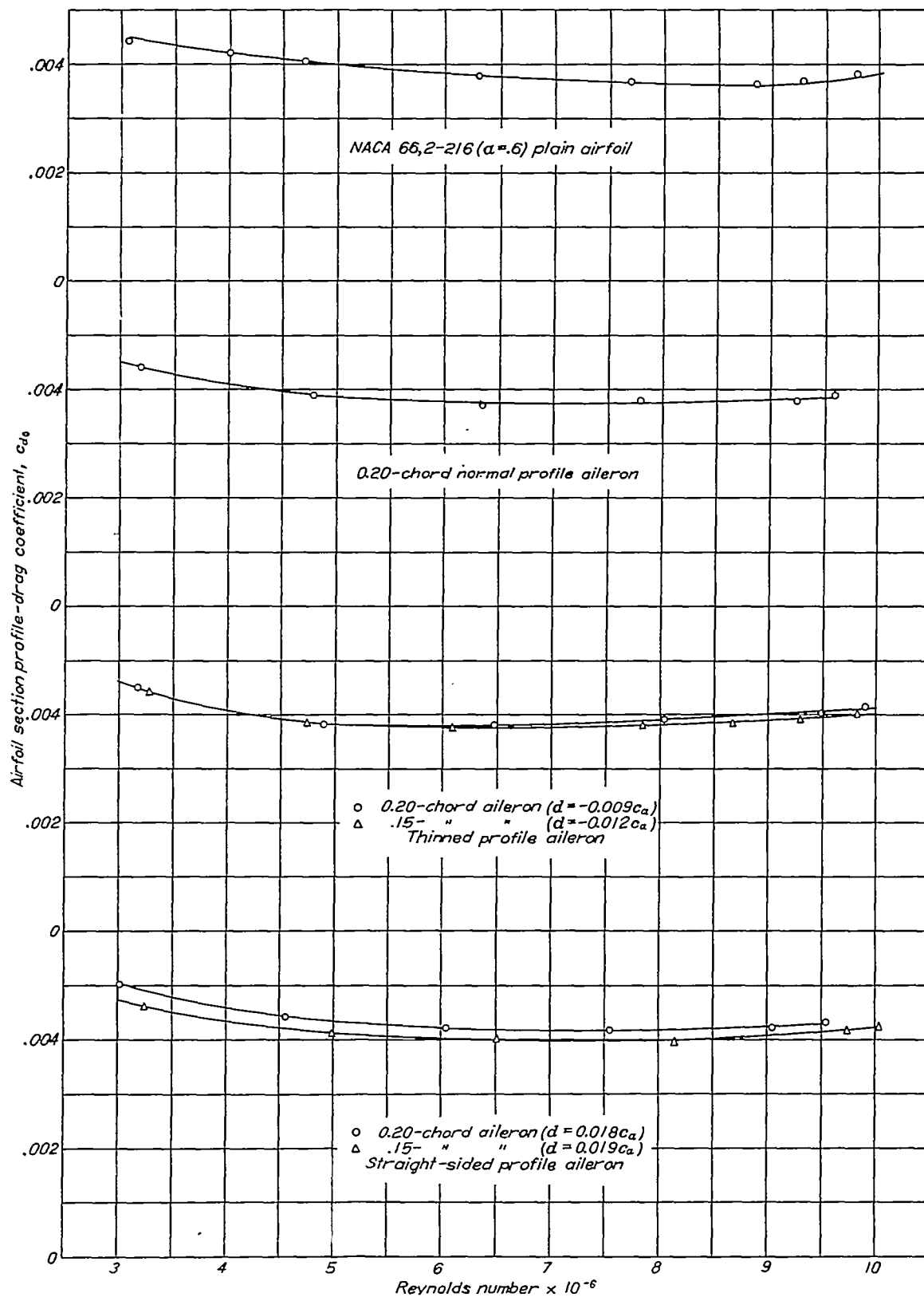
FIGURE 41.—The effect of modification of the aileron profile on the variation of section profile-drag coefficient with Reynolds number for an NACA 66, 2-216 (a=0.6) airfoil, Aileron undeflected. α_o=0.51°.
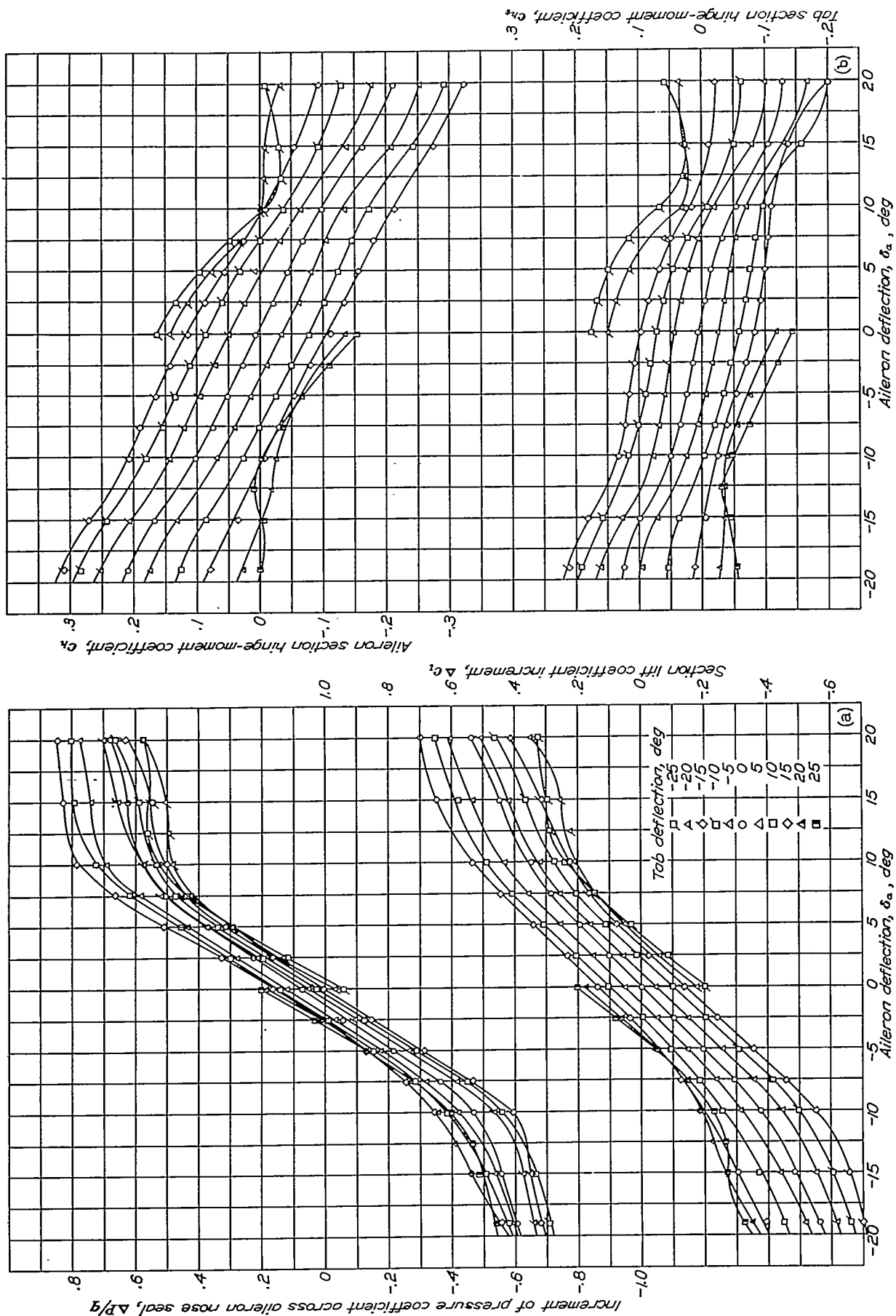
(a) $R=9,000,000.$

(b) $R=3,800,000.$

FIGURE 42.—Section aerodynamic characteristics of an NACA 66, 2-216 ($a=0.6$) airfoil equipped with a 0.20-chord, sealed gap, plain aileron with a 0.40c_a beveled trailing edge.

(a) $R=9,000,000$

(b) $R=3,800,000$.
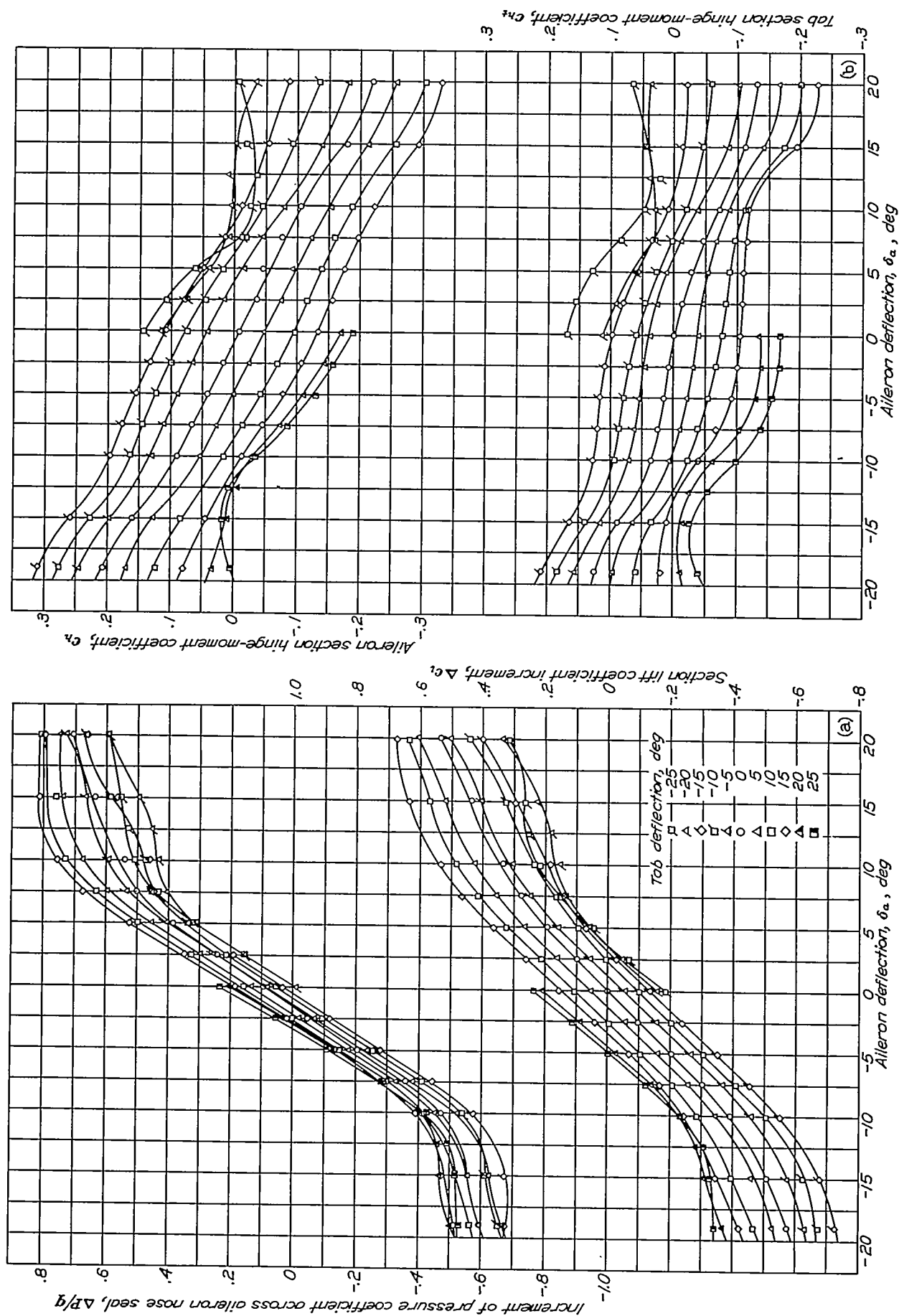
FIGURE 43.—Section aerodynamic characteristics of an NACA 66, 2-216 ($a=0.6$) airfoil equipped with a 0.20 chord, sealed gap, plain aileron with a 0.30c_a beveled trailing edge.

(a) $R = 9,000,000$.

(b) $R = 3,800,000$.

FIGURE 44.—Section aerodynamic characteristics of an NACA 66, 2-216 ($a = 0.6$) airfoil equipped with a 0.20-chord, sealed gap, plain aileron with a 0.20c_a beveled trailing edge.
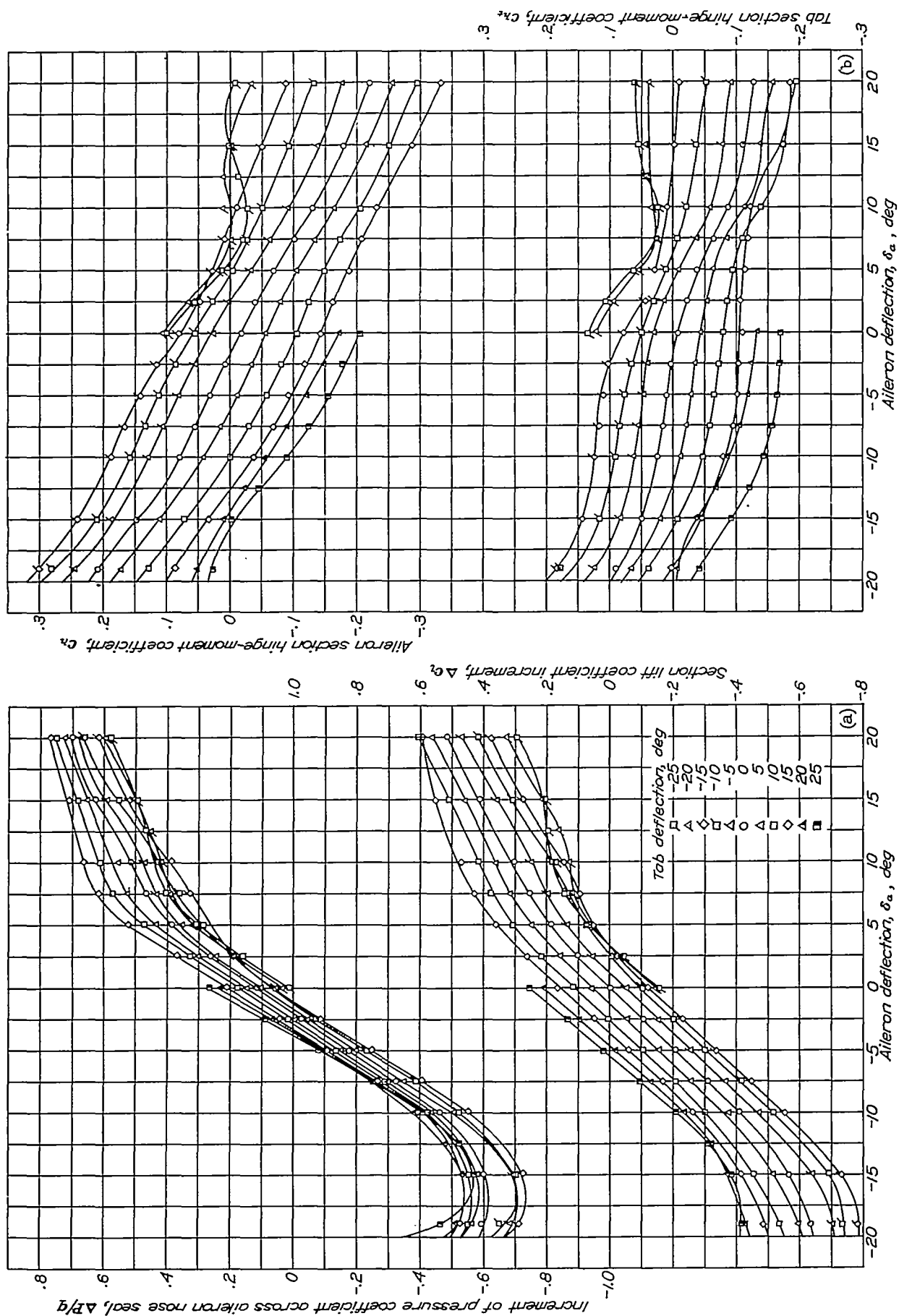
(a) $R=9,000,000$.

(b) $R=3,800,000$.
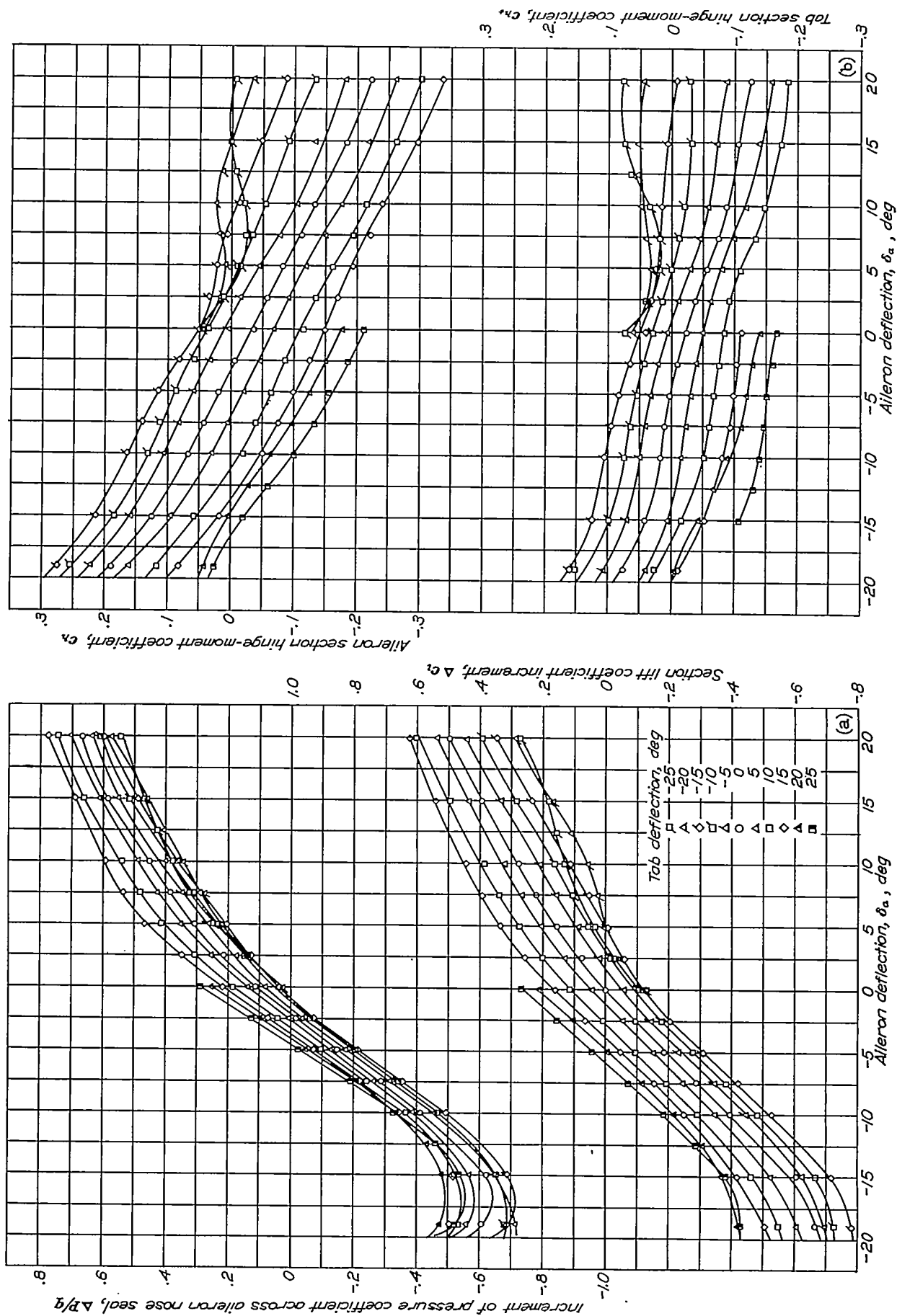
FIGURE 45.—Section aerodynamic characteristics of an NACA 66, 2-216 ($a=0.6$) airfoil equipped with a 0.20-chord, sealed gap, plain aileron with a 0.10c_a beveled trailing edge.

FIGURE 46.—Section aerodynamic characteristics of an NACA 66, 2–216 (a=0.6) airfoil equipped with a 0.20-chord, plain aileron with a 0.20c_a beveled trailing edge and 0.0052c nose gap. R=9,000,000.
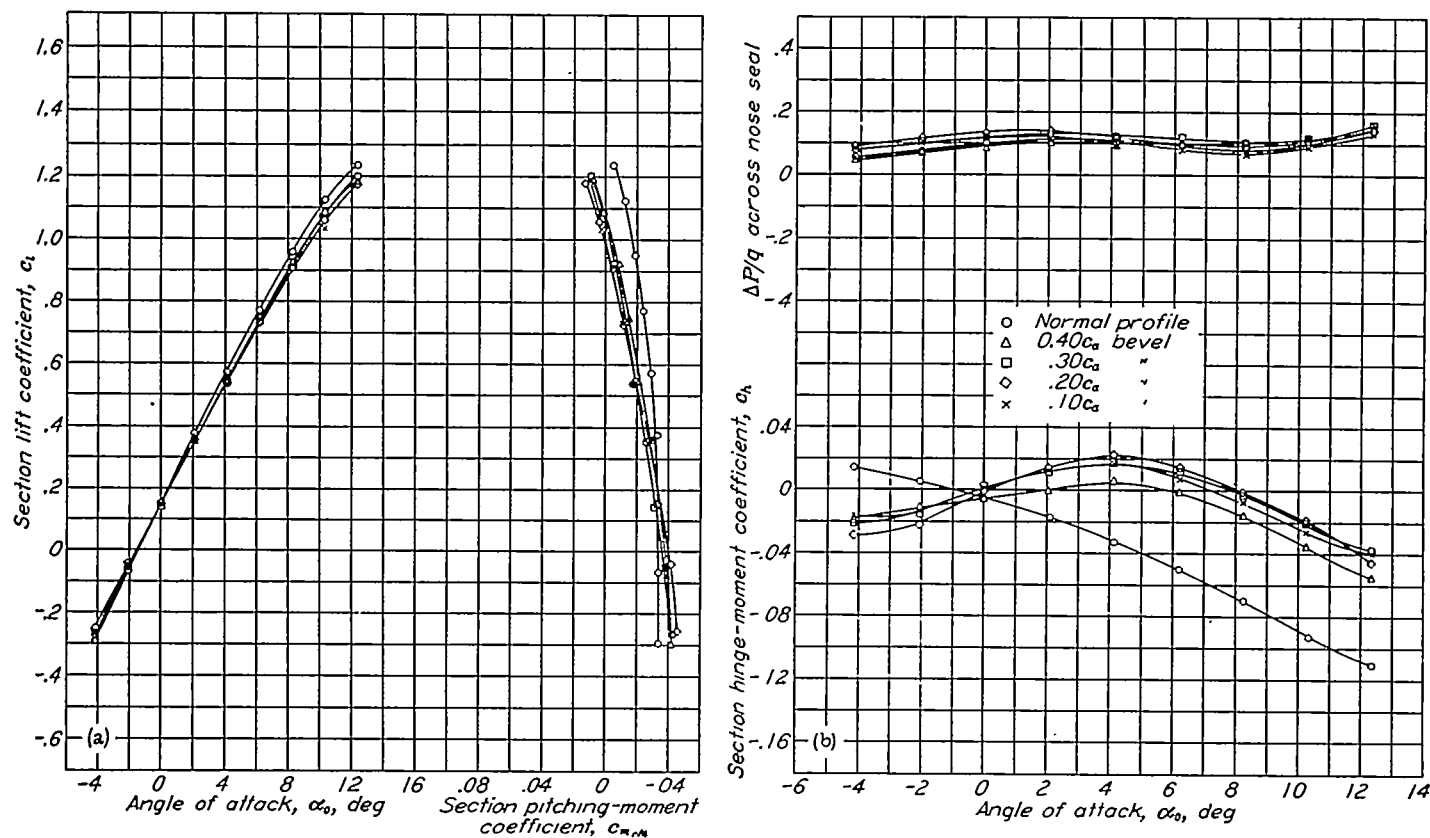
FIGURE 47.—Effect of beveled trailing edge on section aerodynamic characteristics of an NACA 66, 2–216 (a=0.6) airfoil equipped with a 0.20-chord, sealed gap, plain aileron. Aileron undeflected. R=8,200,000.

FIGURE 48.—Effect of beveled trailing edges on variation of section profile-drag coefficient with Reynolds number for an NACA 66, 2-216 ($a=0.6$) airfoil equipped with a 0.20-chord, sealed gap plain aileron. Aileron undeflected. $\alpha_{\bullet}=0.51°$.
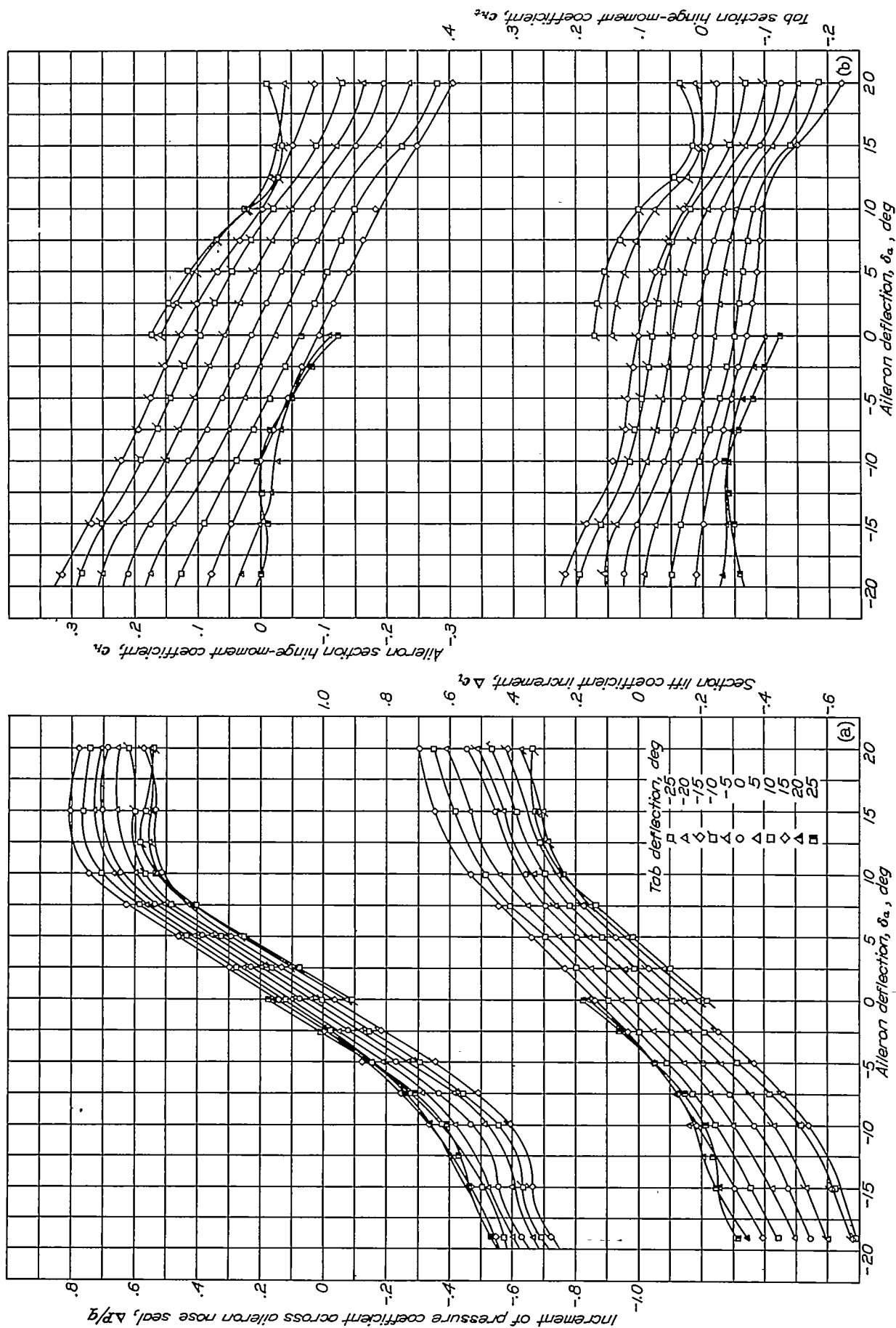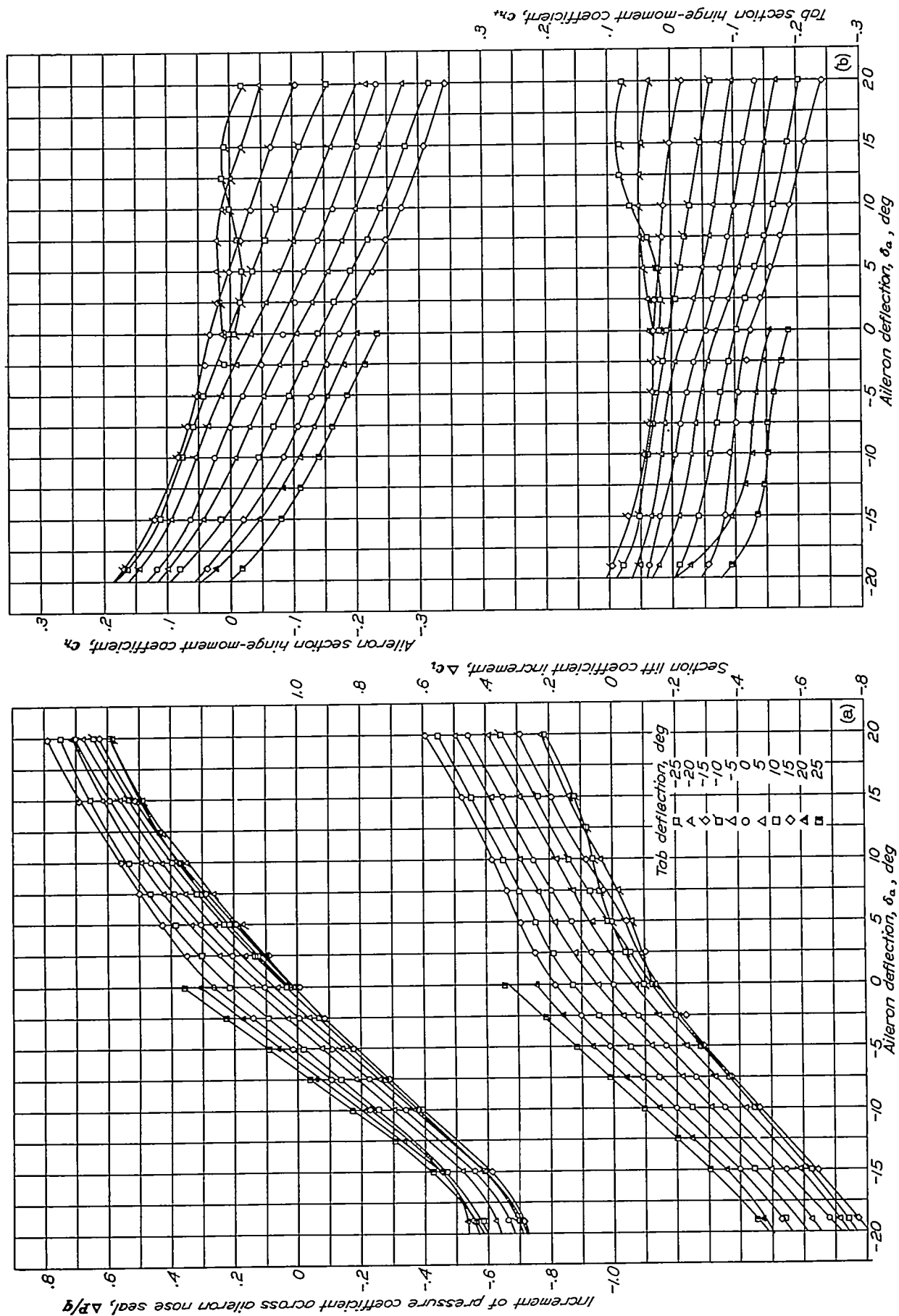
FIGURE 49.—Section aerodynamic characteristics of an NACA 66, 2-216 (a=0.0) airfoil equipped with a 0.20-chord, sealed gap, plain aileron of normal profile with a 0.20c, plain inset tab. R=9,000,000, $\alpha_0 = -4.13°$.
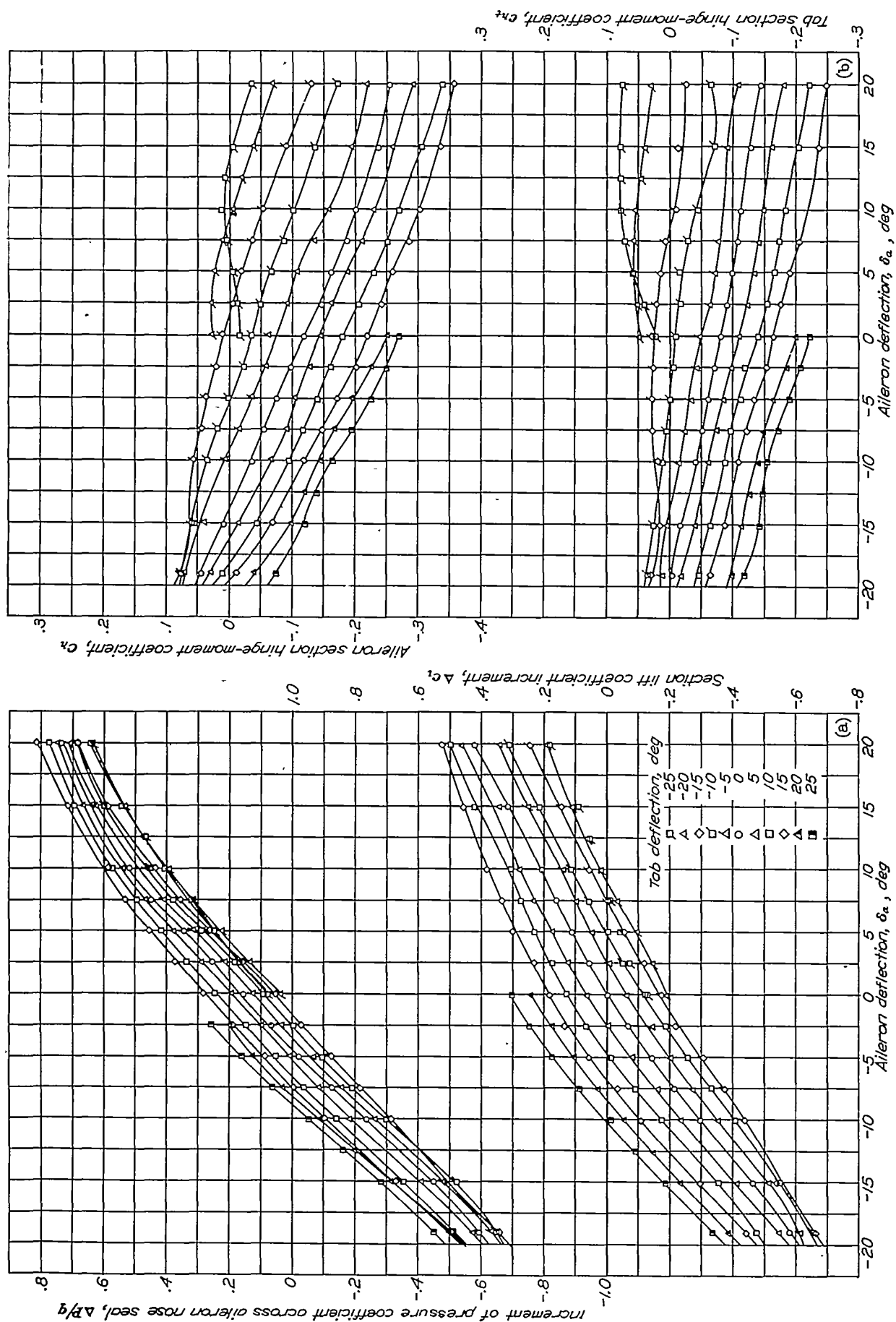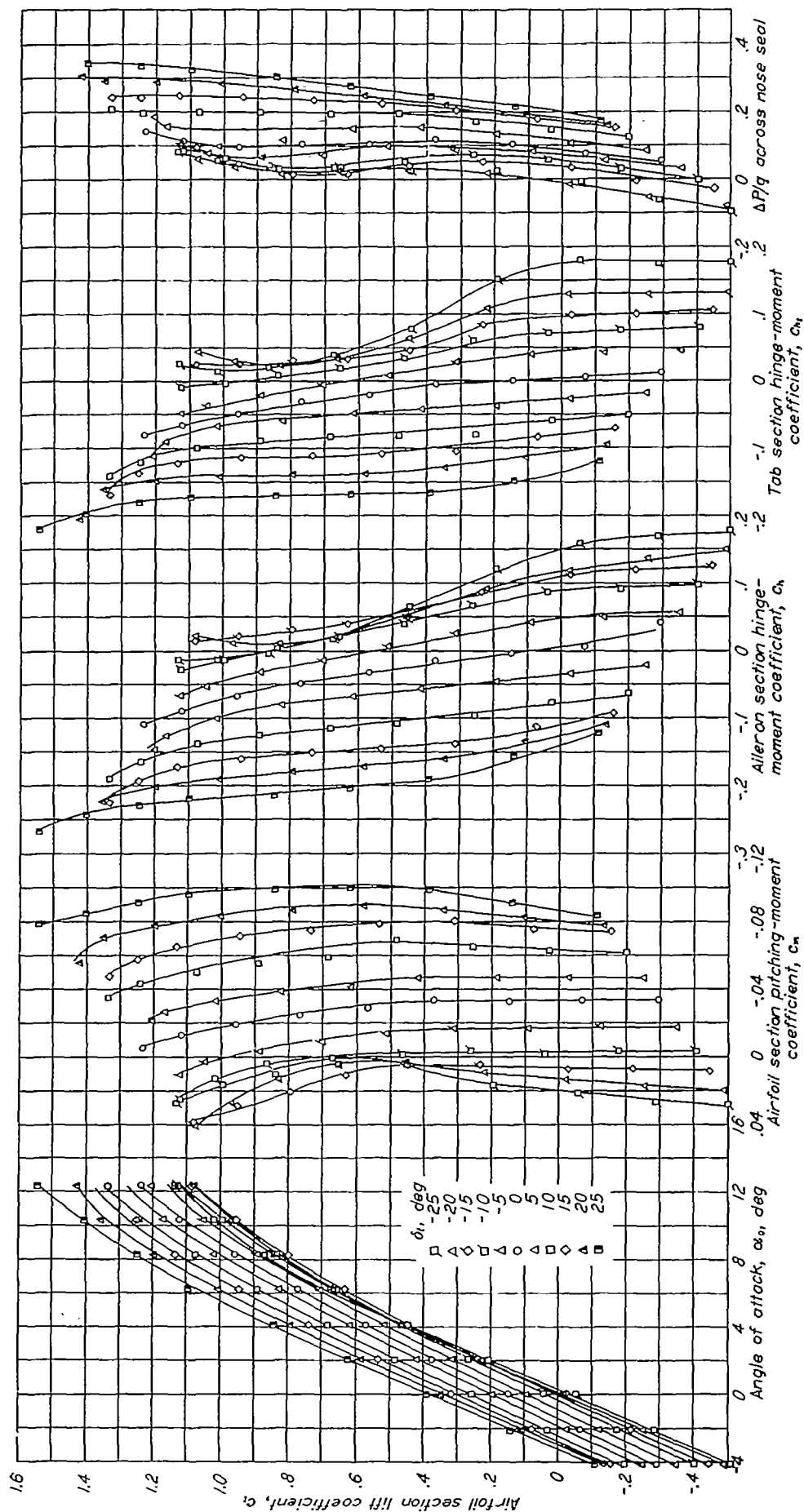
FIGURE 50.—Section aerodynamic characteristics of an NACA 66,2-216 ($\alpha=0.6$) airfoil equipped with a 0.20-chord, sealed gap, plain aileron of normal profile with a 0.20c_a plain inset tab. $R=9,000,000$, $\alpha_0=-2.06°$.

FIGURE 61.—Section aerodynamic characteristics of an NACA 66, 2-210 ($a=0.0$) airfoil equipped with a 0.20-chord, sealed gap, plain aileron of normal profile with a 0.20c_a plain inset tab. $R=9,000,000$, $\alpha_s=0.01°$.
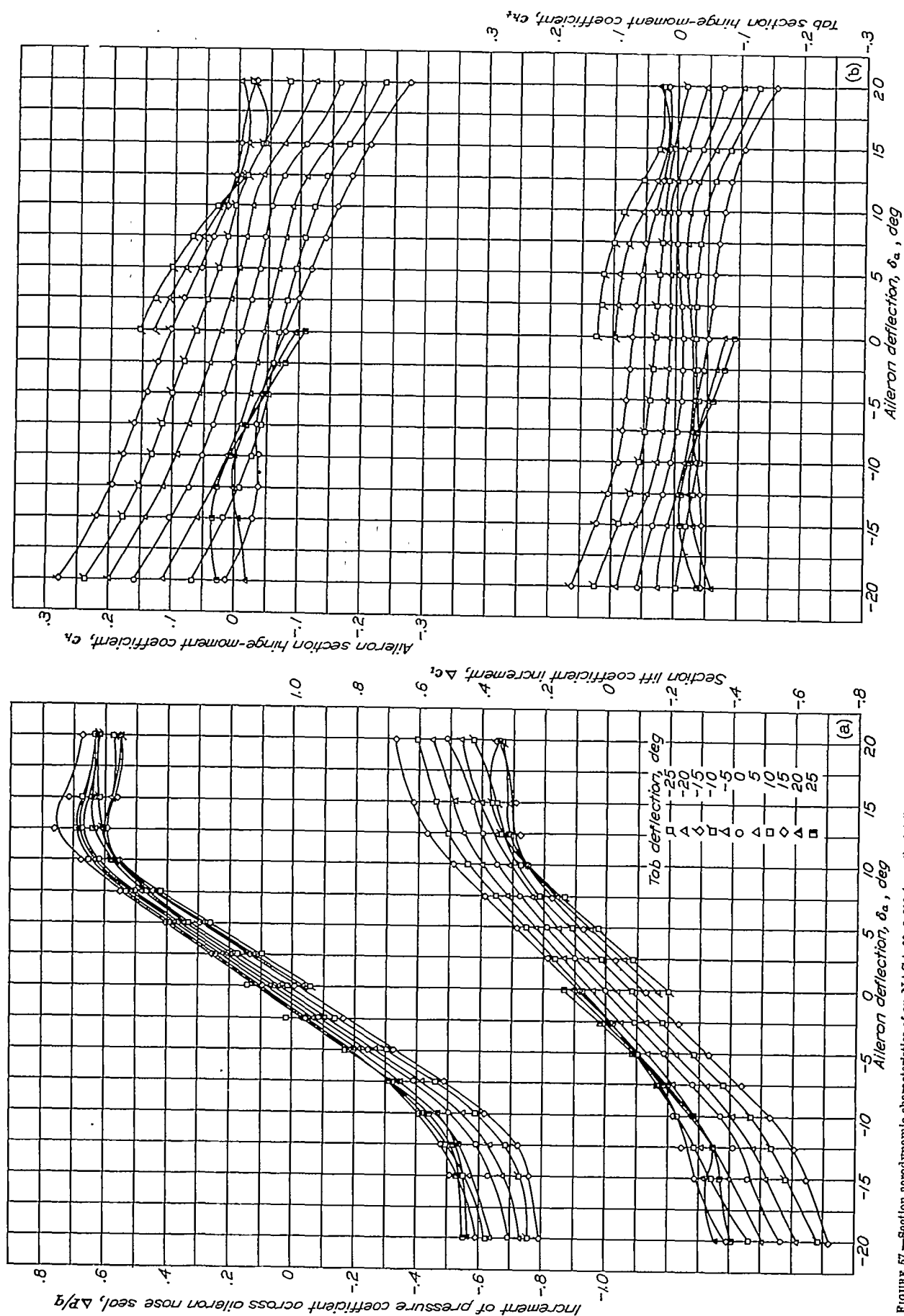
FIGURE 52.—Section aerodynamic characteristics of an NACA 66,2-216 (α=0.6) airfoil equipped with a 0.20-chord, sealed gap, plain aileron of normal profile with a 0.20c_a plain inset tab. R=9,000,000, α_o=2.07°.
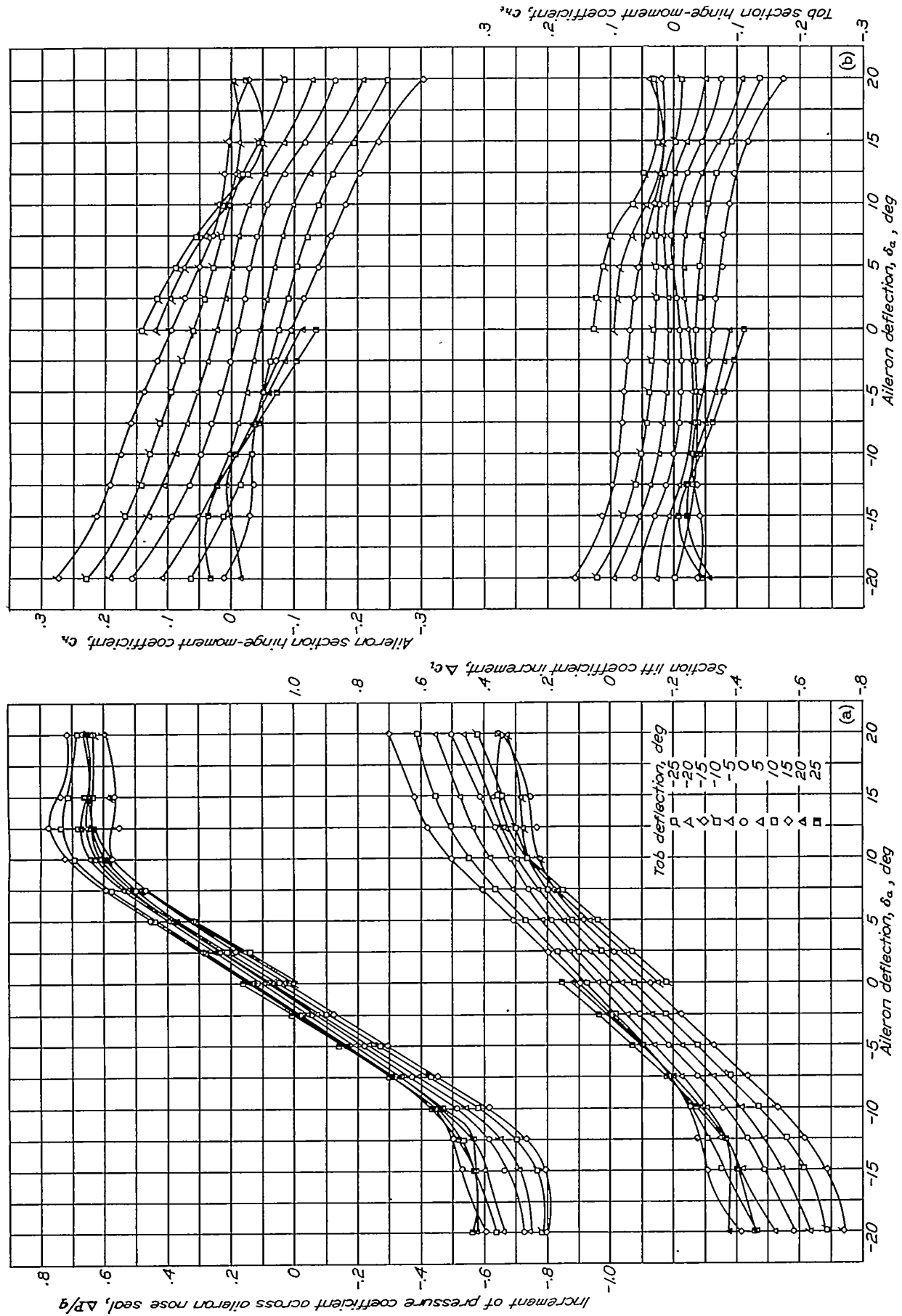
FIGURE 53.—Section aerodynamic characteristics of an NACA 66, 2-216 ($\alpha = 0.0$) airfoil equipped with a 0.20-chord, sealed gap, plain aileron of normal profile with a 0.20c, plain inset tab. $R = 9,000,000$, $\alpha_s = 4.14°$.

FIGURE 54.—Section aerodynamic characteristics of an NACA 66, 2-216 ($\alpha=0.6$) airfoil equipped with a 0.20-chord, sealed gap, plain aileron of normal profile with a 0.20c_a plain inset tab. $R=6,700,000$, $\alpha_o=8.27°$.

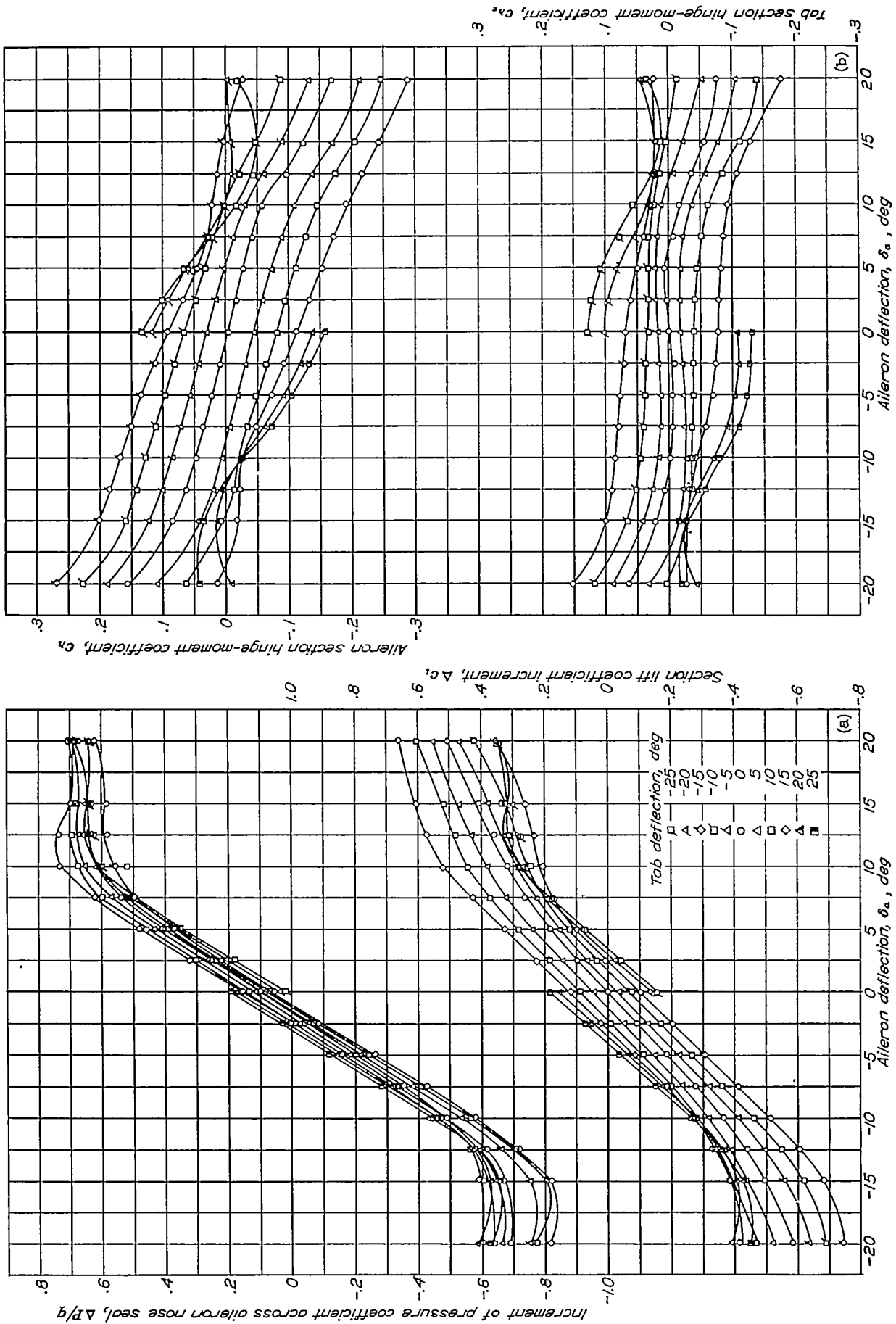FIGURE 56.—Section aerodynamic characteristics of an NACA 66, 2-216 (a=0.0) airfoil equipped with a 0.20-chord, sealed gap, plain aileron of normal profile with a 0.20c. plain inset tab.   R=5,600,000, α₀=12.37°.
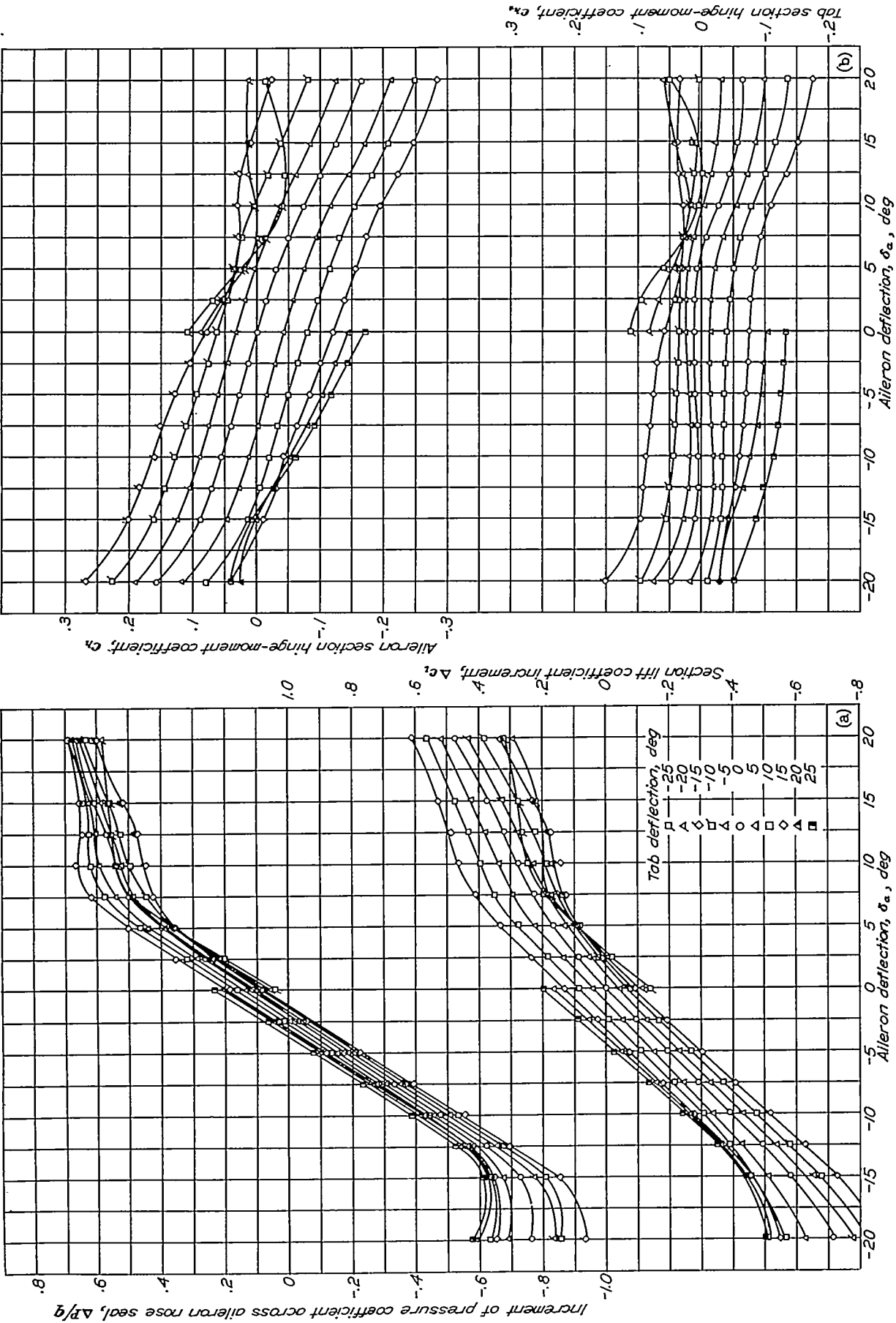
Figure 56.—Section aerodynamic characteristics of an NACA 66, 2-216 (a=0.6) airfoil equipped with a 0.20-chord, sealed gap, plain aileron of normal profile with a 0.20c_a plain inset tab. Aileron undeflected. R=8,200,000.

FIGURE 57.—Section aerodynamic characteristics of an NACA 66, 2-210 (a=0.6) airfoil equipped with a 0.20-chord, sealed gap, plain aileron of straight-sided profile with a 0.20c, plain inset tab. R=9,000,000, α₀=-4.13°.
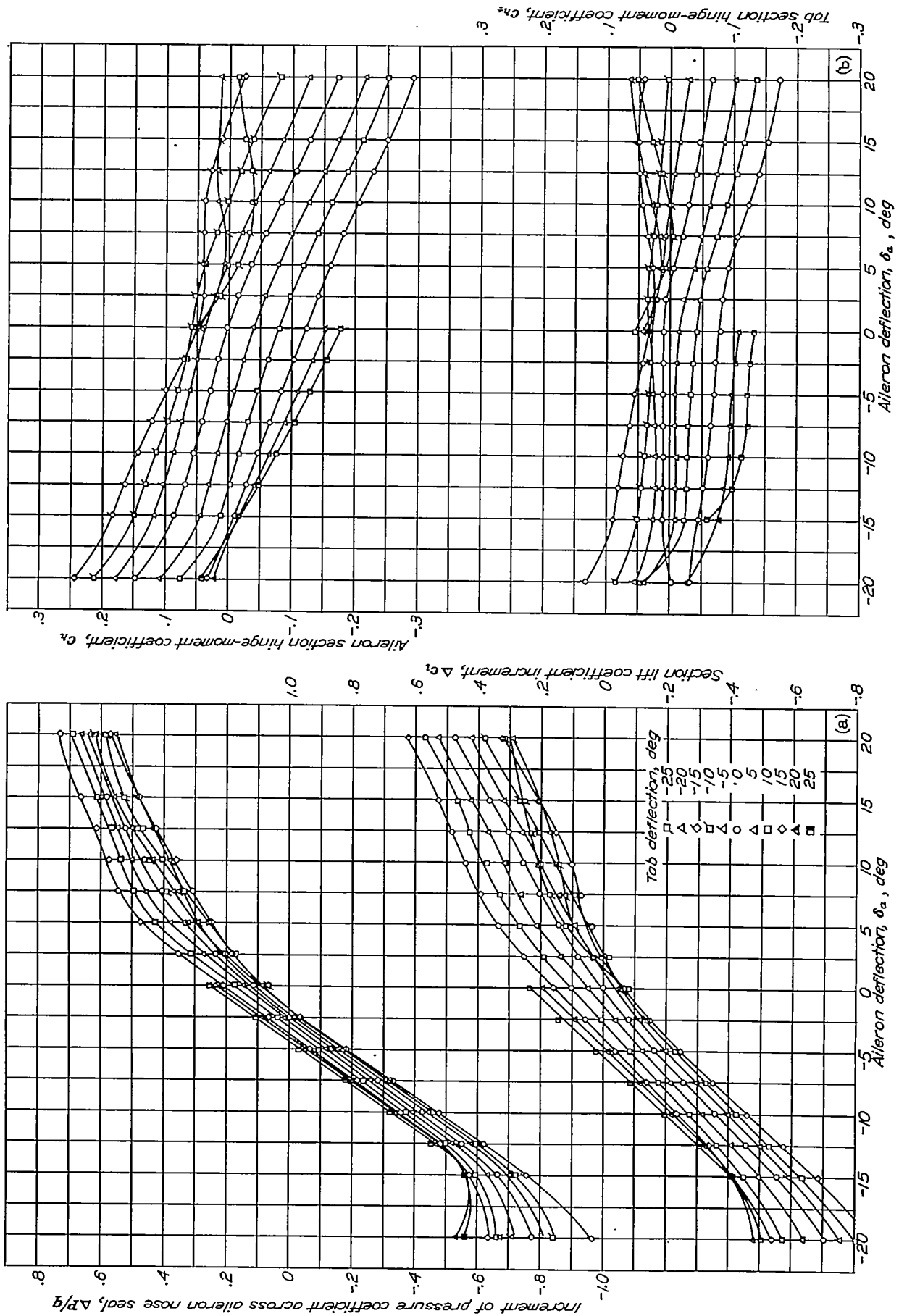
FIGURE 68.—Section aerodynamic characteristics of an NACA 66, 2-216 (a=0.6) airfoil equipped with a 0.20-chord, sealed gap, plain aileron of straight-sided profile with a 0.20c. plain inset tab. R=9,000,00, α₀=−2.08°.

FIGURE 50.—Section aerodynamic characteristics of an NACA 66, 2-210 (a=0.6) airfoil equipped with a 0.20-chord, sealed gap, plain aileron of straight-sided profile with a 0.20c, plain inset tab. R=9,000,000, α=0.01°.
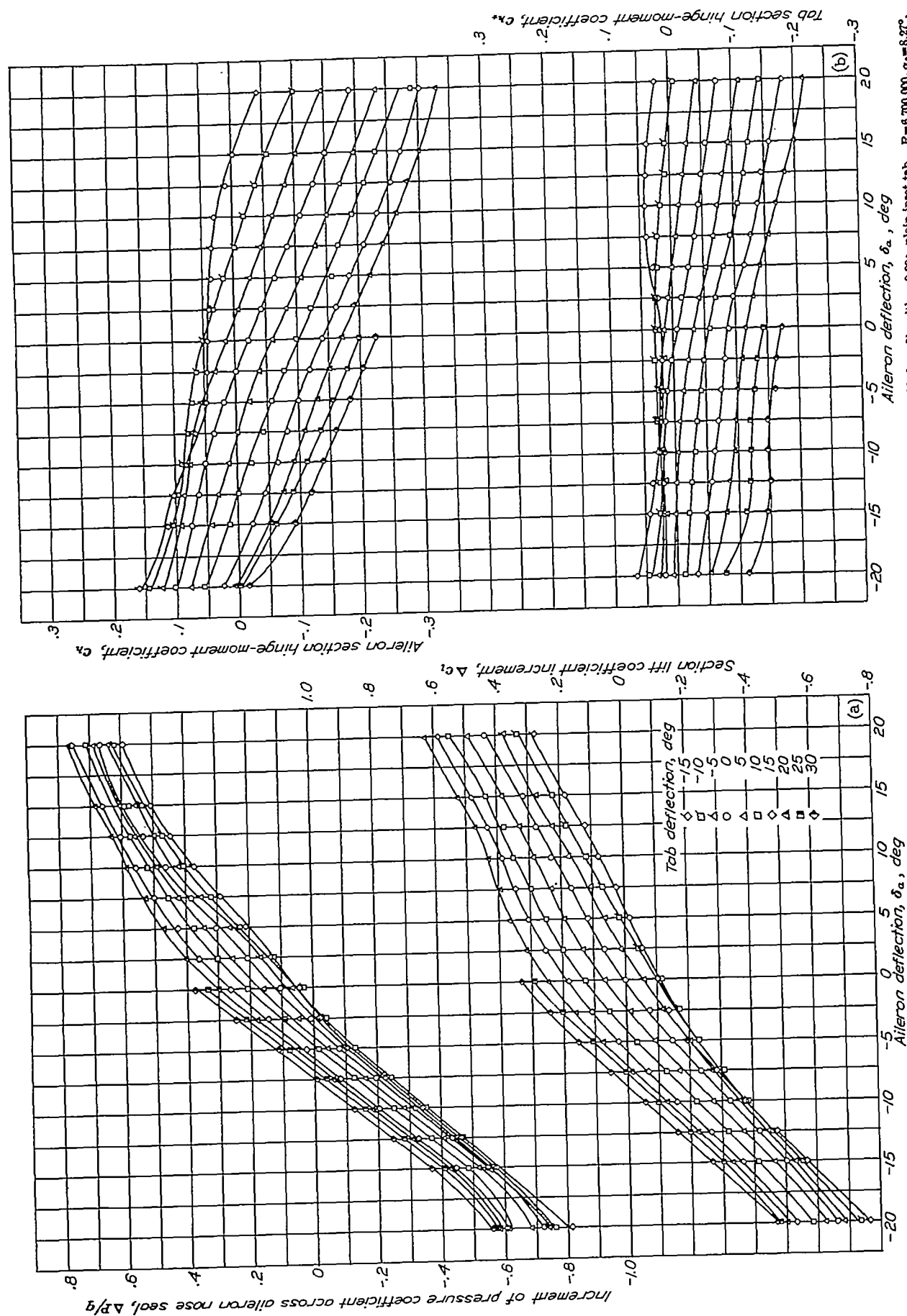
FIGURE 60.—Section aerodynamic characteristics of an NACA 66, 2-216 (α=0.6) airfoil equipped with a 0.20-chord, sealed gap, plain aileron of straight-sided profile with a 0.20c, plain inset tab. R=9,000,000, α_0=2.07°.
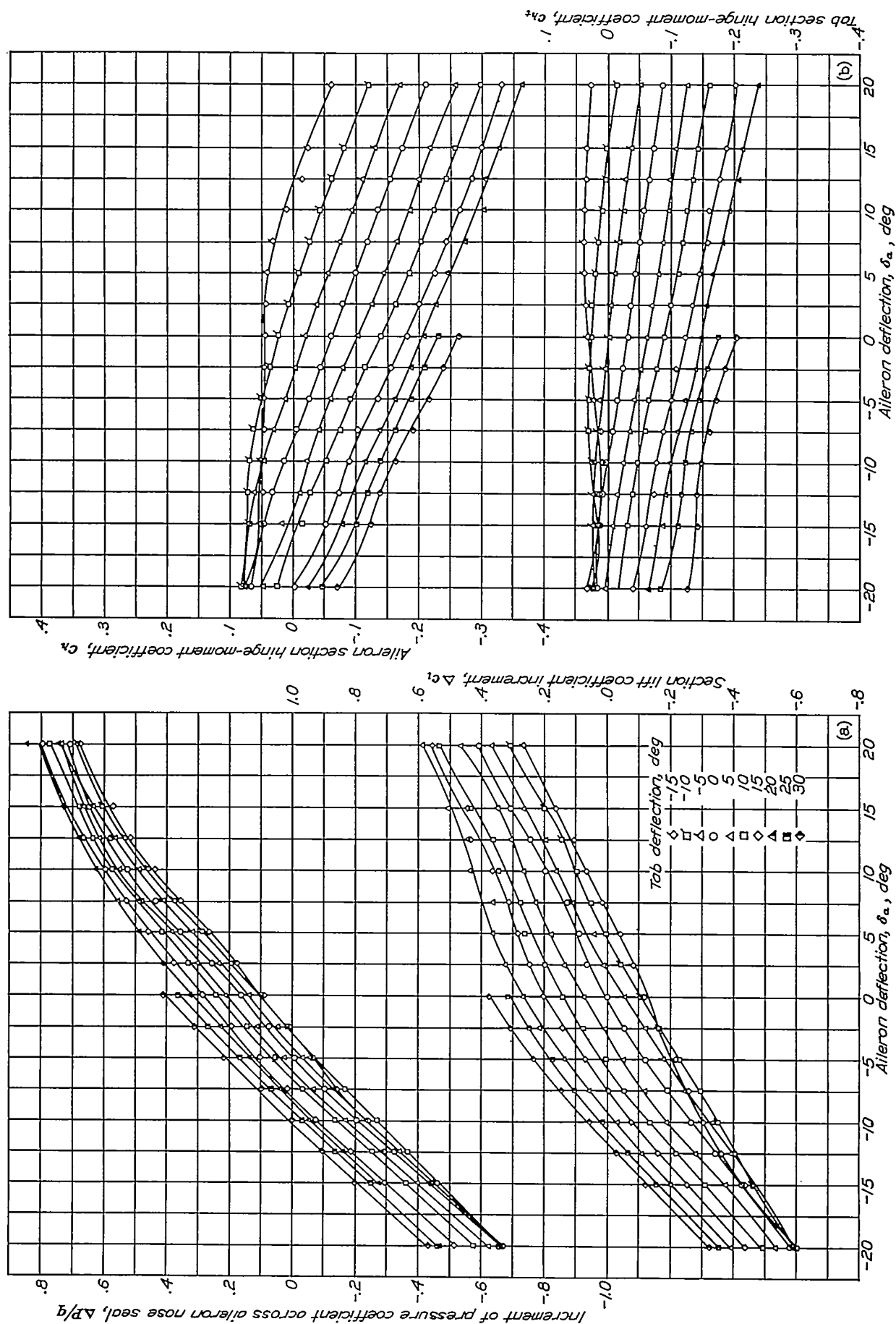
FIGURE 61.—Section aerodynamic characteristics of an NACA 66, 2-210 (a=0.6) airfoil equipped with a 0.20-chord, sealed gap, plain aileron of straight-sided profile with a 0.20c, plain inset tab. $R=9,000,000$, $a_0=4.14°$.

FIGURE 62.—Section aerodynamic characteristics of an NACA 64, 2-216 ($\alpha=0.6$) airfoil equipped with a 0.20-chord, sealed gap, plain aileron of straight-sided profile with a 0.20c_a, plain inset tab. $R=6,700,000$, $\alpha_0=8.27°$.
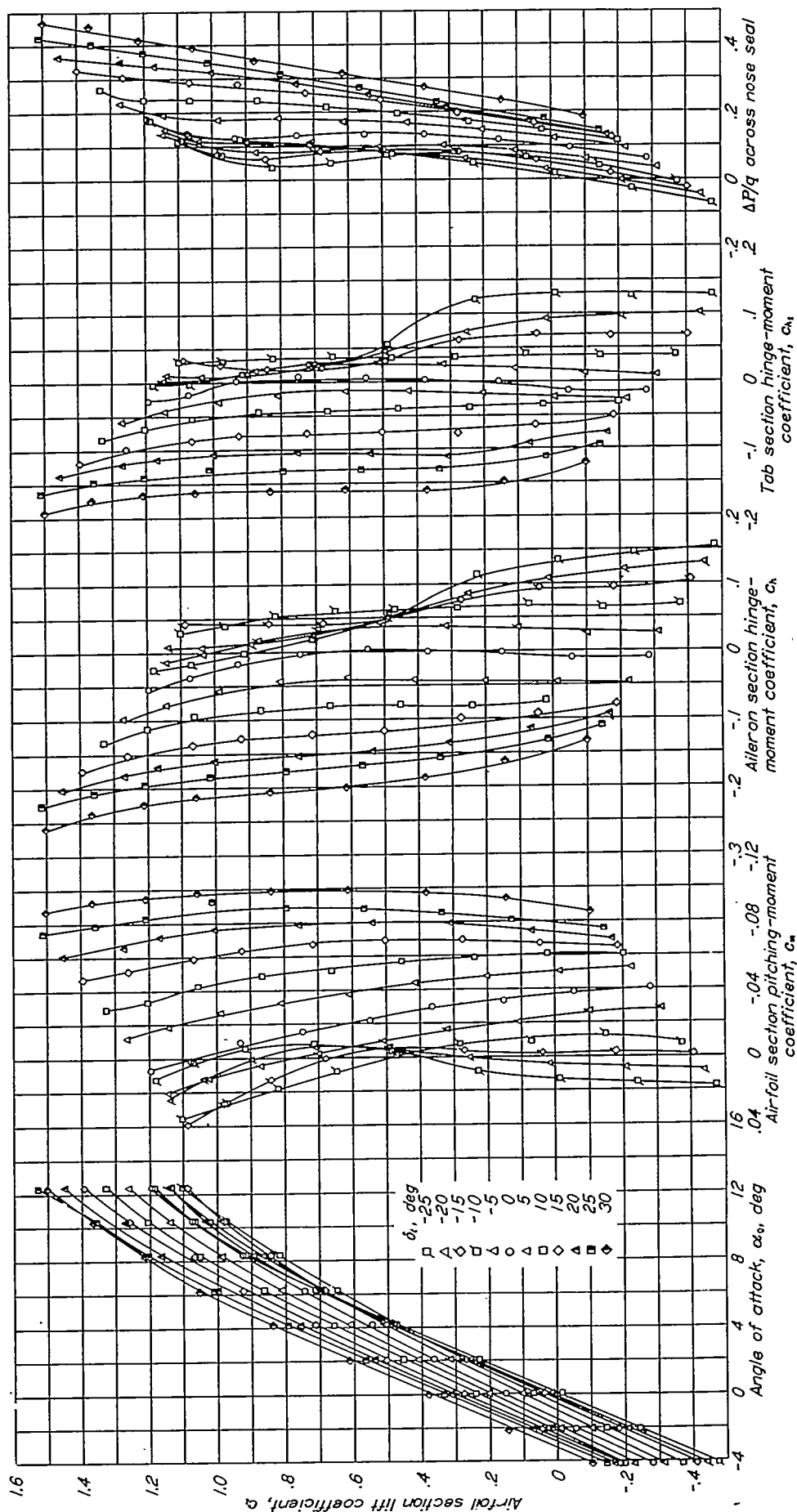
FIGURE 63.—Section aerodynamic characteristics of an NACA 66, 2-216 ($\alpha=0.0$) airfoil equipped with a 0.20-chord, sealed gap, plain aileron of straight-sided profile with a 0.20c_a plain inset tab. $R=5,500,000$, $\alpha_0=12.37°$.

FIGURE 64.—Section aerodynamic characteristics of an NACA 66,2-216 ($\alpha=0.6$) airfoil equipped with a 0.20-chord, sealed gap, plain aileron of straight-sided profile with a 0.20c, plain inset tab.   Aileron undeflected. $R=8,200,000$.

AMER. TITLE: Wind-tunnel investigation of the effects of profile modification and tabs on the characteristics of ailerons on a low-drag airfoil

FORG'N. TITLE:

ORIGINATING AGENCY: National Advisory Committee for Aeronautics, Washington, D. C.

TRANSLATION:

COUNTRY	LANGUAGE	FORG'N.CLASS	U.S.CLASS.	DATE	PAGES	ILLUS.	FEATURES
U.S.	Eng.		Unclass.	1944	53		photo, tables, diagr, graphs

ABSTRACT

Tests were made to determine the effect of control-surface profile modifications on the aerodynamic characteristics of an NACA 66-series airfoil. Thickening aileron profile or thickening and beveling trailing edge of aileron reduced aileron effectiveness, slope of section lift curve, and hinge-moment coefficients. Thinning profile had opposite effect. Effects of profile thickness on aileron characteristics decreased with increasing angle of attack. Basic data are presented from which effect of tabs can be calculated for specific cases.

NOTE: Requests for copies of this r
Washington, D. C.

PIII

& Ailerons.
Loco Drag Airfoils